Aus der Klinik für Endokrinologie und Diabetologie

der Heinrich-Heine-Universität Düsseldorf

Direktor: Univ.-Prof. Dr. Michael Roden

EVALUATION OF URINARY C-PEPTIDE AS A SURROGATE TO SERUM C-PEPTIDE IN ADULT-ONSET DIABETES

Dissertation

zur Erlangung des Grades eines Doktors der Medizin

der Medizinischen Fakultät der Heinrich-Heine-Universität Düsseldorf

vorgelegt von

Tanmay Ramesh Londhe

2026

Als Inauguraldissertation gedruckt mit Genehmigung der
Medizinischen Fakultät der Heinrich-Heine-Universität Düsseldorf

gez.:
Dekan: Prof. Dr. med. Nikolaj Klöcker
Erstgutachter: Prof. Dr. med. Robert Wagner
Zweitgutachter: PD Dr. med. Maximilian Spieker

Dedicated to my family.

“The greatest mistake man ever makes is to assume he has time.”

“Change is the only constant in life.”

Zusammenfassung

Serum C-Peptid (SCP) ist ein etablierter Marker zur Beurteilung der endogenen Insulinsekretion und wird zur Unterscheidung zwischen Typ-1- und Typ-2-Diabetes (T2DM) eingesetzt. Seine klinische Anwendung ist jedoch durch strenge präanalytische Anforderungen limitiert. Die Bestimmung von C-peptid im Urin (UCP) könnte hingegen eine nicht-invasive und präanalytisch robustere Alternative zu SCP darstellen. Ziel dieser Arbeit war, die präanalytische Stabilität von UCP zu untersuchen sowie dessen Eignung zur Abschätzung der β-Zell-Funktion (BCF) und Insulinsensitivität (IS), die üblicherweise aus SCP über die Homeostasis-Model-Assessment-2 (HOMA2)-Indizes der BCF (HOMA2-B) und IS (HOMA2-S) abgeschätzt werden, zu evaluieren. Außerdem wurde geprüft, inwieweit UCP zur Klassifikation der 2018 von Ahlqvist et al. vorgeschlagenen SCP basierten T2DM-Subtypen beitragen kann. Hierfür wurden UCP und Kreatinin retrospektiv in morgendlichen Spontanurinproben aus einer Subgruppe der Deutschen Diabetes Studie mit T2DM und normaler Glukosetoleranz (NGT) bestimmt, die über zehn Jahre bei -20 °C gelagert worden waren. Zusätzlich wurde die Stabilität von UCP bei Raumtemperatur (RT) bis zu 96 Stunden sowie über vier Einfrier-Auftau-Zyklen untersucht. Zur Abschätzung der HOMA2-Indizes aus UCP wurde erst SCP anhand von UCP, Diagnosealter, Geschlecht und Body-Mass-Index (BMI) geschätzt. Anschließend wurden HOMA2-Indizes aus den geschätzten und den gemessenen SCP-Werte berechnet und miteinander verglichen. Die UCP-basierte Subtypenzuordnung wurde mit der etablierten SCP-basierten Klassifikation verglichen. Insgesamt wurden 488 Teilnehmende mit T2DM (medianes Alter: 53 Jahre, 35 % weiblich, medianes BMI: 30 kg/m²) sowie 192 Teilnehmende mit NGT (medianes Alter: 47 Jahre, 38 % weiblich, medianes BMI: 26 kg/m²) eingeschlossen. UCP zeigte über 96 Stunden bei RT keine statistisch signifikante zeitabhängige Veränderung ($\beta = 0{,}13$; $p = 0{,}83$), obwohl eine interindividuelle Variabilität beobachtet wurde. Nach vier Einfrier-Auftau-Zyklen wurde ein statistisch signifikanter, jedoch geringer Abfall beobachtet ($\beta = -0{,}64$, $p < 0{,}001$). Die UCP-basierten HOMA2-Indizes korrelierten stark mit den SCP-basierten Werten (HOMA2-S: Spearman's $\rho = 0{,}81$, HOMA2-B: Spearman's $\rho = 0{,}80$, p jeweils $< 0{,}001$). Die Übereinstimmung der UCP-basierten mit den SCP-basierten Subtypen betrug 77.5 % (Cohen's $\kappa = 0{,}62$, $p < 0{,}001$). Zusammenfassend stellt UCP eine praktikable und nicht-invasive Alternative zu SCP dar, die eine Abschätzung der HOMA2-Indizes und Einordnung in T2DM-Subtypen ermöglicht.

Abstract

Serum C-peptide (SCP) has an established clinical utility in the assessment of endogenous insulin secretion and specifically to differentiate between type 1 diabetes and type 2 diabetes (T2DM). However, its widespread clinical use is limited by stringent pre-analytical requirements. On the other hand, its measurement in urine as urinary C-peptide (UCP) may provide a non-invasive and pre-analytically robust alternative to SCP. In this respect, we aimed to evaluate the pre-analytical stability of UCP, the feasibility of UCP in assessing the β-cell function (BCF) and insulin sensitivity (IS), both of which being usually estimated using the homeostasis model assessment 2 (HOMA2) indices of BCF (HOMA2-B) and IS (HOMA2-S) from SCP, and the ability of UCP to classify individuals to the novel T2DM subtypes, which were introduced in 2018 by Ahlqvist et al. based on SCP. To this end, we retrospectively measured UCP and urinary creatinine from morning spot urine samples, which were collected and stored at -20 °C over ten years, from a subset of the German Diabetes Study comprising participants with T2DM and normal glucose tolerance (NGT). Pre-analytical stability of UCP was assessed at room temperature (RT) over 96 hours and across four freeze-thaw cycles. To estimate HOMA2 indices from UCP, SCP was first predicted from UCP, age at diagnosis, sex, and body mass index (BMI), following which HOMA2 indices were calculated from predicted SCP and measured SCP values and compared with each other. A cluster assignment based on UCP was performed and compared with the SCP-based assignment as per the original Ahlqvist-classification. A total of 488 T2DM participants (median age: 53 years, 35% female, median BMI: 30 kg/m²) and 192 NGT (median age: 47 years, 38% female, median BMI: 26 kg/m²) participants were included in this study. UCP showed no statistically significant time-dependent change over 96 hours at RT ($\beta = 0.13$, $p = 0.83$), although inter-individual variability was seen. UCP did show a statistically significant decay across four freeze-thaw cycles ($\beta = -0.64$, $p < 0.001$), but with a small effect size. The UCP-based HOMA2 indices correlated strongly with SCP-based indices (HOMA2-S: Spearman's $\rho = 0.81$, HOMA2-B: Spearman's $\rho = 0.80$, p in both = < 0.001). UCP-based subtype model prediction achieved an overall accuracy of 77.5% (Cohen's $\kappa = 0.62$, $p < 0.001$) compared with the SCP-based classification. In conclusion, UCP can provide a practical and non-invasive alternative to SCP for the estimation of HOMA2 indices and for subtype classification in T2DM.

List of Abbreviations

ADA	American Diabetes Association
AUC	area under the curve
BMI	body mass index
CI	confidence Interval
CV	coefficient of variation
DDZ	Deutsches Diabetes-Zentrum/German Diabetes Centre
ER	endoplasmic reticulum
GADA	glutamic acid decarboxylase antibodies
GDM	gestational diabetes mellitus
GDS	German Diabetes Study
GST	glucagon stimulation test
EASD	European Association for the Study of Diabetes
ECLIA	electrochemiluminescence immunoassay
HbA1c	haemoglobin A1c
HOMA	Homeostasis Model Assessment
HOMA1/2	Homeostasis Model Assessment 1/2
HOMA/1/2-B	Homeostasis Model Assessment 1/2 of β-cell function
HOMA/1/2-IR	Homeostasis Model Assessment 1/2 of insulin resistance
HOMA/1/2-S	Homeostasis Model Assessment 1/2 of insulin sensitivity
IDF	International Diabetes Federation
IFG	impaired fasting glucose
IGT	impaired glucose tolerance
IL-6	interleukin-6
IQR	interquartile range
IVGTT	intravenous glucose tolerance test
MARD	mild age-related diabetes
MMTT	mixed-meal tolerance test
MOD	mild obesity-related diabetes
MODY	maturity-onset diabetes of the young
NAFLD	non-alcoholic fatty liver disease
NGT	normal glucose tolerance
OGTT	oral glucose tolerance test
PCOS	polycystic ovary syndrome

PI3K	phosphoinositide 3-kinase
PMDI	precision medicine in diabetes initiative
ROC	receiver operating characteristic
SAID	severe autoimmune diabetes
SCP	serum C-peptide
SIDD	severe insulin-deficient diabetes
SIRD	severe insulin-resistant diabetes
T1DM	type 1 diabetes
T2DM	type 2 diabetes
TNFα	tumour necrosis factor α
UCP	urinary C-peptide
UCPCR	urinary C-peptide-to-creatinine ratio
UCr	urinary creatinine
UKPDS	United Kingdom Prospective Diabetes Study
WHO	World Health Organization
×*g*	relative centrifugal force
°C	degrees Celsius
mmol/mol	millimole per mole
nmol/mmol	nanomole per millimole
mmol/L	millimole per litre
mg/dL	milligram per decilitre
mg/mL	milligram per millilitre
ng/mL	nanogram per millilitre
µg/L	microgram per litre
µL	microlitre
mL	millilitre
kg/m^2	kilogram per metre squared

Table of Contents

1 Introduction 1

1.1 Types of Diabetes and Diagnostic Criteria 1

1.2 Type 2 Diabetes 3

1.2.1 Epidemiology 3

1.2.2 Risk Factors and Pathophysiology 4

1.3 Measurement of β-cell function and insulin sensitivity 7

1.4 HOMA Indices of β-cell Function and Insulin Resistance 9

1.5 C-peptide 11

1.5.1 Serum C-peptide 11

1.5.2 Urinary C-peptide 14

1.6 Heterogeneity and Clustering in Type 2 Diabetes 18

1.7 Aims of this Thesis 20

2 Materials and Methods 22

2.1 Study Design 22

2.2 The German Diabetes Study (GDS) 22

2.2.1 Introduction and Aims of the GDS 22

2.2.2 The Cohort of the GDS 23

2.3 Sample Collection and Storage 26

2.4 Laboratory Analysis 28

2.4.1 Measurement of Urinary C-peptide 28

2.4.2 Measurement of Urinary Creatinine 30

2.5 Pilot-Project 31

2.6 Stability-Testing 31

2.7 Statistical Analysis 32

3 Results 34

3.1 Baseline Characteristics 34

3.2 Stability of Urinary C-peptide under various storage conditions 37

3.2.1 Long-term Storage at -20 °C 37

3.2.2 Stability at Room Temperature 38
3.2.3 Stability during Multiple Freeze-Thaw Cycles 42
3.3 Relationship between Urinary C-peptide and Serum C-peptide 46
3.4 Prediction of Serum C-peptide and HOMA2 Indices 48
3.5 Cluster Analysis 50
4 Discussion 52
4.1 Baseline Characteristics 52
4.2 Pre-Analytical Stability of Urinary C-peptide 53
4.3 Relationship of Urinary C-peptide and Serum C-peptide 57
4.4 Prediction of HOMA2 Indices from Urinary C-peptide 59
4.5 Cluster Analysis in Type 2 Diabetes using Urinary C-peptide 61
4.6 Limitations 62
5 Conclusions 65
6 Outlook 66
7 Bibliography 67
8 Appendix 76
8.1 Supplementary Tables 76
8.2 Supplementary Figures 79

1 Introduction

Diabetes mellitus is a chronic metabolic disorder signifying a state of enduring hyperglycaemia, leading to macrovascular and microvascular complications and resulting in long-term morbidity and/or mortality. As per the International Diabetes Federation (IDF) estimates of diabetes prevalence, as of 2024, approximately 589 million adults (20–79 years of age) are living with diabetes worldwide, with most of the disease prevailing in low- and middle-income countries [1]. The disease burden is expected to rise to 853 million by 2050 [1], posing a great challenge not only to the well-being of the population but also to the overburdened health services throughout the world.

1.1 Types of Diabetes and Diagnostic Criteria

The American Diabetes Association (ADA) [2] classifies diabetes into four major types:

1. Type 1 diabetes (T1DM): autoimmunity-induced destruction of the pancreatic β-cells.
2. Type 2 diabetes (T2DM): progressive loss of the pancreatic β-cell function, with insulin resistance being a common concurrent occurrence.
3. Specific diabetes types: pancreatogenic diabetes, medications-/chemical-induced diabetes, monogenic diabetes, etc.
4. Gestational diabetes mellitus (GDM): diabetes exclusively occurring and being diagnosed during the second or third trimester of pregnancy.

The diagnostic criteria proposed by the ADA and the German Diabetes Association, which are in accordance with those recommended by the World Health Organization (WHO) and the IDF, involve the use of plasma glucose values and haemoglobin A1c (HbA1c) for the diagnosis of diabetes in non-pregnant individuals [2] [3] [4]. Plasma glucose values can either be measured after a period of minimum 8 hours of fasting or two hours post oral glucose tolerance test (OGTT) with a 75 g standardized meal or from a random blood sample [2]. The latter, when combined with typical symptoms of hyperglycaemia such as polyuria, polydipsia, unexplained weight loss, or hyperglycaemic emergencies like diabetic ketoacidosis and hyperglycaemic hyperosmolar state, is enough for the diagnosis of diabetes [2]. In the absence of clinical signs for diabetes, the diagnosis can be made with the help of two of the criteria

listed below, either measured at the same time or at two different points in time [2]. If two different points in time are used for the diagnosis, either the same criterion or two different criteria can be used [2]. The laboratory assay used for HbA1c must be certified by the National Glycohemoglobin Standardization Program and standardized to the assay used in the Diabetes Complications and Control Trial [2]. The following diagnostic criteria have been proposed by the ADA [2]:

1. HbA1c ≥ 6.5% (≥ 48 mmol/mol)
2. Fasting plasma glucose ≥ 126 mg/dL (≥ 7.0 mmol/L)
3. 2-hours post OGTT plasma glucose ≥ 200 mg/dL (≥ 11.1 mmol/L)
4. Random plasma glucose ≥ 200 mg/dL (≥ 11.1 mmol/L) along with symptoms of hyperglycaemia or hyperglycaemic crisis

Although the detection of hyperglycaemia is the sole diagnostic marker of diabetes in general, each type of diabetes has a different underlying pathophysiology. T1DM accounts for 5%–10% of the total diabetes cases and is characterized by autoimmune-mediated destruction of the pancreas, which leads to absolute insulin deficiency [2, 5]. The resulting severe hyperglycaemia can trigger ketosis in these patients, and a glucose-lowering insulin therapy is needed right from the diagnosis [2]. Although this disease can occur in all ages, a typical patient with T1DM is young and lean [2]. Islet cell antigen 512 antibodies also called islet antigen 2 antibodies, glutamic acid decarboxylase antibodies (GADA), anti-insulin antibodies, and zinc-transporter 8 antibodies can be detected in most of the patients with T1DM [6]. However, in 10% of these patients, no antibodies can be identified [5]. The early period after diagnosis is said to be the “honeymoon period”, in which residual insulin secretion can still be detected [7]. As time progresses, β-cell destruction ensues, but 30–80% of the patients retain their β-cell function, the so-called “insulin micro-secretors” [7]. The entity “Latent Autoimmune Diabetes of Adults” , which implies the autoimmune-mediated destruction of the β-cells in adults, has been clubbed together with T1DM in the recent classification of diabetes by the ADA [2]. In the monogenic form of diabetes, as the name itself suggests, a mutation in a single gene contributes to the development of hyperglycaemia [6]. Several genes involved in β-cell function have been identified to cause monogenic diabetes [2]. Examples are hepatocyte nuclear factor 1-α, hepatocyte nuclear factor 4-α, glucokinase, etc., which are responsible for the maturity-onset diabetes of the young (MODY), a monogenic form of diabetes occurring

in children and in early adulthood [2]. Although the prevalence of monogenic diabetes is rare, many of these patients get misdiagnosed as T1DM and are started on insulin treatment, which they do not usually need [2]. GDM is the development of hyperglycaemia during the gestational period, which confers not only an increased risk of birth defects in the foetus but also a lifelong risk for the development of T2DM in the mother [2]. T2DM is a chronic metabolic disorder that develops when insulin secretion cannot keep up with the increased demand of insulin action on the background of insulin resistance, the consequence of which is the development of hyperglycaemia and its complications [2]. Unlike the detection of autoantibodies in T1DM or the detection of a mutation in monogenic diabetes, T2DM cannot be identified by a test of a single biomarker [5], owing to its multifactorial causation.

1.2 Type 2 Diabetes

1.2.1 Epidemiology

Among the various types of diabetes, T2DM represents the most frequently occurring type comprising more than 90% of the cases [1] [3]. As mentioned above, parallel to the projected increase in the cases of diabetes in 2050, this disease will become the 2nd largest disease of the global disease burden in 2050 [1]. In Germany as of 2025 about 9 million adults are affected by diabetes, by 2040 this number is projected to rise to 12 million adults [8]. According to the third European Health Interview Survey (2018–2020), prevalence of diabetes is higher in Germany as compared to other European countries [9]. The number of undiagnosed adults with diabetes is estimated to be 2 million in Germany, which is similar to the estimate of the IDF that about 1 in 3 adults with diabetes in high-income countries is undiagnosed [1, 8]. This may well be attributed to the fact that T2DM, especially in the early years of the disease, is relatively silent with respect to signs and symptoms, with the diagnosis being made only with the onset of cardiovascular, nephrological and neurological complications in many of the cases [1]. In 2010, about €30 billion were spent by the German healthcare system for people with diabetes and this expenditure is expected to more than double till the year 2040 [8]. Thus, even though in a country like Germany, which has a high public health expenditure, the prevalence of diabetes is still increasing [6]. As diabetes is frequently accompanied by other chronic diseases such as hypertension, obesity,

hyperlipidaemia and kidney disease, the required expenditure of these diseases taken together would put a huge burden on healthcare systems.

1.2.2 Risk Factors and Pathophysiology

The pathophysiological origin of T2DM is multifactorial in nature [10]. The interplay of genetic, metabolic, environmental and lifestyle factors contribute together to the development of persistent hyperglycaemia on the grounds of decreased insulin secretion and sensitivity [11]. The non-modifiable risk factors such as age, familial predisposition, ethnic background and genetic susceptibility confer an increased risk of developing diabetes [12]. The incidence of T2DM increases with increasing age [13]. A single parent with T2DM alone increases the risk of developing the same in a first degree relative approximately 2.5 times and this risk doubles when both the parents are affected [14]. The risk is also higher in ethnicities such as Japanese and Hispanics and the disease is more prevalent in Asians than in other populations [12]. Since the advent of genome-wide association studies, more than 100 gene loci have been identified which confer a genetic susceptibility to defective insulin secretion and action [12, 15]. Although there is a substantial amount of genetic diversity associated with T2DM, the role of this diversity contributing to the development of T2DM is limited in comparison to that of other factors [16].

The development of hyperglycaemia is preceded by the stage of dysglycaemia, also known as prediabetes or intermediate hyperglycaemia [1, 2]. Prediabetes represents a state where plasma glucose levels are not high enough to meet the criteria for diabetes but are also not low enough to fall within the normal range, thereby increasing the risk of diabetes [1, 2]. Prediabetes encompasses the two entities of impaired glucose tolerance (IGT) and impaired fasting glucose (IFG) [1, 2]. As per the ADA, prediabetes is said to prevail when one or more of the following criteria are met: Fasting plasma glucose in the range of 100–125 mg/dL (IFG), 2-h post 75 g-OGTT plasma glucose ranging from 140 to 200 mg/dL (IGT) or HbA1c from 5.7 to 6.4% (39 to 47 mmol/mol) [2]. Although the pathophysiological mechanisms underlying the development of prediabetes revolve around a reduction in insulin secretion and sensitivity, IFG and IGT are said to be distinct metabolic entities [17, 18]. In IFG, a reduced hepatic insulin sensitivity results in increased hepatic glucose output, and although the early-phase insulin secretion in response to a glucose load is deranged,

plasma glucose levels return to baseline at 120 minutes owing to a normal muscular insulin sensitivity [17-19]. On the other hand, the increased 2-h plasma glucose level in IGT arises due to an increased insulin resistance primarily at the muscular level, together with a defective early-phase and late-phase insulin response [17-19]. The prevalence of IFG and IGT differs according to age and sex, wherein IGT is more prevalent in older age and IFG in males [17]. It is seen that approximately 25% of patients with IFG or IGT progress to diabetes within a period of 3 to 5 years [18]. The presence of IFG and IGT both together doubles the risk of diabetes as compared to the presence of only one of the two [18]. As with IFG and IGT, increasing HbA1c levels also elevate the risk of T2DM in a progressive manner [2].

The epidemic of T2DM has been growing in parallel to the epidemic of obesity, as obesity increases the susceptibility for T2DM manyfold [1, 20]. Since the prevalence of obesity in children and adolescents has been increasing worldwide, the incidence of T2DM has also increased in these groups [21]. Obesity and overweight can potentiate the risk of diabetes through insulin resistance, changes in fatty acid metabolism, as well as through dysfunction at the mitochondrial level [22, 23]. It is observed that every kilogram of weight gain contributes to an increased diabetes risk of up to 9% [24]. Moreover, increased central adiposity with visceral fat plays a much more important role than the deposition of fat in the periphery [22]. This is in concordance with the observation that a lack of physical activity increases the risk of diabetes independent of obesity, and regular physical exercise is beneficial to promote insulin sensitivity and prevent progression from prediabetes to T2DM [25-27]. The intake of foods with high glycaemic index, consumption of sugary soft drinks and red meat have been found to be associated with an increased incidence of T2DM [28]. Smoking contributes to an increased risk of T2DM through insulin resistance, with the risk being elevated both for former and current smokers [29, 30]. Taken together, obesity arises out of sedentary lifestyle, physical inactivity, consumption of unhealthy foods, and smoking, finally giving rise to T2DM [30, 31]. In women, polycystic ovary syndrome (PCOS) is associated with obesity, IGT, and T2DM, with insulin resistance being common to all [32].

The development of overt hyperglycaemia leading to T2DM takes place under the umbrella of β-cell dysfunction parallel to increased insulin resistance [10]. Insulin secretion from the β-cells in response to an intraarterial glucose load consists of an

early-phase response achieving a maximum in 2–4 minutes and a late-phase response which peaks at 2–3 hours [33]. Insulin action is defined as the ability of insulin to dispose of glucose in fat and skeletal muscles and suppress gluconeogenesis in the liver [10, 34]. Resistance to insulin action or insulin resistance can therefore be present in the periphery (fat and skeletal muscles) and/or in the liver, and this resistance is seen to develop very early in the course of the disease [10, 35, 36]. At the cellular level, insulin action takes place through the binding of insulin to its tyrosine kinase receptor on the cell membrane [37]. This receptor consists of various intracellular substrates called insulin receptor substrates 1–4, which, upon phosphorylation, begin insulin signalling by activating phosphoinositide 3-kinase (PI3K) [37]. PI3K activates a serine-threonine kinase AKT which stimulates a downstream-cascade responsible for the diverse anabolic effects of insulin, such as glucose and protein uptake, inhibition of gluconeogenesis and lipolysis, glycogen storage, lipid synthesis, protein synthesis, etc. [10, 11, 37, 38]. Obesity, which is a strong risk factor for insulin resistance, causes an expansion in the central adipose tissue [10]. As more and more triglycerides get deposited, an enlargement in the size of the adipocytes takes place and these adipocytes blunt the anti-lipolytic action of insulin with a consequent increase in the circulating levels of free fatty acids and glycerol [10, 31]. The adipose tissue is also a site of chronic inflammation, so that inflammatory cytokines such as tumour necrosis factor α (TNFα) and interleukin 6 (IL-6) are released from the adipose tissue [10, 31]. Increased levels of free fatty acids and glycerol trigger hypoxia in adipose tissue, subsequently leading to adipose tissue dysfunction [31]. Additionally, free fatty acids cause phosphorylation in the serine-threonine kinase AKT, thereby creating a disturbance in the insulin signalling [10, 11]. TNFα not only hampers the phosphorylation process in the signalling cascade but also promotes lipolysis in the adipose tissue so that free fatty acid levels further increase [10, 31]. IL-6 enhances the degradation of proteins involved in the signalling cascade [10]. Apart from this, oxidative stress and mitochondrial dysfunction have also been found to disrupt the downstream cascade in insulin signalling [11]. On the other hand, the levels of Adiponectin, which is protective against insulin resistance, fall in obesity [10]. The consequence of insulin resistance is the increased demand on β-cells to secrete higher amounts of insulin to achieve the same level of glucose disposal at the target organs [33, 39]. However, the resulting hyperinsulinemia itself aggravates insulin resistance owing to a downregulation of the tyrosine kinase receptors along with a simultaneous

low-grade stimulation of lipid metabolism [37, 39]. Resulting hyperlipidaemia and an increase in adipose tissue exacerbate adipose tissue dysfunction, thereby worsening insulin resistance [35].

An impairment in insulin secretion owing to β-cell dysfunction has been shown to prevail early in the course of the disease, so that β-cell response cannot sufficiently meet the increasing secretory demand and hyperglycaemia results with dysglycaemia ensuing in between [40]. Therefore, β-cell dysfunction usually goes in tandem with an increased insulin resistance, synergistically giving rise to T2DM, however the relative contribution varies [10, 33]. For example, although the prevalence of T2DM in Pima Indians and Asian Indians is high, Pima Indians are much more insulin resistant than Asian Indians, whereas β-cell dysfunction is much more common in Asian Indians [41]. Defects in β-cell secretion have been observed in first-degree normoglycemic relatives of T2DM individuals, which suggests that the β-cell dysfunction has a genetic cause [10]. Indeed, majority of the genes found to be associated with T2DM are those that give rise to secretory defects [12]. After the onset of hyperglycaemia, chronically elevated glucose levels aggravate the deterioration of the β-cell function, causing damage to β-cells through hyperglycaemia-induced oxidative stress and apoptosis [10, 33]. Parallel to glucotoxicity, increased levels of circulating non-esterified fatty acids or saturated fats due to obesity or dietary consumption also contribute to a diminishing insulin secretion, inducing inflammation within the pancreas itself, this phenomenon being referred to as lipotoxicity [10, 42]. Glucotoxicity also promotes local inflammation in the islet cells through deposition of amylin, inducing mitochondrial stress and endoplasmic reticulum (ER) stress, which enhances the release of inflammatory cytokines [12]. Apart from the effect of glucotoxicity on β-cell function, high glucose levels can also interfere with insulin signalling, thus worsening insulin resistance [37].

1.3 Measurement of β-cell Function and Insulin Sensitivity

In the 1960s, Andres and his colleagues introduced the glucose clamp techniques of the hyperglycaemic clamp and the euglycemic hyperinsulinaemic clamp for the assessment of β-cell function and insulin sensitivity, respectively [43]. The hyperglycaemic clamp and the intravenous glucose tolerance test (IVGTT) are considered the gold standard methods for the assessment of β-cell function, whereas the euglycemic hyperinsulinaemic clamp is considered the gold standard method for

the assessment of insulin sensitivity [43, 44]. In the hyperglycaemic clamp, glucose is infused to rapidly induce hyperglycaemia in the subject, and this level of hyperglycaemia is maintained (“clamped”) through continuous glucose infusion throughout the study [43-45]. The induced hyperglycaemia provokes endogenous insulin secretion from the pancreas under maximal stimulation, and both the phases of insulin secretion vis-á-vis the early first-phase (first 5–10 minutes) and the second phase (after 10 minutes) can be assessed through serial measurements of plasma insulin [43-45]. In the IVGTT, the incremental area under the curve (AUC) in the levels of insulin following an intravenous glucose load is measured, which reflects the β-cell function of the pancreas [45, 46]. The use of a glucose infusion in both the hyperglycaemic clamp as well as the IVGTT circumvents the confounding gastrointestinal effects on insulin release, such as the incretin effect (as observed in an OGTT), thereby providing a direct reflection of the β-cell secretory response to a glucose stimulus [45-47]. In the euglycemic hyperinsulinaemic clamp, as the name itself suggests, high doses of insulin are continuously administered to suppress the endogenous hepatic glucose production, and a parallel continuous glucose infusion maintains (“clamps”) the plasma glucose at euglycemic levels, thereby preventing an endogenous insulin secretory response from the pancreas [43-45]. After the achievement of a steady state, the rate of glucose infusion is a direct reflection of the rate of glucose uptake in the tissues and the resulting M index is primarily a function of insulin sensitivity at the muscle level (as majority of the glucose uptake takes place physiologically in the muscle) with higher values implying a better insulin sensitivity [43, 44, 48]. Additionally, a tracer labelled glucose can be deployed to assess the endogenous glucose production and gauge the hepatic insulin sensitivity [44]. As both the clamp techniques operate at the maximal state of stimulation, they enable an isolated observation of the feedback loop between glucose and insulin, thereby providing a sound physiological basis for the assessment of glucose metabolism in healthy as well as in disturbed states [45, 46]. However, as the aforementioned gold standard techniques are not only time- and labour-consuming but also require trained technical staff, their use in the routine clinical practise is not feasible and is therefore restricted to research settings. Hence, various proxy measures to assess β-cell function and insulin resistance have been developed, which are commonly used in clinical practise. These proxy measures are either based on simple measurements of plasma glucose and insulin in the fasting state (e.g. Matsuda-Index, Stumvoll-Index

etc.) or are derived from the OGTT (e.g. insulinogenic index, oral disposition index etc.) [45, 49]. These surrogate measures have been comprehensively validated against the gold standard methods, with some of them exhibiting a high degree of correlation and reproducibility [47-50]. One of the most widely accepted and validated surrogate measures of β-cell function and insulin resistance are the indices of the Homeostasis Model Assessment (HOMA) [34, 47].

1.4 HOMA Indices of β-cell Function and Insulin Resistance

In 1985, a mathematical model was developed by Matthews et al., assessing the insulin resistance and β-cell function known as the HOMA [51]. This model was based on the feedback loop between β-cells and the liver in the fasting state [51]. Levy et. al. [52] published an updated version in 1998, which came to be known as HOMA2. According to these models, insulin resistance and β-cell function can be estimated at various concentrations of plasma glucose and insulin at basal fasting steady-state, being respectively known as HOMA1-/HOMA2-IR and HOMA1-/HOMA2-B [51, 52]. The term HOMA1-/HOMA2-S signifies insulin sensitivity, which is inversely proportional to HOMA1-/HOMA2-IR [51, 52].

Especially in persons with T2DM, this model is helpful in assessing changes in the β-cell function and insulin resistance not only over the natural course of the disease but also under treatment [34, 53]. The first HOMA model is a simple linear mathematical equation using fasting plasma insulin and fasting plasma glucose values to calculate HOMA1-B and HOMA1-IR [51]. The β-cell function is modelled around plasma glucose values (decreasing β-cell function would increase plasma glucose), whereas the insulin sensitivity is modelled around plasma insulin values (decreasing insulin sensitivity would mean higher insulin levels) [54]. As the equation was calibrated using insulin assays of the 1980s, there is a tendency of the HOMA1 model to overestimate the β-cell function and underestimate the insulin sensitivity, if newer assays were used to measure plasma insulin [34]. Therefore, HOMA1 model should not ideally be used to calculate an individual's HOMA1-B and HOMA1-S but should be used to longitudinally observe these values over a period for e.g., in epidemiological studies [34, 55]. HOMA1 model assumes that insulin resistance is the same for liver and fat/skeletal muscles, on the other hand, HOMA2 model is a non-linear computer model taking into account variations in hepatic and peripheral insulin resistance, is able

to compute HOMA2-B and HOMA2-IR at insulin levels over 10 mmol/L, takes into account the urinary glucose excretion during hyperglycaemia and incorporates an estimate of proinsulin secretion, thereby enabling the use of radioimmunoassay or specific insulin assays for insulin measurements [34]. Both the HOMA models have been validated against the gold standard methods of insulin sensitivity and β-cell function in persons with normal glucose tolerance (NGT) as well as in patients with diabetes [51, 56-58].

Clinically, the HOMA model predicts risk of developing diabetes as shown in the Women Health Initiative Observational Study in which women from multiple ethnicities in the age group of 50 to 79 years of age were followed up for a period of 5.9 years [59]. Results of this study showed a strong association between increased diabetes risk and high levels of HOMA1-IR with low levels of HOMA1-B [59]. The San Antonio Heart Study showed similar results [60]. In the Bruneck study, a higher HOMA1-IR has been shown to be associated with increased risk of cardiovascular events such as myocardial infarction, stroke and transient ischaemic attack, even after adjusting for classical risk factors [61]. The United Kingdom Prospective Diabetes Study (UKPDS) used HOMA1-B to monitor the β-cell function under different treatment regimens in T2DM [62]. HOMA-IR can be used to monitor insulin resistance in patients undergoing treatment for T2DM [63, 64]. Apart from this, many studies have used HOMA indices complementary to gold standard methods to study the pathophysiology of the two prediabetic states of IFG and IGT [65, 66]. As insulin resistance is an integral part of the pathogenesis of the metabolic syndrome, HOMA-IR can detect and predict the risk of metabolic syndrome in adults, children and adolescents [67, 68].

However, the HOMA model has several limitations. Firstly, the insulin-independent glucose uptake in the brain has not been incorporated in the model [69]. Secondly, the validation of the HOMA model against gold standard techniques such as the euglycemic hyperinsulinaemic clamp test assumes that there is a high correlation between insulin resistance at fasting basal steady-state (HOMA) and at maximally stimulated steady state (euglycemic hyperinsulinaemic clamp test) [70]. However, in fact in the fasting state, insulin action is at the liver and in the maximally stimulated state, insulin action occurs at the muscle [70]. Thirdly, the model assumes that the secretion of insulin from the β-cells is a measure of the β-cell mass; however, in reality, many factors, such as amino acids, fatty acids, neurotransmitters, and hormones,

affect insulin secretion [69, 71]. Despite these limitations and although many other surrogate methods of assessing insulin resistance and β-cell function have been developed, the ease of estimating both these parameters through a single blood collection in the fasting state has ensured that the HOMA model survives [55, 70].

Although the measurement of insulin is a prerequisite for the estimation of HOMA indices, there are several limitations to its use. About half of the insulin secreted in the portal vein by the pancreas undergoes hepatic extraction [72]. Furthermore, this hepatic extraction is not constant, but variable depending on the load of glucose ingestion [72]. The value of the measured insulin, therefore, may not accurately reflect the pancreatic insulin secretion [73, 74]. Moreover, the measurement of insulin may be unreliable due to the presence of exogenous insulin and insulin-autoantibodies in the serum of patients with diabetes [75]. Instead, the measurement of C-peptide is said to be a better alternative to the measurement of insulin to assess the pancreatic insulin secretion [76].

1.5 C-peptide

1.5.1 Serum C-peptide

In 1967, during experiments carried out on a human islet cell adenoma, Steiner and colleagues postulated the existence of a connecting segment linking the two polypeptide chains of insulin in the precursor molecule proinsulin. [77]. A year later, Chance and his team successfully identified the amino acid sequence of this connecting segment in porcine proinsulin and named it the “connecting peptide” [78]. The term “C-peptide” was first used by Clark et al., and it was suggested that C-peptide is secreted in equimolar amounts to insulin after the cleavage of proinsulin, which was then confirmed in further studies [79, 80]. Subsequent research also showed that the structure of C-peptide is variable in different species, the human C-peptide consisting of 31 amino acids [81].

Insulin biosynthesis is triggered through a rise in the blood glucose level, which is registered by the β-cells of the islets of Langerhans, leading to the synthesis of preproinsulin in the ER [82]. Enzymatic cleavage of preproinsulin yields proinsulin in which C-peptide is essential for promoting the proper folding of proinsulin, thereby enabling the formation of two disulfide bonds between cysteine residues located on

the α- and β-chains of the insulin molecule [82]. This proinsulin gets temporarily stored in the Golgi bodies, following which proconvertases and carboxypeptidases act tandemly to yield insulin and C-peptide, both of them getting secreted in a 1:1 ratio in the portal circulation [82].

As previously mentioned, the peripheral measurement of insulin may not accurately reflect the pancreatic insulin secretion, as up to half of the secreted insulin undergoes first-pass metabolism, with the hepatic insulin uptake varying under various physiological circumstances [73]. On the other hand, C-peptide, after getting secreted in the portal circulation, gets minimally metabolized in the liver, thereby assuming concentrations in the periphery which are approximately five times higher than those of insulin, with the half-life of C-peptide being approximately 20–30 minutes as compared to 3–5 minutes for insulin [82]. Because of the longer half-life of C-peptide, the unsteady β-cell response can be better captured with the measurement of C-peptide [83]. C-peptide is thus said to be a surrogate marker to insulin for the assessment of β-cell function, with the peripheral concentrations of insulin and C-peptide showing significant correlations at fasting and stimulated states [84, 85].

Clinically, the measurement of C-peptide takes place as part of either a routine blood draw or comprehensive β-cell stimulation tests [76]. The comprehensive β-cell stimulation tests to assess the β-cell response include tests such as OGTT, mixed-meal tolerance test (MMTT), or glucagon stimulation test (GST) [86]. In these tests, the β-cell stimulation can be assessed in the following ways: by computing the area under the curve of rise in C-peptide levels after a standardized 75-g glucose load at 120 minutes (OGTT) or after a liquid meal at 120 minutes (MMTT), or by measuring C-peptide levels at 6 minutes after the intravenous application of glucagon (GST) [76, 86, 87]. OGTT and MMTT mirror the physiological dynamics of the β-cell response after a meal through the glucose load and incretin effect; on the contrary, in the GST, the acute response can be assessed, surpassing the glucose-induced stimulation and the incretin effect [86]. However, in day-to-day practise, as the stimulation tests, although having a higher accuracy and reproducibility, are time-consuming and not practicable to perform, more commonly, C-peptide is measured as part of a routine blood draw either in the fasting state or randomly [76]. As concomitant hypoglycaemia interferes with the β-cell response, the simultaneous measurement of glucose along with C-peptide is recommended [86].

The spectrum of clinical utility of C-peptide ranges from the diagnosis of diabetes to the differential diagnosis of hypoglycaemia. In insulin-treated patients with diabetes, if there is difficulty in differentiating between T1DM and T2DM, a fasting C-peptide level of less than 0.6 ng/mL suggests the diagnosis of T1DM [76, 83]. This cut-off has been recently incorporated in the ADA guidelines, when T1DM is clinically suspected but no islet cell autoantibodies can be serologically identified [2]. On the other hand, the detection of considerable levels of C-peptide may help to re-classify a patient with a long-term T1DM in T2DM or monogenic diabetes [76]. Irrespective of the type of diabetes, the decision to initiate insulin therapy in patients with diabetes can be aided through the measurement of C-peptide levels, which can detect an absolute insulin deficiency [76, 83]. On the contrary, in patients with unclear diagnosis of T1DM or T2DM, who have been treated with insulin since diagnosis, the detection of considerable levels of C-peptide may aid in deciding discontinuation of insulin therapy [76]. Prognostically, low levels of C-peptide in T1DM have been shown to be associated with poor glycaemic control, higher HbA1c levels, and the development of microvascular complications such as retinopathy [76, 86]. In opposition, high C-peptide levels in prediabetes and T2DM have been associated with the development of metabolic syndrome and macrovascular complications [76, 86]. C-peptide levels also find use to differentiate between factitious and real hypoglycaemia [88]. Low C-peptide levels point towards a surreptitious use of exogenous insulin, whereas higher levels suggest overdose of sulfonylureas or an insulinoma [88]. The HOMA indices of β-cell function and insulin resistance can also be calculated with C-peptide and glucose, instead of insulin [34]. Especially in insulin- treated patients with diabetes, the assessment of insulin resistance and β-cell function cannot be reliably carried out with HOMA indices based on insulin [34].

Despite these various applications of C-peptide, the pre-analytical phase, starting from the blood draw till the actual measurement of C-peptide in the laboratory, poses a hindrance to its widespread acceptance in diabetes. It is recommended that C-peptide, which can be measured either in serum or plasma, needs to be rapidly transported on ice to the laboratory, followed by immediate separation of serum/plasma from the cellular components [89, 90]. This means practically that a blood draw for C-peptide at a doctor’s office that is closer to a laboratory is the only viable option. In reality, however, as most of the patients with diabetes are treated by a physician in an outpatient setting, a pre-centrifugation delay is unavoidable. Previous studies indicate

that a prolonged delay before centrifugation results in rapid degradation of C-peptide in whole blood [91-93]. Therefore, the use of serum/plasma C-peptide for these clinical applications, owing to its pre-analytical instability, is indeed problematic. Instead, C-peptide in urine is an alternative to the measurement of serum/plasma C-peptide [76].

1.5.2 Urinary C-peptide

In 1975, a group of Japanese scientists first reported the presence of C-peptide in human urine, its concentrations not only being higher than serum but also increasing in parallel to serum concentrations after a glucose ingestion [94]. Research showed that after the passage of the secreted C-peptide through the liver, approximately 85–90% reaches the systemic circulation, and the kidneys represent the leading organ of C-peptide excretion, with muscle and adipose tissues showing no uptake [95, 96]. The majority of C-peptide from the systemic circulation undergoes glomerular filtration and subsequent metabolism through peritubular uptake [95]. Finally, around 5% of the daily secretion of C-peptide can be found in 24-hour urine collections, assuming concentrations in urine that are ten to twenty times higher than plasma [76, 97, 98]. Due to the absence of proteases in urine, C-peptide in urine has been shown to have a better stability at room temperature after collection [76]. As urine is subject to dilutional variability, the urinary C-peptide-to-creatinine ratio (UCPCR) is suggested to nullify this dilutional effect [76, 94].

Additional advantage of measuring urinary C-peptide (UCP) instead of serum C-peptide (SCP) is the fact that some amounts of proinsulin is always released from the β-cells along with insulin and C-peptide and as the commercially used C-peptide assays do show some amount of cross-reactivity with proinsulin, erroneous measurements of C-peptide may take place depending on the amount of proinsulin in the blood [99, 100]. The amount of proinsulin secreted from the β-cells is variable, and higher amounts are seen in patients with diabetes [85]. As the concentration of proinsulin in urine is very scarce, the measurement of UCP is advantageous from this view as well [99].

Studies with UCP started initially with 24-hour collections with the goal to stably assess the β-cell function over an entire day, because firstly a single blood draw cannot capture the fluctuating insulin secretions over the course of the day and secondly the

measurement of urinary insulin excretion was not practical owing to the fact that only 0.1% of daily insulin secretion can be found in urine [101]. Various studies have shown a significant correlation between 24-hour UCP excretion and SCP/insulin secretion in both fasting and stimulated states, indicating that UCP excretion reflects β-cell function relatively well [94, 99, 102-104]. 24-hour UCP excretion also correlated well with C-peptide and insulin secretion under differing metabolic conditions such as exercise [105]. In a study conducted by Aurbach-Klipper et al. in children diagnosed with T1DM within first six years of disease onset, the decline in β-cell function could be captured through progressive measurements of UCP from 24-hour collections [106]. A study conducted on Caucasoids and Pima Indians showed better discriminatory ability of UCP as compared to SCP to differentiate between insulin-dependent T1DM and T2DM [107]. Apart from this, the progressively declining β-cell secretion in both the diabetes types could also be observed with the measurement of 24-hour UCP in the same study [107]. A Japanese study pointed out an association between lower levels of 24-hour UCP and the need of insulin use in the future in T2DM [108].

However, as the 24-hour collection procedure is inconvenient to the patient and insufficient collection is seen in many cases, focus soon shifted to the measurement of UCP from spot urine samples [109, 110].

In 2011, in studies conducted by the Exeter group, fasting UCPCR and two-hour post-prandial (or post-MMTT) UCPCR showed significant correlations with stimulated SCP values after the MMTT in patients with T1DM and T2DM on insulin therapy; thus UCPCR was proposed as an alternative to MMTT to assess the endogenous β-cell function [111, 112]. UCPCR and SCP measured two hours after the intake of a standardized meal in patients with T2DM showed significant correlations with each other [113]. When this test was repeated thrice, the reproducibility of fasting and post meal UCPCR was similar to that of SCP itself [113]. In patients with diabetes on insulin therapy, two-hour post meal UCPCR has been shown to reliably detect absolute insulin deficiency which may help guide clinical decisions on whether to continue insulin therapy or switch to oral hypoglycaemic agents. [111, 114].

As many patients with MODY get falsely diagnosed as T1DM [115], many studies have used UCPCR as a tool to avoid this misdiagnosis. In a study conducted by the Exeter group comparing post-prandial UCPCR levels between patients with adult MODY and T1DM, the measurement of UCPCR levels > 0.2 nmol/mmol several years after

diagnosis showed a good sensitivity and specificity to identify patients with MODY who were initially classified as having T1DM [115]. A cut-off of 0.7 nmol/mmol UCPCR two hours post-prandial had a sensitivity of 100% and a specificity of 97% to differentiate between T1DM and MODY/T2DM in children with a diabetes duration of more than 2 years [116]. Similar cut-offs have been proposed to differentiate between T1DM and T2DM/MODY in children and adults in Egyptian, Turkish and Chinese studies [117-119]. In a systematic review by Pappachan et al., the same cut-off of 0.2 nmol/mmol UCPCR was found best to make a distinction between T1DM and T2DM/MODY [120].

Even a random spot UCPCR was shown to be a practical alternative to MMTT to assess endogenous β-cell function in long-standing insulin-treated T2DM [121]. In long-standing T1DM, UCPCR has been used to determine residual β-cell function and Shields et al. used UCPCR to identify two phases of decline in β-cell function in T1DM [122-124].

Although in one study, UCPCR was seen to be 1.48 times higher in women than in men irrespective of diabetes type or control group, this observation could not be confirmed in another study and no difference has been found in C-peptide excretion rates between men and women [125, 126]. According to the first study, this difference in the UCPCR between the genders was observed because of lower creatinine excretion rates in women owing to their lower muscle mass [125].

UCPCR also has a predictive value. As per the Biomarkers in Personalized Medicine (BioPersMed) Cohort Study in Austria, UCPCR had a negative predictive value of 60.2% when adult study participants with NGT were followed up to screen for prediabetes [126]. Higher UCPCR levels were associated with the development of macrovascular complications such as coronary heart disease, stroke, and diabetic kidney disease in patients with T1DM and T2DM, even after adjusting for other relevant risk factors [127, 128].

A possible association between insulin resistance and UCP levels has been observed. Chung et al. in 1986 observed higher levels of UCP in T2DM as compared to healthy controls, and a correlation was seen between higher body fat mass and higher levels of UCP [129]. They postulated that higher levels of insulin get secreted to compensate the effect of insulin resistance in T2DM [129]. A few years later Kato et al. observed a weak correlation between UCP and body mass index (BMI) in T2DM [130]. A study conducted by the Exeter group in participants with NGT pointed out a significant

correlation between fasting UCPCR and HOMA2-IR (insulin-based) [131]. The same was also seen in children and adolescents with obesity as well as in patients with T2DM [128, 132]. Keeping in line with these observations, Farghaly et al. found that UCPCR was the strongest predictor of non-alcoholic fatty liver disease (NAFLD) in obese children [133]. Thus, several studies have shown a significant correlation between UCPCR and HOMA-IR with UCPCR having a potential to be used as non-invasive surrogate marker for insulin resistance. However, the estimation of HOMA indices themselves using UCP has not been undertaken to date.

With respect to the pre-analytical phase, second void fasting UCPCR showed lesser intra-individual variability than first void fasting UCPCR as well as a better correlation with 24-hour UCP [134]. Studies evaluating the stability of UCP under various storage conditions are limited. Kuzuya et al. conducted a storage experiment with UCP at various temperatures and concluded that urine samples without additives remained stable at room temperature for 1–2 days, however better stability could be achieved with the use of sodium azide [135]. Samples stored in a refrigerator at 4 °C also remained stable for at least 2 days, and samples frozen at -20 °C remained stable for at least up to a year [135]. Several years later, the Exeter group conducted similar experiments with UCPCR [134]. Their findings point to a rapid deterioration of UCPCR at room temperature after 24 hours; by using boric acid as a preservative, UCPCR remained stable for up to 72 hours [134]. At 4 °C, all samples remained stable for up to 72 hours, and seven freeze-thaw cycles had no effect on the stability of UCPCR [134]. However, both these studies had very low sample sizes (n = 6 in Kuzuya et al.; n = 2–4 in McDonald et al.). Therefore, a comprehensive study on the effect of various storage conditions on UCP is needed. Of note, the stability of urinary creatinine under freezer storage over several years, at room temperature over many days, as well as during multiple freeze-thaw cycles, has already been established [136-140].

In most of the studies conducted by the Exeter group using UCPCR, a sample tube filled with boric acid was sent to the study participants, which was then sent back by post to the measuring laboratory [111, 114-116]. This kind of home-based method would not only simplify the use of C-peptide in clinical decision-making in diabetes but also potentially increase participation in future decentralised studies and make the implementation of screening programs easier. A better clinical implementation of C-peptide in diabetes could also reduce expenditure in the health care system.

1.6 Heterogeneity and Clustering in Type 2 Diabetes

The conventional classification of diabetes into its two main types is blind to the heterogeneity of patients, especially with T2DM. Although guidelines recommend that the diagnosis of diabetes be made based on blood glucose levels, T2DM is diagnosed when other diabetes types are excluded [2, 141]. Even when a diagnosis has been made, clinical experience points to a very heterogeneous nature of the disease with a spectrum of phenotypes. The wide range in age of onset, from adolescence to older adulthood, the higher prevalence in men, and the presence or absence of obesity or other features of metabolic syndrome at presentation all point to a disease with multifaceted forms of presentations and differing progression and complication profiles [141-143]. This kind of heterogeneity can especially be observed in various diabetes cohorts in newly diagnosed patients with T2DM [16]. These cohorts, having patients relatively early in the course of diabetes, have shown a substantial person-to-person variability in the prevalence and progression rates of diabetes-related complications underscoring the heterogenous nature of this disease [16]. On one hand, some patients rapidly progress to a β-cell failure, requiring a therapy with insulin, sometimes right from the clinical diagnosis; on the other hand, some patients never need any insulin therapy during their lifetime [143]. This kind of heterogeneity and that too in a single disease entity, underlines the pathophysiological complexity of the disease with this complexity being a summation of various risk factors at the genetic and environmental level, along with lifestyle habits [16]. This complexity is not reflected in the current classification of diabetes and therefore a need was always felt to identify subtypes in T2DM which would, depending on the subtype, help in clinically point out the direction, a patient would take, so that specific complications or a specific treatment response could be predicted [6, 16, 141].

In the year 2018, the precision medicine in diabetes initiative (PMDI) was started by the ADA, in cooperation with the European Association for the Study of Diabetes (EASD) [6]. The PMDI defines precision medicine in diabetes as the use of every available form of data, be it clinical, behavioural, geographical or genomic, to optimise diagnostic, therapeutic, prevention and monitoring strategies for subgroups of patients with common disease characteristics, ultimately facilitating personalised decisions at the individual level [6]. Therefore, one of the several objectives of the PMDI involves

stratification of T2DM in subsets with the aim of refining therapy decisions and prognostic predictions [6].

Keeping in line with this objective of the PMDI, in 2018, Ahlqvist et al. introduced a novel classification of adult-onset diabetes with five clusters, each having a different risk of disease progression and complications [144]. Using k-means clustering based on six variables namely, age at disease diagnosis, BMI, HOMA2-B, HOMA2-IR (both indices being C-peptide based), HbA_{1c} and serological presence or absence of GADA, this research group proposed five distinct clusters in diabetes: severe autoimmune diabetes (SAID) corresponding to T1DM, severe insulin-deficient diabetes (SIDD), severe insulin-resistant diabetes (SIRD), mild obesity-related diabetes (MOD) and mild age-related diabetes (MARD), with the latter four clusters representing T2DM [144]. The presence of GADA determined the classification of a patient in SAID, whereas its absence meant classification into the other four clusters [144]. It was found that patients with SIDD were younger, leaner, had a lower HOMA2-B, and a higher prevalence of diabetic retinopathy, and although insulin-deficient, they were the ones who received the maximum number of metformin prescriptions [144, 145]. The SIRD group had a higher BMI, higher values of the HOMA indices, higher prevalence of NAFLD and diabetic nephropathy, and although insulin resistant, this group received a lower number of metformin prescriptions [144, 145]. The MOD cluster had a higher BMI but was less insulin resistant than the SIRD cluster [144]. The MARD group was significantly older in age and had a level of metabolic disturbance which was similar to that of the MOD group [144]. A genetic analysis identified no genetic variant that was common to all clusters [144]. This method of clustering was applied to five different cohorts in Sweden, not only in patients with new onset of diabetes but also in long-standing disease states under treatment [144]. As this study reported differing outcomes depending on the underlying cluster, a potential was seen to develop cluster-tailored treatment strategies and was perceived as an important step towards precision medicine in diabetes [145].

In 2019, Zaharia et al. validated the clusters in the German Diabetes Study (GDS) cohort using gold standard methods of insulin secretion and insulin resistance, thereby confirming the presence of a substantial insulin resistance at the level of muscle and adipose tissue in the SIRD group and primarily at the level of adipose tissue in the MOD group [146]. The poor β-cell function in the SIDD group could also be confirmed

[146]. Moreover, it was seen that a cluster assigned at the stage of diagnosis was not the same after a follow-up period, suggesting that the membership of a cluster can change depending upon the metabolic changes during the disease course and under therapy [146].

In the years thereafter, this method for cluster assignment was applied in various cohorts throughout the world, and the same clusters could be identified in more than 20 studies, albeit with differing prevalence in different areas of the world [141]. As an example, in India and China, the phenotype of SIDD is seen to be much more prevalent than in Europe [33]. Wagner et al. undertook the task of identifying subgroups in prediabetes, and 6 phenotypes with differing rates of progression to T2DM could be brought to the surface [147].

Precision medicine in diabetes demands the discovery of these clusters in various ethnicities throughout the world [141]. To make sure that this discovery takes place, there is a need to improve the practicability and ease of finding clusters by using variables that are robust and show strong correlation with the original variables, but are also as non-invasive as possible to enable broad application in the community [6, 16, 145]. The ADA-EASD consensus statement on precision medicine in diabetes recognizes the lack of clinical usage of SCP as one of the hindrances to the application of precision diagnostics in diabetes [6]. It is at this stage that a marker like UCP can play an important role. The implementation of UCP instead of SCP for cluster identification would enable an at-home cluster assignment in diabetes, in which the urine samples would be sent by mail either directly to a laboratory or through the family physician, provided that sufficient biochemical stability during transport is ensured. If realised, this would also go a long way towards simplifying recruitment strategies in future decentralised diabetes studies, without the need for physical contact with the study centre.

1.7 Aims of this Thesis

Against this heterogeneous background of T2DM, this study envisioned the use of UCP as a surrogate marker for SCP to enable non-invasive cluster identification and the assessment of β-cell function and insulin resistance in T2DM. Additionally, a pre-analytical study of stability was performed to check if urine samples can be sent back to the treating physician or a laboratory by post.

The following were the aims of this study:

1. to assess the stability of UCP under various pre-analytical conditions:
   a. during long-term storage at -20 °C,
   b. at room temperature,
   c. across multiple freeze-thaw cycles.
2. to test whether UCP can be used to calculate the HOMA2 indices.
3. to test whether UCP can be used to subclassify T2DM.

These aims were tested through the retrospective measurement of UCP from urine samples years after being collected from the participants of the GDS, which is an ongoing prospective longitudinal study in diabetes since 2005 in Germany. The samples that were used in this study were collected and immediately frozen at the German Diabetes Centre in Düsseldorf during the first of the many visits of the study participants in the GDS. The study participants included those with a recent onset of T2DM as well as those with NGT.

As the stored urine samples were collected starting from the year 2008 till 2022, the first step was to determine the presence of C-peptide in these samples, the samples being thawed for the first time in 2022. Following the measurement of 488 samples from participants with T2DM and 192 samples from participants with NGT, statistical analysis was carried out to test if UCP can be used to estimate the HOMA2 indices and to correctly identify the novel clusters in T2DM. The last step in this study was to test the effect of various storage conditions on UCP.

2 Materials and Methods

2.1 Study Design

This study was a retrospective clinical study, which analysed a subset of the GDS. In this study, we analysed urine samples of 488 recently diagnosed patients with T2DM and 192 participants with NGT registered with the GDS from the year 2008 to 2022. This study took place within the framework of the GDS, which was reviewed by the Ethics Committee of the University of Düsseldorf, under the reference number 4508. The urine samples were measured for UCP and urinary creatinine (UCr) at the Central Institute for Clinical Chemistry and Laboratory Diagnostic, University Hospital Düsseldorf (hereinafter referred to as Central Laboratory). C-peptide was measured using an electrochemiluminescence immunoassay (ECLIA), while Creatinine was measured using the enzymatic method, both performed on a *cobas 8000*® analyser from Roche Diagnostics (Mannheim, Germany).

2.2 The German Diabetes Study (GDS)

2.2.1 Introduction and Aims of the GDS

The GDS is an ongoing longitudinal prospective observational study, started in 2005 at the German Diabetes Centre (in German: Deutsches Diabetes-Zentrum or DDZ), a Leibniz Centre for Diabetes Research, Heinrich-Heine University, Düsseldorf, and as of today is taking place at multiple centres throughout Germany in accordance with the Declaration of Helsinki [148]. After a written informed consent to the study, participants with diabetes undergo extensive phenotyping with investigations such as taking medical history, anthropometric measurements, baseline blood testing, assessment of β-cell function, metabolic assessment of cardiovascular and respiratory system, neurological and musculoskeletal investigations, as well as multiple questionnaires to ascertain lifestyle and behavioural activities [148]. With the help of these investigations, the GDS aims to

1. identify sub-phenotypes in diabetes,
2. develop individualized treatment strategies based on the sub-phenotypes,
3. identify predictors of diabetes-related comorbidities at an early stage,

4. identify the effect of various risk factors on the progression and comorbidities in diabetes [148].

Participants are followed up every 5 years till 20 years, with the above-mentioned investigations being carried out at baseline and during every follow-up visit [148]. Between follow-up visits, annual telephone interviews are carried out with standardised questionnaires [148].

2.2.2 The Cohort of the GDS

The cohort of the GDS includes recently diagnosed patients with T1DM, T2DM, and MODY from the ages 18 to 69, being included in the GDS within one year of their clinical diagnosis [148]. The diagnostic criteria for inclusion in the study depend on the current recommendations of the ADA for the diagnosis of diabetes [148]. Since 2015, participants with NGT matched for age, sex, and BMI have been included in the GDS [148]. The GDS excludes patients with other forms of diabetes, such as pancreatogenic diabetes or GDM [148]. The inclusion and exclusion criteria of the GDS are listed in detail in Table 1. The investigations carried out are listed in detail in Table 2.

Table 1: Inclusion and exclusion criteria of the GDS.

Inclusion criteria	- Adults aged 18 to 69 years
	- Diagnosis of T1DM and T2DM, including MODY, following ADA guidelines
	- Individuals diagnosed with T1DM exhibiting ketoacidosis or having immediate insulin dependence, and at least one islet cell autoantibody or undetectable C-peptide values
	- Individuals with recent-onset diabetes (diagnosed within the past 12 months)
Exclusion criteria	- Individuals with forms of diabetes other than those mentioned above (e.g., pancreatogenic diabetes) or GDM
	- Poorly controlled diabetes (HbA1c > 9.0%)
	- Metabolic conditions: those with severe lipid disorders (triglycerides or LDL cholesterol ≥ twice the upper reference limit)

	- Organ dysfunction: individuals with heart failure (NYHA stage II or higher), renal impairment (serum creatinine ≥ 1.6 mg/dL), or liver dysfunction (elevated GOT, GPT, or GGT)
	- Vascular disease: presence of advanced peripheral artery disease or a history of venous thromboembolic events
	- Individuals who have donated blood or have been part of a clinical trial in the last three months
	- Anaemia, severe infections and autoimmune conditions: presence of acute infections, leucocytosis, autoimmune diseases, HIV, or active malignancies
	- Individuals on immunosuppressant therapy
	- Mental health considerations: individuals with severe psychiatric disorders or those who may have difficulty following study protocols
Exclusion criteria for specific tests	- With respect to the neurological examination, individuals with corneal abnormalities or neuropathies unrelated to diabetes are excluded
	- Individuals who develop ECG abnormalities, unstable angina, or severe hypertension during spiroergometry
	- MRI & MRS: participants with metallic implants, metal fragments from prior injuries or prior occupational exposure to metal are excluded as also individuals with large tattoos, waist circumference > 135 cm, or those with claustrophobia
	- Tissue biopsies: exclusion applies to individuals on anticoagulation or those on platelet inhibitors (e.g. therapy with acetylsalicylate)

Table 1: Inclusion and Exclusion Criteria (GDS). Adapted from Szendroedi, J. et al. [148]. *T1DM* type 1 Diabetes, *T2DM* type 2 Diabetes, *MODY* maturity-onset diabetes of the young, *ADA* American Diabetes Association, *HbA1c* haemoglobin A1c, *GDM* gestational diabetes mellitus, *LDL* low-density lipoprotein, *NYHA* New York Heart Association, *GOT* glutamic oxaloacetic transaminase, *GPT* glutamic pyruvic transaminase, *GGT* gamma-glutamic transferase, *HIV* human immunodeficiency virus, *ECG* electrocardiography, *MRI* magnetic resonance imaging, *MRS* magnetic resonance spectroscopy

Table 2: Investigations in the GDS at baseline and 5-year intervals.

Demographic data	- Age, sex, marital status, educational status, status of employment, type of medical insurance, frequency of regular medical checks, family history of diabetes, history of present and prior illnesses, anti-diabetic medications including insulin, anti-hypertensive therapy, platelet inhibition, and anti-lipidemic therapy
Clinical and metabolic assessments	- BMI, waist circumference, glucose, C-peptide, HbA1c, total cholesterol, LDL cholesterol, HDL cholesterol, triglycerides, GOT, GPT, GGT, hsCRP, systolic and diastolic blood pressure, VO_2max, NMD, FMD
Assessment of β-cell function and insulin sensitivity	- GST
	- MMTT
	- Botnia Clamp: IVGTT + euglycemic hyperinsulinaemic clamp
	- Hepatic insulin sensitivity: measured via [6,6-$^2H_2$] glucose co-infusion
Assessment of cardiovascular & metabolic fitness	- Cycling ergospirometry
	- Indirect calorimetry
Molecular analysis	- RNA & DNA purification from whole blood and peripheral blood mononuclear cells
Neurological & microvascular assessments	- Neuropathy: nerve conduction studies, quantitative sensory testing, neuropathic symptoms, intraepidermal nerve fibre density, corneal confocal microscopy
	- Autonomic function: heart rate variability, baroreflex sensitivity, pupillography, sudomotor function, sexual function

	- Microvascular function: laser doppler flowmetry, skin autofluorescence
Ophthalmological examinations	- Fundoscopy
	- Corneal esthesiometry
	- Optical coherence tomography
Assessment of body composition & energy metabolism	- Skeletal muscle & adipose tissue biopsy as well as MRI and MRS
	- Phosphorus metabolite quantification (liver)
	- Phosphocreatine recovery (skeletal muscle, post-exercise)
	- Whole-body fat distribution & ectopic lipid storage (Proton Spectroscopy, MRI)
Assessment of patient-reported outcomes	- Lifestyle habits
	- Disease progression
	- Compliance and socio-economic factors
	- Dietary habits
Psychosocial & quality of life assessments	- Quality of Life: e.g., WHO-5
	- Depression: e.g., PHQ
	- Information needs and time for health-related activities: e.g., CPS

Table 2: Investigations in the GDS at baseline and 5-year intervals. Adapted from Szendroedi, J. et al. [148] *BMI* body mass index, *HbA1c* haemoglobin A1c, *LDL* low-density lipoprotein, *HDL* high-density lipoprotein, *GOT* glutamic oxaloacetic transaminase, *GPT* glutamic pyruvic transaminase, *GGT* gamma-glutamyl transferase, *hsCRP* high-sensitivity C-reactive protein, *VO_2max* maximal oxygen uptake, *NMD* nitrogen-mediated vasodilatation, *FMD* flow-mediated vasodilatation, *GST* glucagon stimulation test, *MMTT* mixed-meal tolerance test, *IVGTT* intravenous glucose tolerance test, *RNA* ribonucleic acid, *DNA* deoxyribonucleic acid, *MRI* magnetic resonance imaging, *MRS* magnetic resonance spectroscopy, *WHO-5* World Health Organization 5 questions health survey, *PHQ* Patient Health Questionnaire, *CPS* Control Preference Scale

2.3 Sample Collection and Storage

In addition to the above-mentioned array of work-up, morning spot urine samples are collected as part of the GDS from all participants at baseline, as well as during every follow-up visit. These urine samples are stored frozen at -20° C in the GDS biobank without preservatives for future analysis. In our study, 680 of such anonymized

morning spot urine samples (488 from participants with T2DM and 192 from participants with NGT), stored at the DDZ, were transferred to the Central Laboratory. All the samples were initially thawed at the DDZ, following which aliquots containing 0.7 mL of each sample were prepared and transferred immediately to the Central Laboratory on dry ice in 5 mL 75 mm x 13 mm round bottom tubes made of polystyrene (Sarstedt, Nümbrecht, Germany). Upon arriving at the Central Laboratory, all samples were refrozen at -20 °C till measurement. As part of the routine laboratory workflow, a batch of approximately 24 samples on each day of measurement were passively thawed to room temperature, immediately subjected to centrifugation (3309×*g*, 7 minutes) in a centrifuge (Andreas Hettich GmbH, Tuttlingen, Germany), barcoded, and measured for UCP and UCr. These steps are depicted in Figure 1. After measurement, all samples were again frozen at -20 °C. The measurements took place from July 2023 to January 2024 in the Central Laboratory.

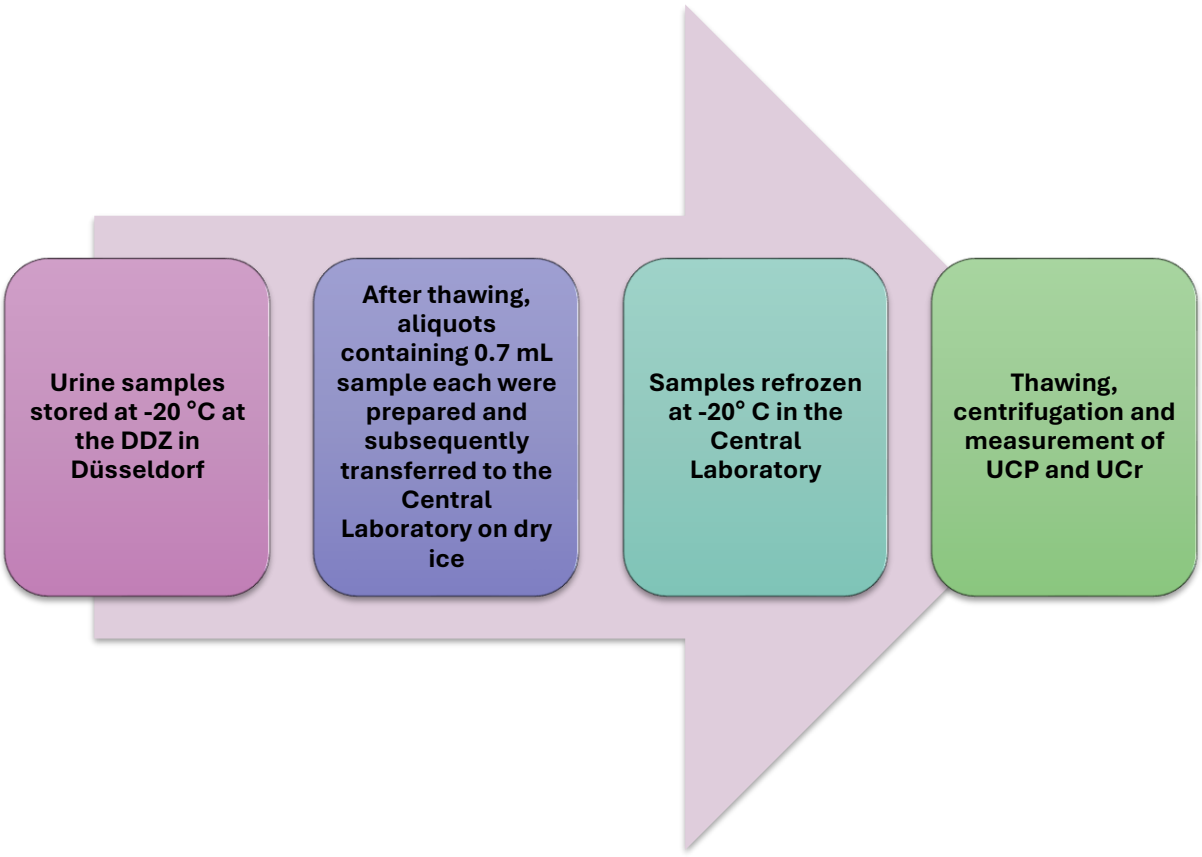


Figure 1: Methodology of this study. Urine samples collected during the first visit of the GDS between 2008 and 2022 were stored at -20 °C in DDZ. Aliquots, 0.7 mL of the sample each, were transferred to the Central Laboratory, subsequently being refrozen at -20 °C. The samples were rethawed, centrifuged, and measured for UCP and UCr. Figure created in "Microsoft PowerPoint". *DDZ* Deutsches Diabetes-Zentrum/German Diabetes Center, *UCP* urinary C-peptide, *UCr* urinary creatinine

2.4 Laboratory Analysis

2.4.1 Measurement of Urinary C-peptide

The Central Laboratory of the University Hospital Düsseldorf uses a *cobas 8000*® analyser (Roche Diagnostics, Mannheim, Germany) for the routine clinical chemistry, which has an e 801 module designed for the ECLIA technique. The Central Laboratory offers the measurement of serum/plasma C-peptide to the University Hospital using the immunoassay *Elecsys C-Peptide* on this e 801 module [100]. As per the official test information, this immunoassay was validated by the manufacturer for the measurement of C-peptide in serum, plasma, and 24-hour urine samples [100], but not specifically for spot urine samples, which were used in this study. However, as previous studies have demonstrated the feasibility of C-peptide measurement in spot urine samples, we proceeded with this method.

The ECLIA for C-peptide is a sandwich-immunoassay and takes 18 minutes to complete [100]. In the first phase, the urine sample (12 µL) is incubated with biotinylated anti-C-peptide monoclonal antibody and ruthenium complex labelled anti-C-peptide monoclonal antibody, all three forming a sandwich [100]. In the second phase of incubation, streptavidin-coated microparticles (0.72 mg/mL) are added to the reaction mixture, thereby inducing a reaction between biotin and streptavidin, leading to the bonding of the sandwich complex to the solid phase (streptavidin-coated microparticles) [100]. In the next step, microparticles get magnetically bound to the electrode following the aspiration of the reaction mixture in the measuring cell [100]. Unbound components of the reaction are washed off by ProCell II M (Roche Diagnostics, Mannheim, Germany), and voltage is applied to the electrode [100]. The resulting emitted chemiluminescence is measured by a photomultiplier, and the concentration of C-peptide is calculated using a 2-point calibration curve [100]. The steps of the C-peptide-ECLIA are depicted in Figure 2. The use of two monoclonal antibodies directed against the same antigen (sandwich-immunoassay) ensures the detection of the antigen in question, even in very small quantities, with a high level of sensitivity and specificity in comparison with the use of only one antibody [149]. The *Elecsys C-peptide* immunoassay is calibrated against the WHO International Reference Reagent for C-peptide of human insulin for immunoassay, IRR code 84/510 [100]. As stated in the test information, all samples were diluted 1:10 using Diluent MultiAssay (Roche Diagnostics, Mannheim, Germany) automatically by the e 801

module before the measurement of UCP, and subsequently, all UCP concentrations above the range of measurement (0.2–400 µg/L) were diluted with a factor of 1:20 using Diluent MultiAssay [100]. Quality assurance is carried out at regular intervals using the materials PreciControl Multimarker Levels 1 and 2 (Roche Diagnostics, Mannheim, Germany). The intra- and inter-assay precision of the assay at various concentrations of UCP was tested by the manufacturer on the e 801 module [100]. The intra-assay coefficient of variation (CV) ranged from 1.4% to 5.5% and the inter-assay CV varied from 2.2% to 6.2% as stated by the test manufacturer based on samples containing urine and *Elecsys* reagents [100] (Supplementary Table 1). This assay shows a cross-reactivity of 28.6% with human proinsulin [100].

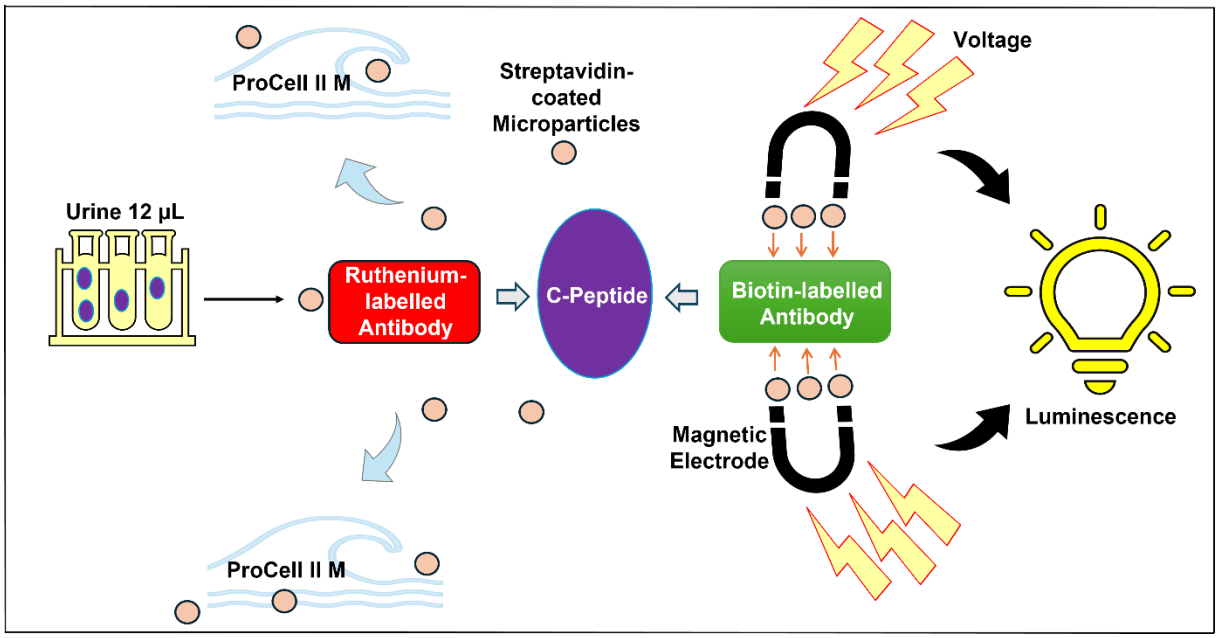


Figure 2: Test principle of the ECLIA. In the first step, 12 µL of the sample is incubated with Ruthenium-labelled anti-C-peptide antibody and Biotin-labelled anti-C-peptide antibody, leading to the formation of a sandwich complex. In the next step, streptavidin-coated microparticles are poured in the reaction mixture, which bind to the biotin of the sandwich complex. Following the aspiration of the reaction mixture in the measuring cell, streptavidin gets magnetically pulled to the electrode. Excess of the streptavidin-coated microparticles is washed away using ProCell II M and in the last step, voltage is applied and the resulting chemiluminescence is measured by a photomultiplier. Figure created in "Microsoft PowerPoint" using information from [100]. *µL* microlitre

2.4.2 Measurement of Urinary Creatinine

UCr is measured in the Central Laboratory using the *CREP2 Creatinine plus ver.2* assay on the c 701 module of *cobas 8000*® [150]. This assay uses the enzymatic method for the measurement of creatinine in human serum, plasma, and urine [150]. In this method, in the first step, creatinine is catalysed by creatininase to creatine, which in turn is catalysed to sarcosine by creatinase [150]. In the next step, sarcosine oxidase converts sarcosine into hydrogen peroxide, formaldehyde, and glycine [150]. Under the action of peroxidase, hydrogen peroxide, along with 4-aminophenazone and 2,4,6-triiodo-3-hydroxybezoic acid, reacts to form quinone imine chromogen, the colour intensity of which is directly proportional to the amount of creatinine in the sample [150]. Figure 3 shows the reactions involved in the measurement of creatinine. This assay is calibrated in regular intervals using a 2-point calibration with Calibrator for Automated Systems as calibrator material and the measurement method is traceable to the isotope dilution mass spectrometry [150]. Quality controls are measured multiple times throughout the day using the materials Liquichek Urine Chemistry Control Levels 1 and 2 (Bio-Rad Laboratories GmbH, Feldkirchen, Germany) in adherence with the German Medical Association's Guideline on Quality Assurance in Medical Laboratory Examinations—Rili-BAEK, the permissible deviation of a control sample being ±12% from the target value [151]. The range of measurement of the assay is 1.1–610 mg/dL [150]. Values above this range can be automatically diluted 1:2.5 through a rerun function [150]. The intra- and inter-assay precision of the assay at various concentrations of UCr was tested by the manufacturer on the c 701 module [150]. The intra-assay CV ranged from 0.5% to 0.9%, whereas the inter-assay CV ranged from 1.4% to 1.5% as stated by the test manufacturer based on materials for quality controls and human urine samples in differing concentrations [150] (Supplementary Table 2).

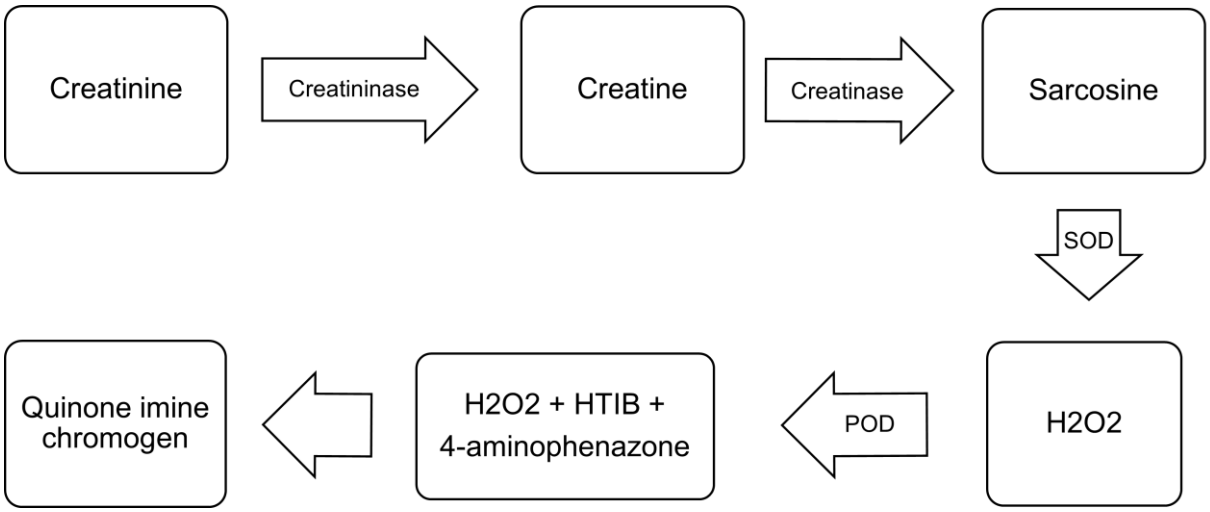


Figure 3: Enzymatic method for the measurement of UCr. At the start, creatininase converts creatinine into creatine, following which, sarcosine is formed from creatine under the action of creatinase. Sarcosine oxidase (SOD) then converts sarcosine to hydrogen peroxide (H_2O_2), glycine, and formaldehyde. In the next step, under the influence of peroxidase (POD), a reaction takes place between H2O2, 4-aminophenazone, and 2,4,6-triiodo-3-hydroxybezoic acid (HTIB), leading to the formation of quinone imine chromogen. The colour intensity of this chromogenic product is measured in the last step. Figure created in "Microsoft PowerPoint" using information from [150].

2.5 Pilot-Project

As none of the samples had been previously analysed for UCP and UCr following collection, 24 urine samples collected from GDS participants with T2DM (at baseline or during follow-up visits) from 2011 to 2022 were measured to ascertain the presence of UCP and UCr. The samples had been stored under identical conditions as the main cohort, i.e. frozen immediately after collection. They were transferred to the Central Laboratory in the same way described above and measured for UCP and UCr, before the measurement of the 680 urine samples. Only after a measurable presence of these two parameters was detected in these 24 samples did the actual study begin. This pilot-project took place in May 2023 at the Central Laboratory.

2.6 Stability-Testing

The stability of UCP and UCr was tested at room temperature for a total period of 96 hours, with both analytes being measured at 0 hours (baseline value) and every 24 hours up to 96 hours. For this purpose, leftover samples from 21 participants with T2DM, which had been stored frozen after the initial measurement of UCP and UCr, were randomly selected. The samples were passively thawed to room temperature,

immediately transferred to false bottom tubes (13 x 75 mm, 2.5 mL; RD Standard False Bottom Tubes, Roche Diagnostics, Mannheim, Germany), centrifuged (3309×*g*, 7 minutes) and measured for UCP and UCr, which constituted the baseline values (0 hours). The samples were then kept at room temperature (21 °C–25 °C), although no continuous temperature monitoring was performed, and were re-measured every 24 hours up to 96 hours. The use of false bottom tubes, which have a smaller residual (dead) volume than the original tubes, enabled the limited remaining sample volume to be utilized for analysis.

Parallel to this experiment, freeze-thaw stability was assessed using leftover samples from a further 20 participants with T2DM that had been stored frozen after the initial measurement. These samples were passively thawed to room temperature, immediately transferred to false-bottom tubes, centrifuged (3309×*g*, 7 minutes), and measured for UCP and UCr. As the false bottom tubes were not intended for storage at -20 °C, the samples were transferred back to the original tubes and refrozen. A total of four freeze-thaw cycles were carried out over five days, and the samples were measured for both the analytes after every cycle.

2.7 Statistical Analysis

Statistical analyses were performed using measured UCP and UCr data together with participant-specific data provided by the GDS. These included age at diagnosis, sex, BMI, SCP, plasma glucose and HbA1c values collected at the first visit. Details regarding the measurement platforms used in the GDS are provided elsewhere [148]. Furthermore, HOMA2-B, HOMA2-S and cluster assignments based on the original Ahlqvist classification were also obtained from the GDS. UCPCR (nmol/mmol) was calculated from UCP (1 nmol/L = 3 µg/L) and UCr (1 mmol/L = 11.3 mg/dL) according to the conversion factors stated by the test manufacturer [76, 100, 150].

Non-normally distributed data is depicted through median and interquartile range (IQR). Comparison of groups was carried out using the Mann-Whitney U test or Kruskal-Wallis test for continuous variables, and the Pearson's chi-squared test for categorical variables. The stability of UCP, UCPCR and UCr at -20 °C over a period of ten years was assessed with a generalized linear regression model. Linear mixed-effects models were used to assess the overall time-dependant changes in UCP, UCPCR and UCr at room temperature and across freeze-thaw cycles. Both

random intercept and random slope and intercept models were fitted, accounting for individual variation across participants. In addition, mean percentage changes relative to baseline were calculated at every measurement time point and the corresponding 95% confidence interval (CI) was compared against a predefined ±10% threshold of clinical stability.

UCP/UCPCR was correlated to SCP using Spearman's rank correlation. HOMA2 indices were predicted using UCP in two steps. Firstly, mixed linear models were applied to predict SCP using UCP, age at diagnosis, sex, and BMI as predictors, following which predicted SCP was correlated to measured SCP with the help of Spearman's rank correlation. Subsequently, HOMA2 indices (HOMA2-S and HOMA2-B) were calculated using the predicted SCP values with the help of the HOMA calculator (University of Oxford, Oxford, UK) [52] and compared with their counterparts derived from measured SCP values using Spearman's rank correlation. Correlation and regression analyses were performed on complete-case data.

To evaluate the ability of UCP to classify diabetes subtypes, UCP, together with age at diagnosis, sex, and BMI (values scaled and centred), was used as input for a multinomial logistic regression model. The dataset was randomly divided into training and testing sets in an 80:20 ratio, and the subtypes predicted using UCP were compared with the subtype assignments based on the original Ahlqvist algorithm, which uses a nearest centroid approach [144, 146]. In this machine-learning approach, the cluster assignment takes place as per the clusters' centroid, where the distance of a particular individual to all cluster centroids is computed using all the provided data and the individual is assigned to the cluster with the minimum distance [144, 152]. Recently, an online tool has been developed by the DDZ, which, after providing all the necessary input, shows a graphical representation of the cluster probability of an individual [152].

P-values reported were two-tailed with a significance level of $\alpha = 0.05$. The entire statistical analysis was carried out using the statistics software "R" version 4.5.1 (R Foundation for Statistical Computing, Vienna, Austria) [153].

3 Results

3.1 Baseline Characteristics

Baseline characteristics of study participants in the NGT group (n = 192) and in the newly diagnosed T2DM group (n = 488) are shown in Table 3, whereas the distribution of missing values across variables is detailed in Supplementary Table 3. Participants in the T2DM group were older, had a higher BMI, and displayed higher fasting blood glucose levels as well as higher levels of SCP and UCP compared to those in the NGT group (all $p < 0.001$). The T2DM group was marked with a higher insulin resistance and a poorer β-cell function in comparison with the NGT group. No statistically significant difference was seen at the levels of UCr.

Baseline characteristics of study participants stratified as per the Ahlqvist classification are shown in Table 4, and the proportions of missing data for each variable are shown in Supplementary Table 4. Participants classified as SIDD were leaner, exhibited the highest fasting glucose levels, with β-cell function being the poorest among the subgroups. SIRD participants demonstrated a pronounced insulin resistance with an increased HOMA2-B, had a higher BMI, and the highest levels of SCP and UCP. MOD participants showed the highest BMI but comparatively lower levels of insulin resistance and UCP as compared to the SIRD subgroup, whereas MARD participants were older with generally milder metabolic disturbances.

Table 3: Baseline characteristics of study participants.

	NGT	T2DM	p-value
Number of participants	192	488	
Age (years)	47.0 (30.3, 55.6)	52.6 (45.4, 59.8)	< 0.001
Sex (males %)	120 (62.5%)	317 (65.0%)	0.608
BMI (kg/m^2)	26.4 (23.4, 29.4)	30.4 (26.4, 34.4)	< 0.001
Fasting SCP (ng/mL)	1.6 (1.2, 2.2)	2.9 (2.0, 4.0)	< 0.001
Fasting UCP (µg/L)	26.5 (13.9, 41.2)	32.1 (16.0, 61.7)	0.001
Fasting UCr (mg/dL)	119.9 (74.3, 181.3)	115.2 (76.9, 158.0)	0.377
Fasting UCP (nmol/L)	8.8 (4.6, 13.7)	10.7 (5.3, 20.6)	0.001
Fasting UCr (mmol/L)	10.6 (6.6, 16.0)	10.2 (6.8, 14.0)	0.377
UCPCR (nmol/mmol)	0.9 (0.5, 1.3)	1.2 (0.6, 1.9)	< 0.001
HOMA2-S	88.4 (65.0, 111.9)	42.4 (31.0, 60.7)	< 0.001
HOMA2-B	110.3 (95.3, 133.9)	97.7 (69.4, 135.5)	< 0.001
Fasting blood glucose (mg/dL)	88.0 (84.0, 92.8)	118.0 (102.0, 137.0)	< 0.001

Table 3: Baseline characteristics of study participants. Data are presented as n (%) for categorical variables and median (IQR) for continuous variables. *NGT* normal glucose tolerance, *T2DM* type 2 diabetes, *BMI* body mass index, *SCP* serum C-peptide, *UCP* urinary C-peptide, *UCr* urinary creatinine, *UCPCR* urinary C-peptide-to-creatinine ratio, *HOMA2-S* homeostasis model assessment 2 of insulin sensitivity, *HOMA2-B* homeostasis model assessment 2 of β-cell function. *n* number of participants, *kg/m^2* kilogram per meter squared, *ng/mL* nanogram per millilitre, *µg/L* microgram per litre, *nmol/L* nanomole per litre, *mg/dL* milligram per decilitre, *mmol/L* millimole per litre, *nmol/mmol* nanomole per millimole

Table 4: Baseline characteristics of study participants with T2DM subtypes and NGT.

	NGT	SIDD	SIRD	MOD	MARD	p-value
Number of participants	192	15	72	190	211	
Age (years)	47.0 (30.3, 55.6)	47.5 (34.5, 51.5)	59.5 (54.5, 64.3)	45.6 (38.7, 51.0)	57.1 (52.0, 62.8)	< 0.001
Sex (males %)	120 (62.5%)	12 (80.0%)	52 (72.2%)	95 (50.0%)	158 (74.9%)	< 0.001
BMI (kg/m^2)	26.4 (23.4, 29.4)	27.8 (25.1, 28.9)	33.4 (31.8, 36.7)	34.1 (30.7, 37.3)	26.9 (24.4, 29.3)	< 0.001
Fasting SCP (ng/mL)	1.6 (1.2, 2.2)	2.3 (1.5, 3.4)	5.1 (4.0, 6.1)	3.3 (2.4, 4.1)	2.3 (1.6, 3.0)	< 0.001
Fasting UCP (µg/L)	26.5 (13.9, 41.2)	34.1 (27.5, 53.3)	45.4 (24.2, 81.8)	28.0 (14.9, 57.3)	29.5 (14.8, 57.6)	< 0.001
Fasting UCr (mg/dL)	119.9 (74.3, 181.3)	141.5 (117.4, 202.6)	133.7 (87.6, 178.0)	115.4 (73.6, 160.9)	110.5 (72.7, 145.6)	0.014
Fasting UCP (nmol/L)	8.8 (4.6, 13.7)	11.4 (9.2, 17.8)	15.1 (8.1, 27.3)	9.3 (5.0, 19.1)	9.8 (4.9, 19.2)	< 0.001
Fasting UCr (mmol/L)	10.6 (6.6, 16.0)	12.5 (10.4, 17.9)	11.8 (7.8, 15.8)	10.2 (6.5, 14.2)	9.8 (6.4, 12.9)	0.014
UCPCR (nmol/mmol)	0.9 (0.5, 1.3)	1.1 (0.6, 1.4)	1.6 (0.8, 2.6)	1.1 (0.5, 1.8)	1.2 (0.7, 1.9)	< 0.001
HOMA2-S	88.4 (65.0, 111.9)	40.9 (33.0, 65.4)	26.5 (20.7, 33.8)	36.7 (28.2, 51.9)	53.1 (42.5, 74.5)	< 0.001
HOMA2-B	110.3 (95.3, 133.9)	42.2 (25.2, 51.1)	172.2 (140.9, 211.5)	102.4 (76.8, 135.4)	84.7 (61.8, 109.7)	< 0.001
Fasting blood glucose (mg/dL)	88.0 (84.0, 92.8)	195.5 (162.5, 222.5)	107.0 (89.8, 119.0)	122.0 (104.0, 141.0)	117.0 (102.0, 133.5)	< 0.001

Table 4: Baseline characteristics of study participants with T2DM subtypes and NGT. Data are presented as n (%) for categorical variables and median (IQR) for continuous variables. *NGT* normal glucose tolerance, *T2DM* type 2 diabetes, *SIDD* severe insulin-deficient diabetes, *SIRD* severe insulin-resistant diabetes, *MOD* mild obesity-related diabetes, *MARD* mild age-related diabetes, *BMI* body mass index, *SCP* serum C-peptide, *UCP* urinary C-peptide, *UCr* urinary creatinine, *UCPCR* urinary C-peptide-to-creatinine ratio, *HOMA2-S* homeostasis model assessment 2 of insulin sensitivity, *HOMA2-B* homeostasis model assessment 2 of β-cell function. *n* number of participants, *kg/m^2* kilogram per meter squared, *ng/mL* nanogram per millilitre, *µg/L* microgram per litre, *nmol/L* nanomole per litre, *mg/dL* milligram per decilitre, *mmol/L* millimole per litre, *nmol/mmol* nanomole per millimole

3.2 Stability of Urinary C-peptide under various storage conditions

3.2.1 Long-term Storage at -20 °C

A generalized linear model showed no evidence of degradation in UCP (Figure 4), UCr (Supplementary Figure 1) or UCPCR (Figure 5) levels over more than 10 years of storage at -20 °C in participants with either NGT (UCP: β = 0.95, p = 0.41; UCr: β = 0.36, p = 0.90; UCPCR: β = 0.02, p = 0.39) or T2DM (UCP: β = -1.59, p = 0.08; UCr: β = -0.41, p = 0.73; UCPCR: β = -0.03, p = 0.26). Even in the pilot-project, a linear regression analysis showed no significant association between storage time and UCPCR concentrations (β = -1.73, p = 0.58).

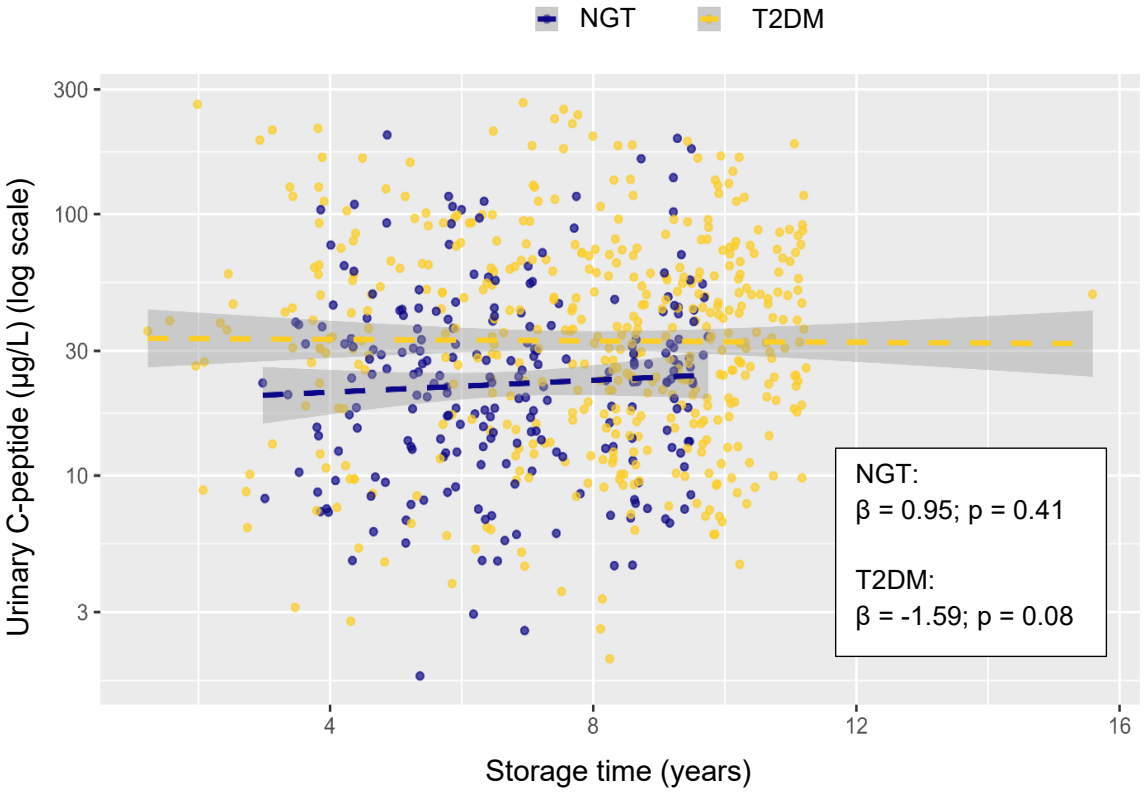


Figure 4: Effect of time on stability of UCP at -20 °C. Scatter plot showing log-transformed UCP (µg/L) on the Y-axis versus elapsed storage time at -20 °C on the X-axis. Group-specific regression lines (dashed) with 95% confidence intervals are shown, with the blue regression line representing participants with NGT and the yellow regression line representing participants with T2DM. Blue and yellow points correspond to individual measurements of participants with NGT and T2DM respectively. A generalized linear model was used. n (total) = 680, NGT: n = 192, β = 0.95, p = 0.41; T2DM: n = 488, β = -1.59, p = 0.08. The figure was created using the software "R". *n* number of participants, *µg/L* microgram per litre

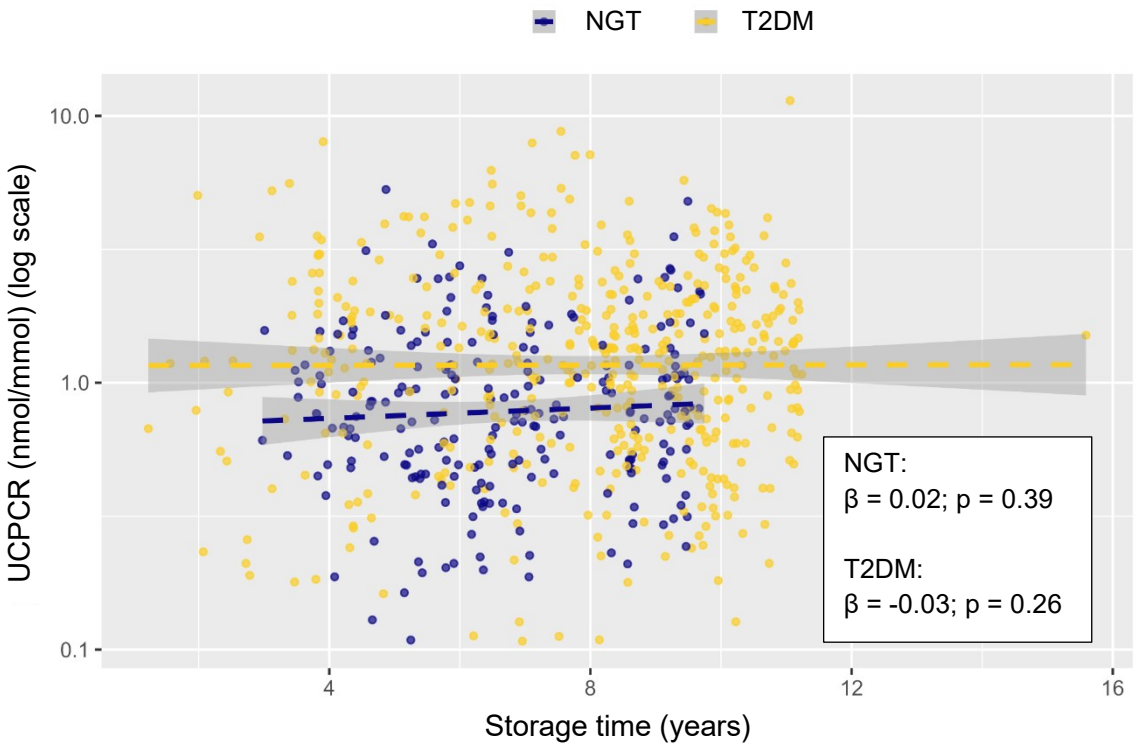


Figure 5: Effect of time on stability of UCPCR at -20 °C. Scatter plot showing log-transformed UCPCR (nmol/mmol) on the Y-axis versus elapsed storage time at -20 °C on the X-axis. Group-specific regression lines (dashed) with 95% confidence intervals are shown, with the blue regression line representing participants with NGT and the yellow regression line representing participants with T2DM. Blue and yellow points correspond to individual measurements of participants with NGT and T2DM respectively. A generalized linear model was used. n (total) = 680; NGT: n = 192, β = 0.02, p = 0.39; T2DM: n = 488, β = -0.03, p = 0.26. The figure was created using the software "R". *n* number of participants, *UCPCR* urinary C-peptide-to-creatinine ratio *nmol/mmol* nanomole per millimole

3.2.2 Stability at Room Temperature

When samples were stored at room temperature for up to 96 hours, a linear mixed-effects model with random slope and intercept demonstrated no evidence of a significant time-dependent change in UCP (β = 0.13, 95% CI -1.06 to 1.32, p = 0.83, Figure 6) and UCPCR (β = -0.05, 95% CI -0.11 to 0.02, p = 0.14, Figure 7) concentrations. In contrast, UCr showed a small but statistically significant increase over time (β = 2.40, 95% CI 0.32 to 4.48, p = 0.024, Supplementary Figure 2).

When considering the predefined threshold of ±10% for clinical stability, UCP and UCPCR remained within acceptable limits for up to 48 hours with a mean change of -2.1% (95% CI -7.6% to 3.5%) for UCP and -3.7% (95% CI -8.6% to 1.3%) for UCPCR at 48 hours. By 72 hours, the 95% CI of the mean percentage change exceeded the threshold limit (for UCP: mean change = -4.8%, 95% CI -15.0% to 5.5%; for UCPCR: mean change = -8.2%, 95% CI -17.4% to 1.1%). In contrast, UCr

concentrations remained within limits for up to 72 hours (mean change = 3.5%, 95% CI -0.3% to 7.4%), whereas the threshold was exceeded at 96 hours (mean change = 8.0%, 95% CI 1.7% to 14.2%). The mean percentage changes with 95% CI are depicted in Figure 8.

Although no consistent time-dependent change was observed in the mixed-effects models, variability increased at later time points (Figure 9). For UCP, 6/21 samples showed bidirectional deviations exceeding ±25% at 96 hours, whereas for UCr, 3/21 samples showed increases in UCr concentrations > 20% at 72 hours and a further 3/21 exceeded 25% at 96 hours.

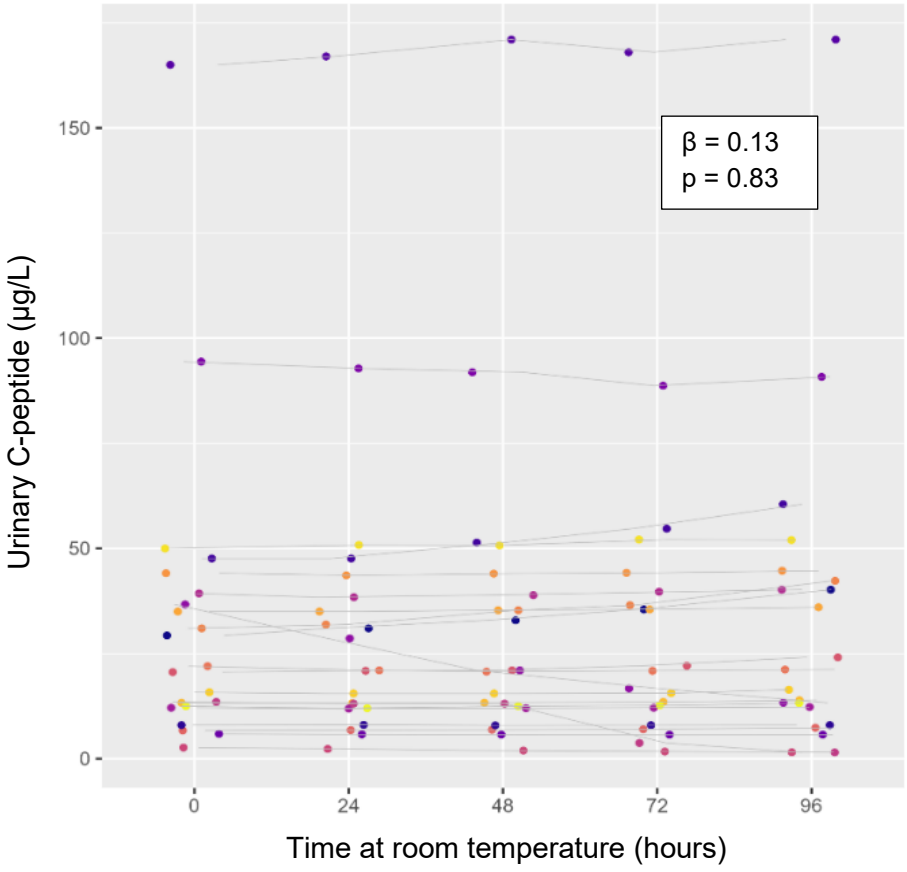


Figure 6: Stability of UCP at room temperature over 96 hours. Spaghetti plot showing individual longitudinal trajectories of UCP concentrations (µg/L, Y-axis) over time (hours) at room temperature (X-axis). Each point represents a single measurement, and lines connect repeated measurements from the same participant across time points. A linear mixed-effects model with random slope and intercept was used. n (participants) = 21, n (measurements) = 105, β = 0.13, 95% CI -1.06 to 1.32, p = 0.83. The figure was created using the software "R". *µg/L* microgram per litre

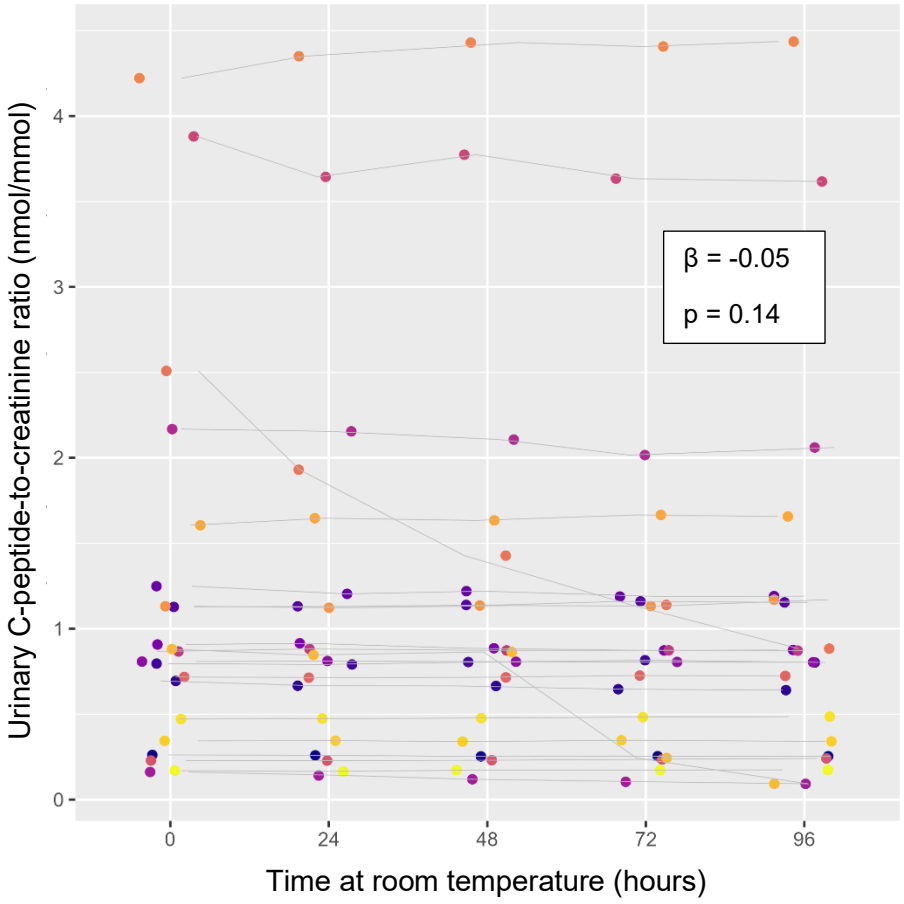


Figure 7: Stability of UCPCR at room temperature over 96 hours. Spaghetti plot showing individual longitudinal trajectories of UCPCR concentrations (nmol/mmol, Y-axis) over time (hours) at room temperature (X-axis). Each point represents a single measurement, and lines connect repeated measurements from the same participant across time points. A linear mixed-effects model with random slope and intercept was used. n (participants) = 21, n (measurements) = 105, β = -0.05, 95% CI -0.11 to 0.02, p = 0.14. The figure was created using the software "R". *nmol/mmol* nanomole per millimole

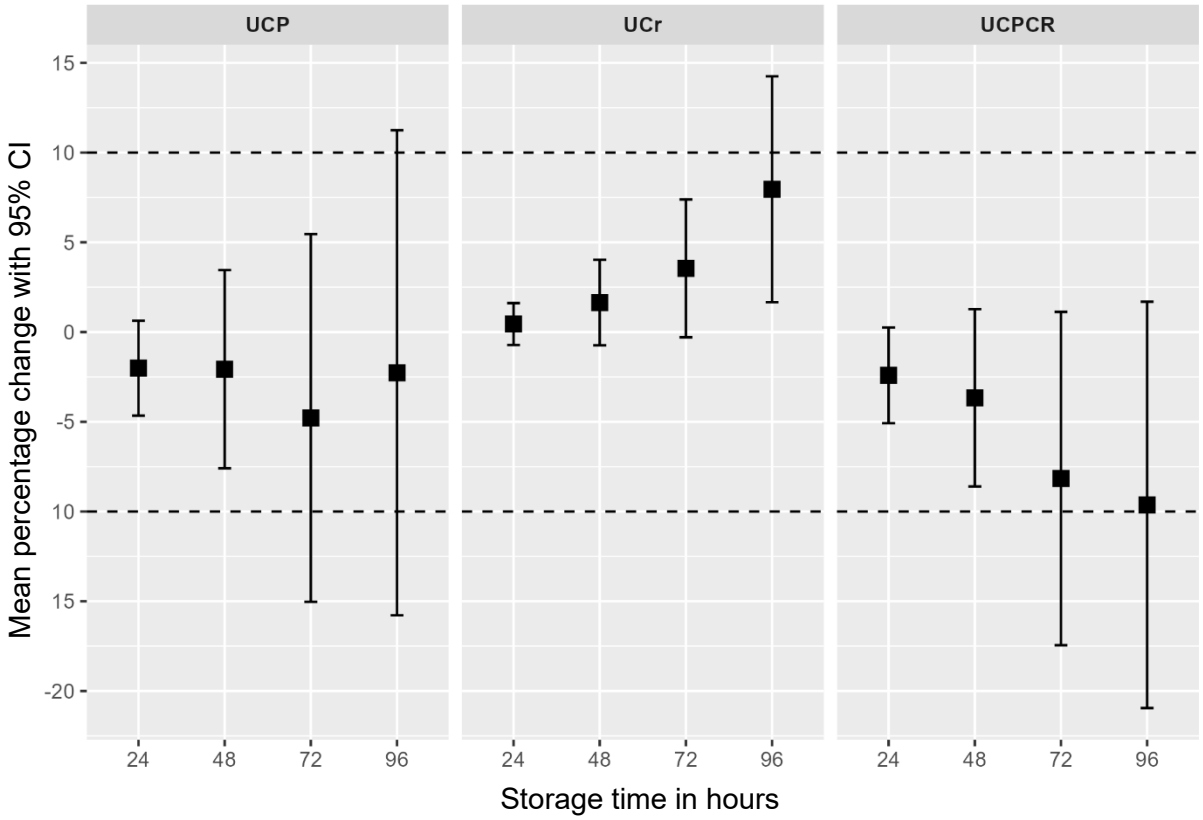


Figure 8: Mean percentage change with 95% CI from baseline for UCP, UCr and UCPCR during storage at room temperature over 96 hours. Black squares represent the mean percentage change relative to the baseline (Y-axis) across storage time in hours (X-axis) with whiskers depicting the respective 95% CI. The dashed lines represent the stability threshold at ±10%. For UCP, UCPCR and UCr: n (participants) = 21, n (measurements every 24 hours) = 21. The figure was created using the software "R". *UCP* urinary C-peptide, *UCr* urinary creatinine, *UCPCR* urinary C-peptide-to-creatinine ratio, *CI* confidence interval

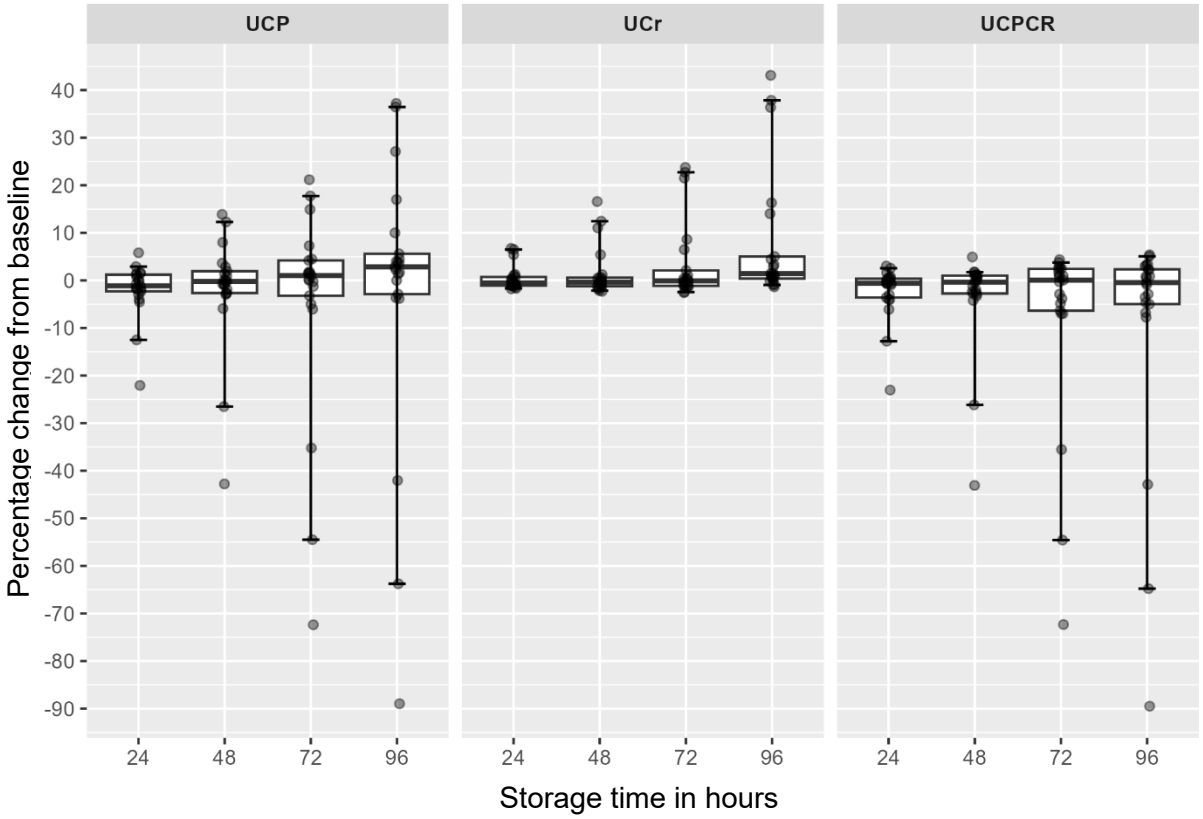


Figure 9: Spread of percentage changes from baseline for UCP, UCr and UCPCR during storage at room temperature over 96 hours. Box plots represent median (horizontal line) with IQR of percentage changes from baseline (Y-axis) across storage time in hours (X-axis). Whiskers represent the 5th to 95th percentiles and each grey dot corresponds to the percentage change of an individual measurement. For UCP, UCPCR and UCr: n (participants) = 21, n (measurements every 24 hours) = 21. The figure was created using the software "R". *UCP* urinary C-peptide, *UCr* urinary creatinine, *UCPCR* urinary C-peptide-to-creatinine ratio

3.2.3 Stability during Multiple Freeze-Thaw Cycles

Across four freeze-thaw cycles, a linear mixed-effects model with random slope and intercept showed a small but statistically significant time-dependent change in UCP (β = -0.64, 95% CI -0.93 to -0.35, p < 0.001; Figure 10), UCPCR (β = -0.03, 95% CI -0.04 to -0.02, p < 0.001; Figure 11) and UCr (β = 1.81, 95% CI 1.28 to 2.33, p < 0.001; Supplementary Figure 3) concentrations. This corresponds to a relative change per freeze-thaw cycle of 2.13% for UCP, 4.34% for UCPCR and 1.17% for UCr, calculated by relating the model-estimated change (β) to the overall mean concentration across all measurements.

Despite statistical significance in the mixed-effects model, UCP remained within the predefined clinically acceptable limits of ±10% for up to three freeze-thaw cycles with the mean percentage change after the third cycle being -6.3% (95% CI -8.9% to -3.8%).

After the fourth cycle, the threshold was not maintained (mean change = -9.8%, 95% CI -13.3% to -6.3%). However, UCPCR maintained the predefined limits for only up to two cycles (mean change after the third cycle = -9.5%, 95% CI -11.8% to -7.2%). In contrast, UCr maintained the threshold limits across all four freeze-thaw cycles. Mean percentage changes with 95% CI are depicted in Figure 12.

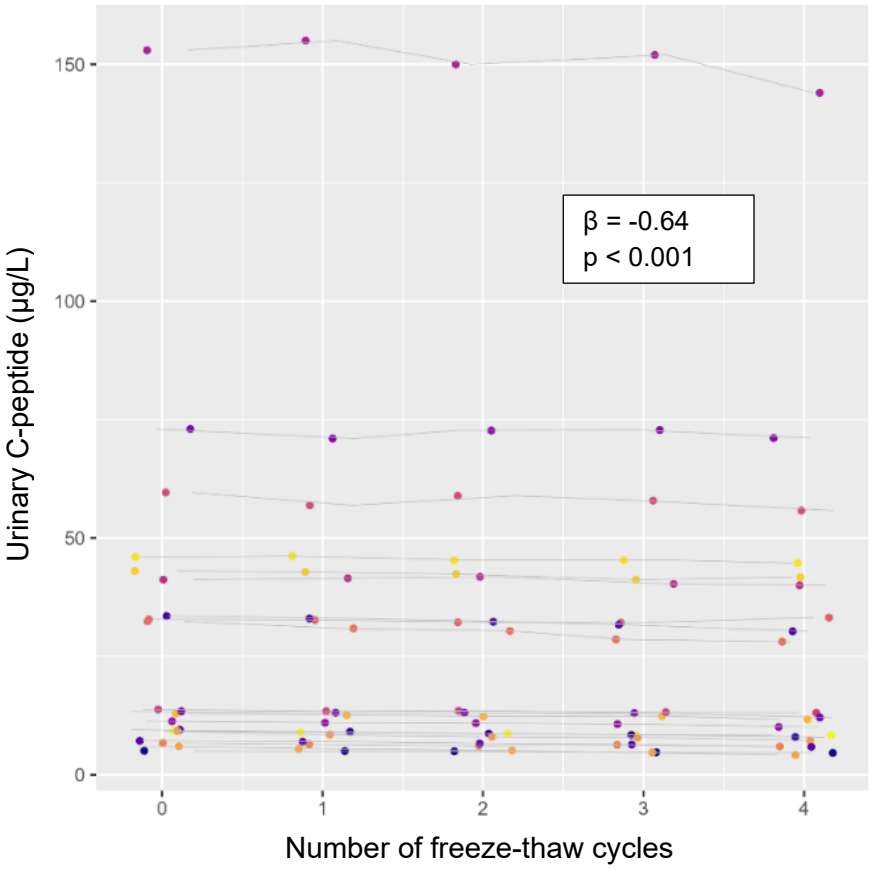


Figure 10: Stability of UCP across four freeze-thaw cycles. Spaghetti plot showing individual UCP concentrations (µg/L, Y-axis) measured across repeated freeze-thaw cycles (X-axis). Each point represents a single measurement, and lines connect repeated measurements from the same participant across cycles. A linear mixed-effects model with random slope and intercept was used. n (participants) = 20, n (measurements) = 100, β = -0.64, 95% CI -0.93 to -0.35, p <0.001. The figure was created using the software "R". *µg/L* microgram per litre

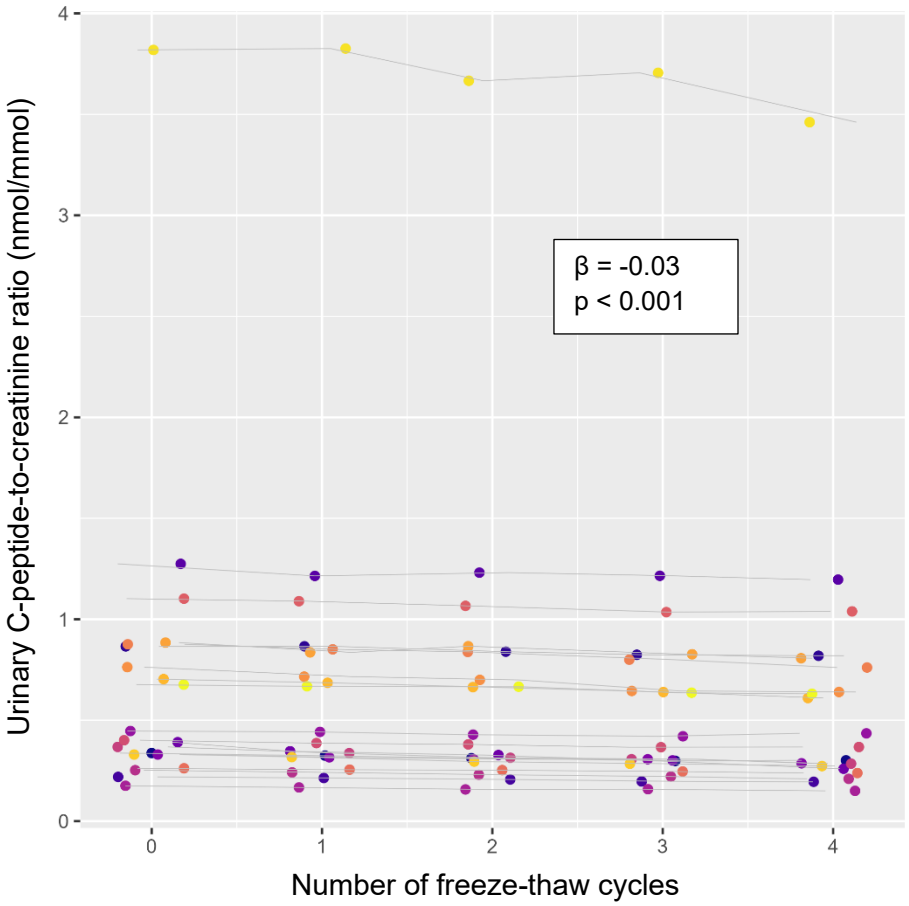


Figure 11: Stability of UCPCR across four freeze-thaw cycles. Spaghetti plot showing individual UCPCR concentrations (nmol/mmol, Y-axis) measured across repeated freeze-thaw cycles (X-axis). Each point represents a single measurement, and lines connect repeated measurements from the same participant across cycles. A linear mixed-effects model with random slope and intercept was used. n (participants) = 20, n (measurements) = 100, β = -0.03, 95% CI -0.04 to -0.02, p <0.001. The figure was created using the software "R". *nmol/mmol* nanomole per millimole

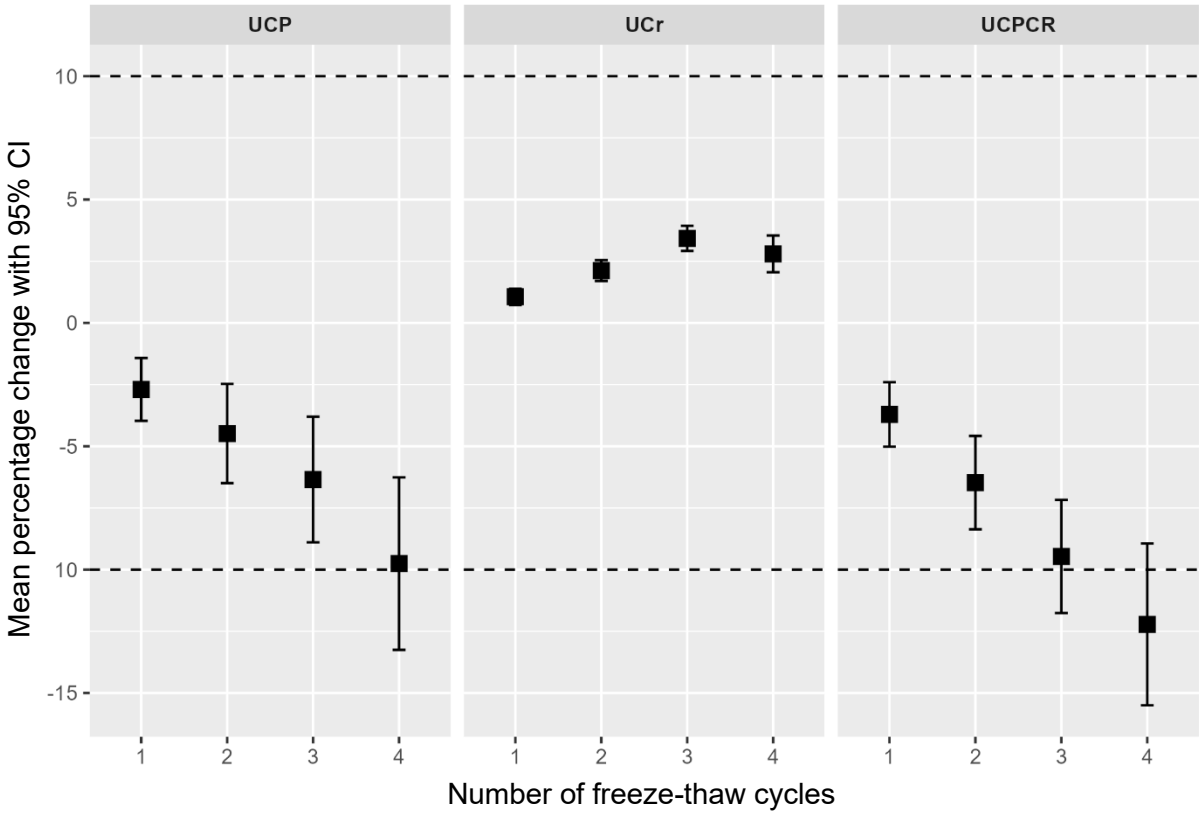


Figure 12: Mean percentage change with 95% CI from baseline for UCP, UCr and UCPCR across four freeze-thaw cycles. Black squares represent the mean percentage change relative to the baseline (Y-axis) across four freeze-thaw cycles (X-axis) with whiskers depicting the respective 95% CI. The dashed lines represent the stability threshold at ±10%. For UCP, UCPCR and UCr: n (participants) = 20, n (measurements after every freeze-thaw cycle) = 20. The figure was created using the software "R". *UCP* urinary C-peptide, *UCr* urinary creatinine, *UCPCR* urinary C-peptide-to-creatinine ratio, *CI* confidence interval

3.3 Relationship between Urinary C-peptide and Serum C-peptide

NGT and T2DM participants taken together, UCP and SCP moderately correlated with each other (Spearman's ρ = 0.32, p < 0.001; Figure 13) and so did UCPCR and SCP (Spearman's ρ = 0.30, p < 0.001; Figure 14).

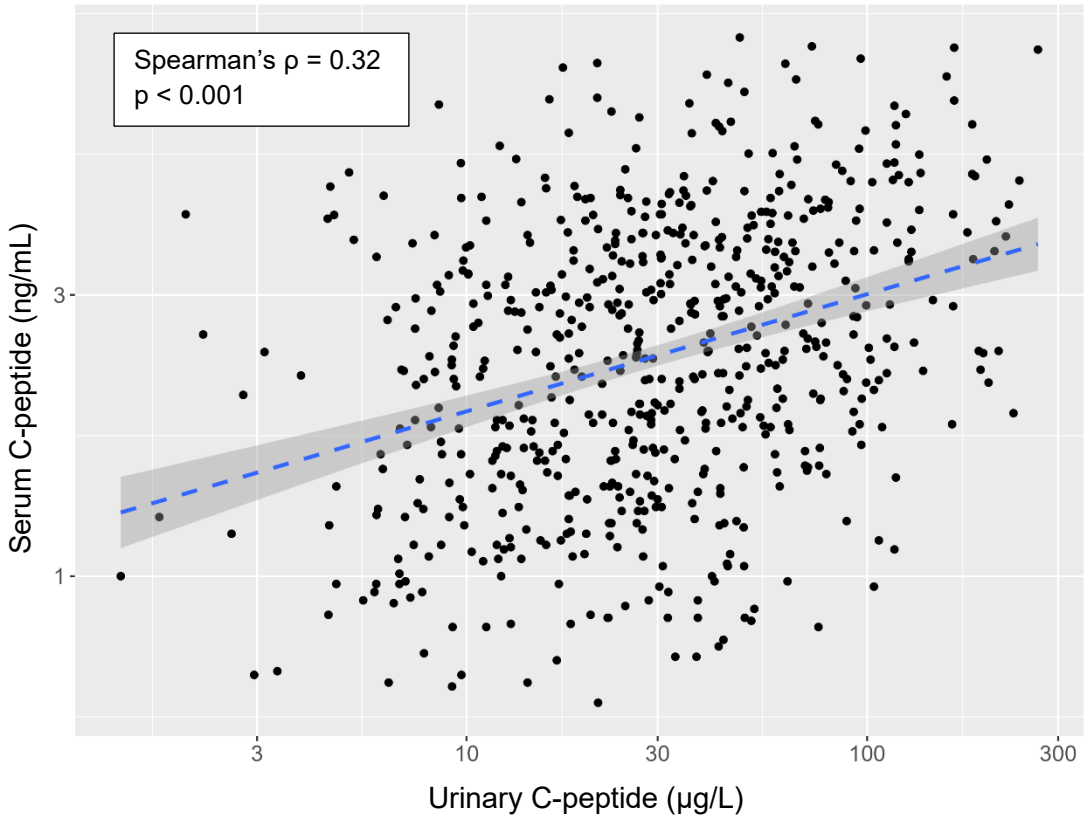


Figure 13: Correlation between UCP and SCP. Scatter plot showing the association between UCP in µg/L (X-axis) and SCP in ng/mL (Y-axis). The blue dashed line represents the regression line with 95% confidence interval. n (participants) = 642, Spearman's ρ = 0.32, p < 0.001. X- and Y-axes are log-scaled. The figure was created using the software "R". *µg/L* microgram per litre, *ng/mL* nanogram per millilitre

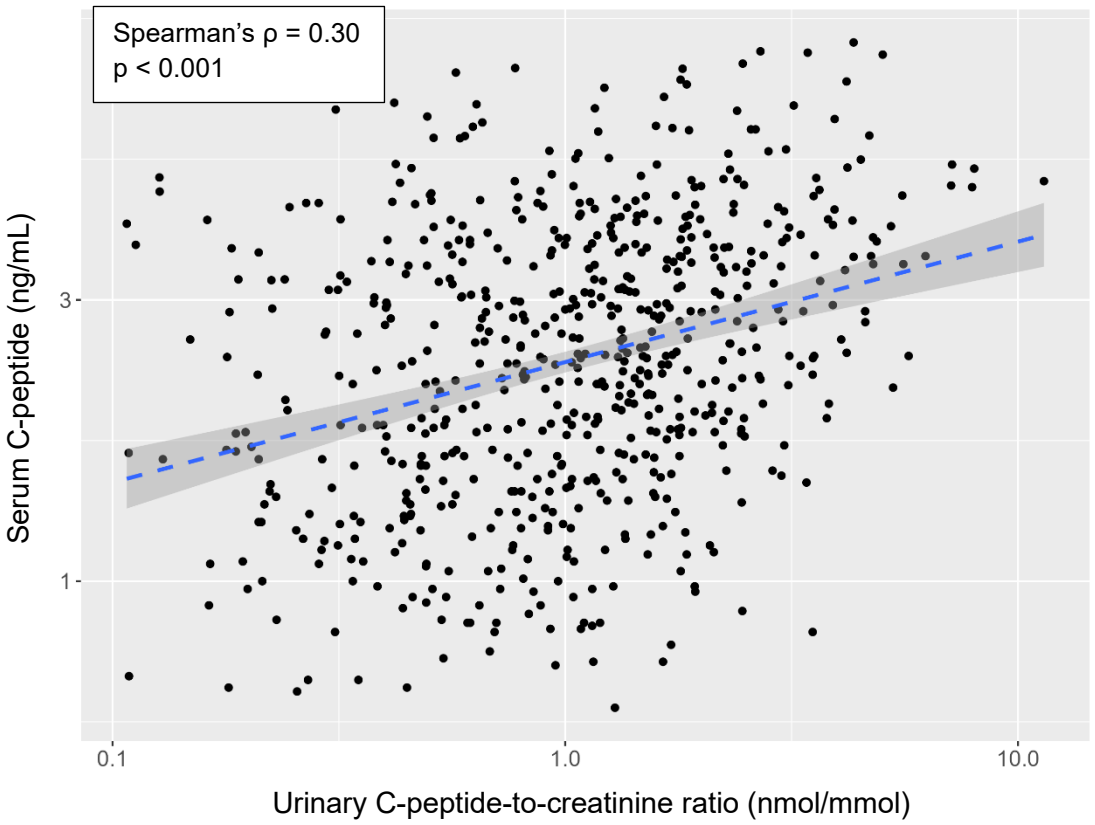


Figure 14: Correlation between UCPCR and SCP. Scatter plot showing the association between UCPCR in nmol/mmol (X-axis) and SCP in ng/mL (Y-axis). The blue dashed line represents the regression line with 95% confidence interval. X- and Y-axes are log-scaled. n (participants) = 642, Spearman's ρ = 0.30, p < 0.001. The figure was created using the software "R". *ng/mL* nanogram per millilitre, *nmol/mmol* nanomole per millimole

3.4 Prediction of Serum C-peptide and HOMA2 Indices

Prediction of HOMA2 indices from UCP was performed in a two-step process for NGT and T2DM participants together. First, SCP values were predicted using the variables UCP, age at diagnosis, sex, and BMI. In the next step, the predicted SCP values were used to calculate the HOMA2 indices.

Predicted SCP derived from UCP, age at diagnosis, sex, and BMI strongly correlated with measured SCP (Spearman's ρ = 0.78, p < 0.001; Figure 15). Predicted HOMA2-S and HOMA2-B, calculated using predicted SCP values, also correlated strongly with their counterparts derived using measured SCP (Spearman's ρ = 0.81 for HOMA2-S, p < 0.001; Spearman's ρ = 0.80 for HOMA2-B, p < 0.001; Figures 16 and 17).

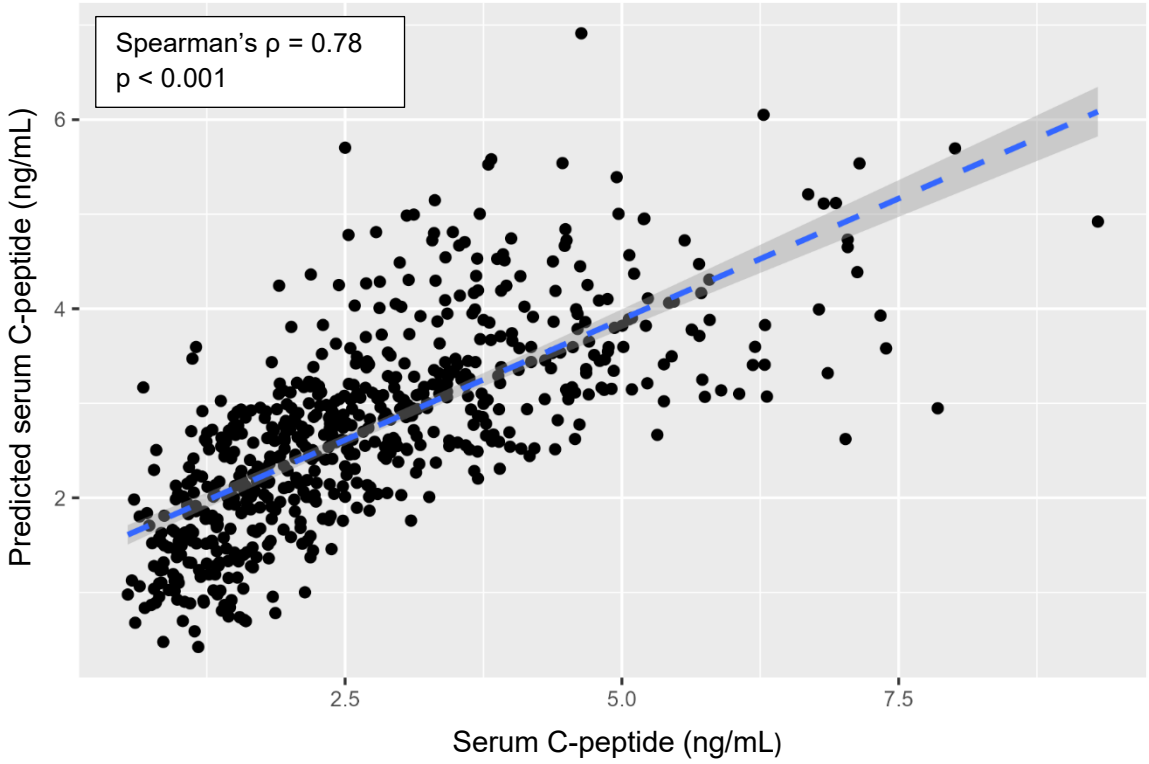


Figure 15: Correlation between predicted SCP and measured SCP. Scatter plot showing the association between measured SCP in ng/mL (X-axis) and predicted SCP in ng/mL (Y-axis). The blue dashed line represents the regression line with 95% confidence interval. n (participants) = 642, Spearman's ρ = 0.78, p < 0.001. The figure was created using the software "R". *ng/mL* nanogram per millilitre

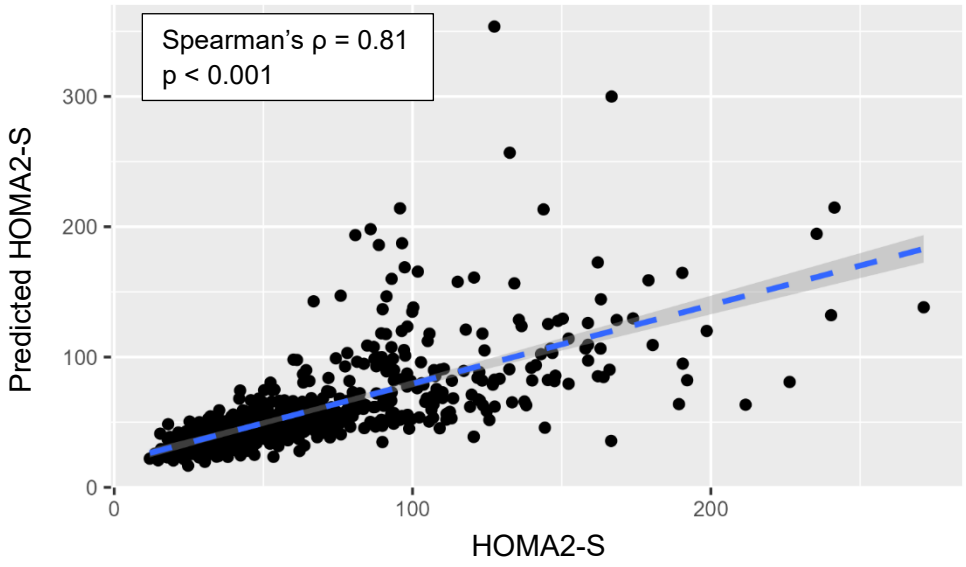


Figure 16: Correlation between predicted HOMA2-S and HOMA2-S. Scatter plot showing the association between HOMA2-S values derived from measured SCP (X-axis) and HOMA2-S values derived from predicted SCP values (Y-axis). The blue dashed line represents the regression line with 95% confidence interval. n (participants) = 642, Spearman's ρ = 0.81, p < 0.001. The figure was created using the software "R". *HOMA2-S* homeostasis model assessment 2 of insulin sensitivity

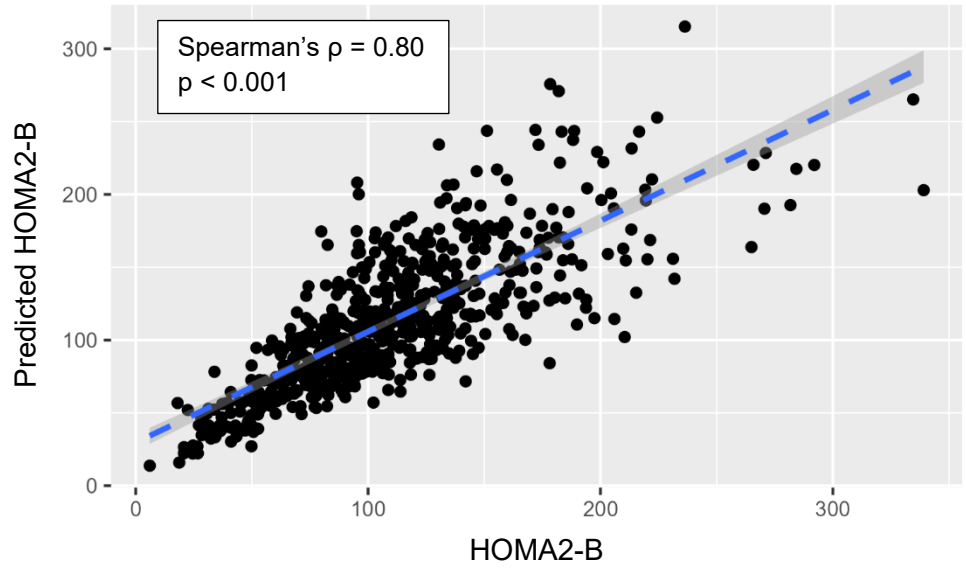


Figure 17: Correlation between predicted HOMA2-B and HOMA2-B. Scatter plot showing the association between HOMA2-B values derived from measured SCP (X-axis) and HOMA2-B values derived from predicted SCP values (Y-axis). The blue dashed line represents the regression line with 95% confidence interval. n (participants) = 642, Spearman's ρ = 0.80, p < 0.001. The figure was created using the software "R". *HOMA2-B* homeostasis model assessment 2 of β-cell function

3.5 Cluster Analysis

A multinomial logistic regression model was used to determine whether UCP-based measures could classify T2DM participants into the four established T2DM subtypes. Model variables included UCP, age at diagnosis, sex, and BMI. The receiver operating characteristic (ROC) curves are shown in Figure 18. The model was trained on 80% of the dataset and tested on the remainder. Cluster analysis was restricted to study participants with complete data required for the prediction models and all the model variables were centred and scaled during pre-processing. Number of cases used in the training set and the test set are shown in Table 5.

Table 5: Number of cases for the training set and test set of the model.

T2DM subtype	$n_{\text{Training set}}$ (80%)	$n_{\text{Test set}}$ (20%)
SIDD	12	3
SIRD	40	10
MOD	124	31
MARD	145	36

Table 5: Number of cases for the training set and test set of the model. *T2DM* type 2 diabetes, *SIDD* severe insulin-deficient diabetes, *SIRD* severe insulin-resistant diabetes, *MOD* mild obesity-related diabetes, *MARD* mild age-related diabetes. *n* number of participants

Overall model performance showed an accuracy of 77.5% (95% CI 66.8% to 86.1%), exceeding the no-information rate of 45% ($p < 0.001$). Agreement between predicted and original subtypes was substantial (Cohen's $\kappa = 0.62$).

The highest discriminative performance, as depicted by the AUC, was observed for the mild subgroups:

- MOD**:** AUC 0.96
- MARD**:** AUC 0.96
- SIDD: AUC 0.93
- SIRD: AUC 0.81

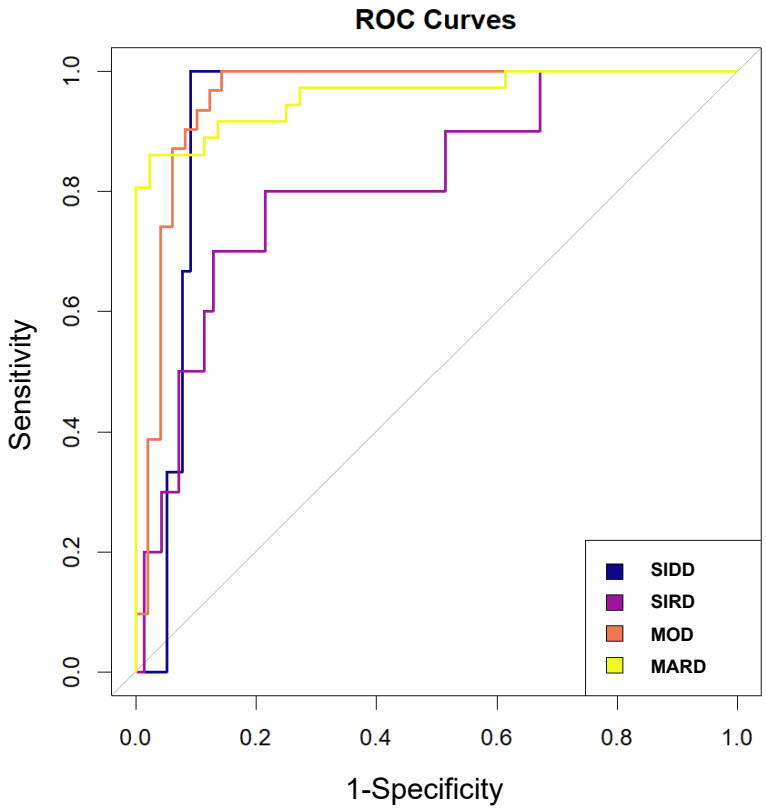


Figure 18: ROC curves for the multinomial prediction model predicting T2DM subtypes. ROC curves are shown for four predicted T2DM subtypes: SIDD (blue), SIRD (purple), MOD (orange), and MARD (yellow). Overall accuracy of the model was 77.5% (95% CI 66.8% to 86.1%), exceeding the no information rate of 45% ($p < 0.001$) with Cohen's κ being 0.62. AUC for SIDD: 0.93, for SIRD: 0.81, for MOD: 0.96, for MARD: 0.96. Variables: UCP, age at diagnosis, sex, and BMI. The figure was created using the software "R". *ROC* receiver operating characteristic, *SIDD* severe insulin-deficient diabetes, *SIRD* severe insulin-resistant diabetes, *MOD* mild obesity-related diabetes, *MARD* mild age-related diabetes

4 Discussion

The aim of this retrospective clinical study was to ascertain the feasibility of UCP as a non-invasive and stable surrogate to SCP for the assessment of insulin secretion and resistance, as well as for subtype classification in the recent-onset T2DM cohort of the GDS. To start with, a stability assessment under various storage conditions suggests no significant time-dependent change in UCP concentrations at room temperature and during frozen storage. Secondly, the data demonstrate that UCP correlates positively with SCP and allows meaningful prediction of both the HOMA2 indices. Lastly, it could be shown that in recently diagnosed diabetes, a prediction model using UCP performs well to identify the established T2DM subtypes, especially MOD and MARD, with good accuracy. The results of this thesis shall encourage to overcome the pre-analytical hurdles for clinical applicability of UCP as a non-invasive alternative to SCP, as well as allow a decentralised and at-home approach for cluster identification in future studies in T2DM.

4.1 Baseline Characteristics

When compared with other European cohorts comprising newly diagnosed T2DM participants, this subset of the GDS was broadly comparable, with participants being older and having a relatively higher BMI [144, 154-157]. A comparatively higher proportion of male participants with T2DM in the GDS has been reported previously by Szendroedi et al. [148], and this sex distribution is also reflected in the present subset.

When all T2DM participants were considered together, UCP levels were higher than those observed in participants with NGT, a finding that is consistent with observations from the Austrian BioPersMed cohort [126]. Studies examining UCP in recent-onset T2DM remain limited; however, from a pathophysiological perspective, this finding is plausible. As demonstrated in the UKPDS, β-cell function is relatively preserved in the early stages of T2DM compared with long-standing disease [158], although the precise onset of diabetes in newly diagnosed individuals cannot be determined with certainty. Another explanation to the finding above could be attributed to the observation of a higher insulin resistance in the T2DM group, which is reflected by lower levels of the HOMA2-S as compared to the NGT group, an observation which is consistent with the BioPersMed study [126]. Of note, a higher insulin resistance leads to hyperinsulinemia

[159], which could lead to higher levels of C-peptide being found in urine. Furthermore, hyperinsulinemia itself, has been proposed to have a causal relationship with the development of impaired glucose metabolism, T2DM, obesity and insulin resistance [160]. This hyperinsulinemia may arise independent to the defects in β-cell function that are otherwise commonly agreed upon to be the earliest cause for the onset of dysglycaemia [160]. To what extent does a causal hyperinsulinemia contribute towards an increase in C-peptide levels in T2DM or in some of its subtypes needs to be examined in future studies.

When the T2DM group was stratified according to the novel subclassification, the observed patterns of metabolic derangements were consistent with the expected clinical profiles of the four clusters [144]. The highest UCP levels were observed in the SIRD group, which also exhibited the highest SCP concentrations. This finding is biologically plausible, given the pronounced hyperinsulinemia associated with severe insulin resistance in this subgroup, which can be inferred from the lowest HOMA2-S values among the clusters in various cohorts [144, 157, 161]. Similar observations concerning UCPCR in the SIRD group are evident in Wang et al. in a cohort of hospitalised T2DM participants, albeit with a substantially longer mean disease duration [128].

Interestingly, despite lower SCP concentrations and lowest HOMA2-B in the SIDD group, UCP levels were not the lowest. This pattern is also evident in Wang et al. [128]. One potential explanation for this observation is concomitant hyperglycaemia, which has been shown to potentiate renal excretion of C-peptide [162]. Notably, participants classified as SIDD exhibited the highest fasting plasma glucose levels, a feature consistently reported across multiple cohorts [157, 161, 163]. However, given the small sample size of the SIDD cluster in the present study, this finding should be interpreted with caution and warrants confirmation in larger datasets.

4.2 Pre-Analytical Stability of Urinary C-peptide

Despite the manifold clinical applicability of SCP in diabetes, the pre-analytical requirements of rapid transport on ice and quick separation of cellular components from the liquid phase act as limiting factors for its widespread clinical utility. The acceptable pre-centrifugation delay, which, depending upon the type of sample tube used, is reported to be 4–24 hours [90-93, 164, 165]. Owing to this varied and

restrictive time frame, the pick-up of these blood samples from the doctor's place needs to be meticulously planned multiple times a day, so that whole blood samples reach the distant measuring laboratory on time. The infrequent clinical use of SCP was specifically observed as attempts were made to replicate Ahlqvist's clusters in multiple cohorts throughout the world, where the data of the parameter, which was most frequently missing, was that of fasting C-peptide [16]. To offer a practicable and non-invasive alternative for this pre-analytical issue, we investigated the stability of UCP under various storage conditions.

The results of the mixed-effects model with random slope and intercept suggest that 96 hours of exposure to room temperatures had no statistically significant impact on UCP and UCPCR concentrations at the population level. This observation differs from two previous studies of Kuzuya et al. and McDonald et al., who reported a stability of 1–2 days at ambient temperatures, albeit with a smaller sample size [134, 135]. However, when considering a change of more than ±10% relative to baseline as clinically significant, UCPCR and UCP concentrations maintained their stability for up to 48 hours, in agreement with the literature mentioned above. Of note, this threshold was also used by McDonald et al. and many others dealing with pre-analytical stability of proteins in blood and urine [91, 134, 140, 166, 167], The statistically significant change in UCr concentrations at room temperatures observed in our study is, however, inconsistent with previous literature [137, 138]. Strikingly, we observed a trend of increasing UCr concentrations with storage time. A similar pattern is also evident in Herrington et al. in patients with albuminuria and in Silva Junior et al. with bovine urine [138, 168]. The latter study postulated a conversion of urinary creatine in UCr as storage temperatures rise [168]. Nevertheless, we cannot rule out effects related to sample-handling or evaporation and may need confirmation in future studies.

At the same time, however, our data showed high sample-to-sample variation in UCP concentrations over time. While most samples remained close to their baseline values, 10%–15% displayed decreases greater than 25% and some showed increases of similar magnitude. This observation suggests that much of the fluctuation may be attributable to analytical and sample-handling variation rather than a unidirectional degradation process. Apart from this, the stability of C-peptide in urine samples also seems to be affected by bacterial contamination. Kuzuya et al. observed a rapid degradation of UCP at room temperature in samples with bacteriuria in comparison to

those without, the addition of sodium azide preventing this decay [135]. The Exeter group experimented using three bacteriostatic agents (sodium azide, sodium carbonate, and boric acid) and concluded that UCPCR remains stable for 72 hours at room temperature when boric acid or sodium carbonate was used [134]. Therefore, it is plausible that at least part of the observed sample-to-sample fluctuations in our study could be due to bacterial degradation of UCP.

We chose the statistical method of mixed-effects model to appropriately account for the repeated-measures design of the experiment, as multiple measurements were obtained from the same urine samples at predefined time points, resulting in non-independent observations. In addition, marked heterogeneity in baseline UCP concentrations was observed across samples, which is expected given biological variability between individuals and differences in initial analyte concentrations. By incorporating random intercepts, the model allows each urine sample to have its own baseline concentration, while random slopes permit individual samples to vary in their trajectories. This is particularly relevant in stability experiments, where a uniform degradation pattern across all samples cannot be assumed, as observed by Herrington et al., wherein the stability of urinary albumin differed with the level of albuminuria [138]. Moreover, sample-specific fluctuations may arise due to pre-analytical handling, bacterial contamination, or analytical variation. Importantly, this modelling strategy enables the distinction between population-level time effects and sample-to-sample variability. Consequently, the absence of a statistically significant fixed effect of time in the mixed-effects model indicates that, despite individual fluctuations in UCP concentrations, there was no consistent, systematic degradation of UCP at the population level over the investigated period. To summarize, while considering the absence of a consistent decay pattern at the population level till 96 hours of exposure to ambient temperatures found in our study, UCP may appear well-suited for large-scale decentralized epidemiological studies, where conclusions are to be drawn from population averages. In this scenario, study participants can be provided with sample tubes, which could be sent back to the study centre or to a laboratory by mail. In contrast, our findings also indicate that in clinical settings, where precise individual-level decision making is required, the use of sample tubes without preservatives may not be the safest option. For this purpose, the use of commercially available sample tubes with pre-added bacteriostatic agents should be preferred for longer transport durations to the laboratory, as recommended by McDonald et al. To

sum up, the practical challenges associated with pre-centrifugation delays in SCP measurements could be mitigated using UCP.

Our findings suggest that UCP, UCPCR and UCr remain stable after more than 10 years of storage at -20 °C, with the generalized linear model showing no evidence of systematic decay over time. In contrast to this, a significant decline in UCPCR was seen at 90 days of freezer storage in a similar study conducted by the Exeter group, although with a sample size of only two urine samples [134]. In our study, despite the lack of fresh baseline measurements, the data from our large sample size suggest no obvious time-dependent drifts in the stored concentrations of UCP at -20 °C, which is in line with the observations of Kuzuya et al [135]. The long-term stability of UCr at freezing temperatures has already been noted in previous studies [136, 139, 140] and our observation is consistent with this. Studies on long-term parameter stability are highly relevant for large biobanking studies, such as the GDS, where urine samples of study participants, who have undergone meticulous phenotyping, have been archived for more than a decade. It is a prerequisite for future analyses from such stored samples that reliable data is known regarding the pre-analytical stability of parameters.

Together with stability at freezer temperatures, the effect of multiple freeze-thaw cycles on analyte concentrations is also relevant not only in research but also in clinical settings. It is not infrequent that in a routine laboratory some measurements are ordered after a sample has already been analysed for other parameters. In this case, a frozen sample needs to be rethawed and measured for the parameter in question, thereby avoiding the need for a repeat sample collection. In some cases, repeat sampling may not be meaningful at all if an intervention has already taken place. In this context, we examined the stability of UCP over four freeze-thaw cycles and analysed the results using mixed-effects models. Although our findings reveal a statistically significant decline in UCP, UCPCR and UCr concentrations across multiple freeze-thaw cycles, the magnitude of the change per freeze-thaw cycle was small and unlikely to affect clinical interpretation. Considering the stability threshold of ±10%, it may be prudent to limit the number of freeze-thaw cycles for UCP and UCPCR to maintain their stability. Our findings are inconsistent with those of the Exeter group, who observed a stability of UCPCR for up to seven cycles [134], albeit with only two urine samples. However, this discrepancy may reflect sample-handling effects, as samples were transferred between original tubes and false bottom tubes at every cycle

in our study. Although not in full alignment with the results of the mixed-effects model, our threshold-based findings for UCr are in line with previous literature [138].

4.3 Relationship of Urinary C-peptide and Serum C-peptide

When considering participants with T2DM and NGT together, UCPCR and SCP showed a moderately positive correlation in the fasting state. This observation is broadly consistent with previously published literature. Bowman et al. reported a moderately positive correlation ($r = 0.31$, $p = 0.007$, $n = 77$) between fasting UCPCR and SCP in T2DM [113]. In healthy participants, the BioPersMed cohort study of Austria showed a weakly positive correlation ($r = 0.227$, $p < 0.001$, $n = 317$) between the two; however, the correlation observed by Oram et al. was strongly positive ($r = 0.73$, $p < 0.0001$, $n = 37$) [126, 131]. This variability in the observed strength of the relationship between fasting UCPCR and SCP could be explained by methodological and physiological factors. Firstly, first-void fasting UCPCR has been shown to exhibit a higher intra-individual coefficient of variation compared with second-void sampling (52% vs 33%, respectively) in healthy subjects and 28% in T2DM (second-void), likely reflecting the influence of the previous evening's meal [113, 134]. Consequently, the previously mentioned studies were methodologically designed to use second-void fasting UCPCR. In contrast, the GDS does not explicitly mandate the collection of second-void fasting urine samples from its study participants. Of note, even SCP seems to show higher biological variability. A recent meta-analysis on biological variation of C-peptide in serum/plasma reported an intra-/inter-individual coefficient of variation of up to 21% in healthy adults, and the Exeter group reported a much higher value (38%) for the same in T2DM [169]. Secondly, hyperglycaemia potentiates the urinary excretion of C-peptide [162], which could suggest that fasting hyperglycaemia may act as a confounding factor in some study participants. Thirdly, previous studies have reported better correlations between UCP and SCP when the β-cell function was poor, and the correlations worsened with improving β-cell function [170]. As in the previously mentioned studies, including our study, no stratification was made as per the level of β-cell function; this may also, in part, explain the variability in the relationship found between UCP and SCP. Conversely, various studies found a stronger correlation between UCPCR and SCP in the stimulated state [111-113].

The role of creatinine correction in improving the interpretability of UCP measurements remains debated. The dilutionary correction of UCP using creatinine did not improve its relationship with SCP in our study. Similar observations were made by Kaneko et al. and Horwitz et al [94, 97]. Kaneko et al. reported that post-stimulation changes in UCP correlated similarly with changes in SCP, regardless of whether UCP was corrected for creatinine [94]. Horwitz et al. observed that the day-to-day variability in UCP excretion could not be improved with corrections using creatinine [97]. On the other hand, Hassan et al. could demonstrate a better correlation of UCPCR to markers of obesity as compared to UCP [132]. In our study, although the correlation between UCPCR and SCP was not better in comparison with UCP, we nevertheless recommend the use of UCPCR due to two reasons; Firstly, to maintain consistency with established practise for other urinary biomarkers, such as urinary albumin, which are routinely corrected for urinary dilution. Secondly, as mentioned previously, hyperglycaemia was not only seen to potentiate the renal excretion of C-peptide but also concomitantly increase creatinine clearance [162], so that the ratio of the two may be the better option. Together, these findings support the concept that UCP reflects endogenous insulin production and may serve as a reliable alternative to blood sampling. Although second-void sampling exhibits lesser biological variability, all findings taken together, we cannot definitively conclude whether second-void sampling is a better option than first-void sampling to achieve a closer agreement with SCP, especially if better patient compliance could be achieved with first-void samples. Additionally, it has been recommended that concomitant hypoglycaemia needs to be ruled out before interpreting C-peptide values, as hypoglycaemia would inhibit the release of C-peptide [76].

It is important to consider the fact that the primary organ of C-peptide metabolism is the kidney itself, and many of the aforementioned studies, including our study, selected participants with a normal renal function. However, the impact of a deranged renal function on UCP excretion remains to be concretely elucidated. While some studies have reported no significant effect on the clinical utility of UCPCR in renal insufficiency, others have shown no correlation between UCPCR and SCP in chronic kidney disease [113, 131, 171]. On one hand, Horwitz et al. found no impact on UCP excretion in two-hour urine samples in patients with kidney disease, not only over a wide range of creatinine clearance but also during proteinuria [97]. On the other hand, in studies done on 24-hour urine samples, UCP correlated poorly with SCP, and a statistically

significant reduction in UCP excretion was found in patients with kidney disease, although the reduction in the ratio of UCP to UCr did not assume statistical significance [99, 135]. Even a difference in renal handling of C-peptide has been observed between healthy subjects and patients with diabetes in previous studies [96, 172, 173]. Ten dam et al. noticed a reduced peritubular uptake of C-peptide in T2DM, resulting in an increased fractional excretion, and this fractional excretion, as observed by Tillil et al., showed a high inter- and intra-individual variation of up to 29% [96, 110]. Even C-peptide clearance was seen to be reduced during exercise, as seen by Blix et al. [105]. Therefore, when interpreting changes in UCP concentrations in clinical practise, the potential influence of renal handling of C-peptide should also be considered, rather than attributing such changes solely to altered insulin secretion.

4.4 Prediction of HOMA2 Indices from Urinary C-peptide

The use of SCP for calculating HOMA2 indices, as one of the variables used to define novel subtypes in diabetes, is already established [144]. It is also well known that UCP shows a close association with clinical and anthropometric markers of insulin resistance as well as with HOMA2-IR in T2DM and healthy cohorts [128, 131-133]. However, UCP itself has not been used to estimate HOMA2 indices directly to date. To achieve this, we first predicted SCP from UCP, age at diagnosis, sex, and BMI using mixed linear models, after which HOMA2-B and HOMA2-S were calculated using the predicted SCP values. Our data suggests that UCP, when combined with basic clinical variables, could be used to predict SCP with good agreement and generate reliable estimates of HOMA2-B and HOMA2-S.

The preservation of good correlation between UCP-based and SCP-based HOMA2 indices is especially important given the nonlinear nature of the HOMA2 model [34]. Small errors in SCP prediction could, in principle, be amplified during the use of the model. However, the observed correlation indicates that prediction error remains within a physiologically acceptable range, thereby supporting the validity of using predicted SCP values as inputs for HOMA2 modelling, at least at the population-level.

Of note, Oram et al. demonstrated a strong correlation between UCPCR and insulin-based HOMA2-IR in participants with NGT but postulated that this relationship may be disrupted with the onset of hyperglycaemia [131]. In contrast, our findings suggest that a meaningful relationship between UCP-derived indices and HOMA2

indices is preserved even in the presence of early T2DM, as many of our study participants were recently diagnosed and exhibited fasting hyperglycaemia.

However, it is important to consider that our model of the UCP-based indices needs to be validated against the gold standard methods for the assessment of insulin resistance and β-cell function, as mere correlation with serum-based indices does not necessarily imply interchangeability. Accordingly, the present findings should be interpreted as proof of concept rather than evidence of clinical interchangeability. As the calculation of HOMA indices also requires the measurement of plasma glucose, the practicability of the model can only be achieved if glucose readings based on a glucometer can replace plasma glucose measurements in the HOMA indices. Consideration also needs to be given to the differential performance of such surrogate indices in different ethnicities as well as in different states of glucose tolerance. As an example, Pisprasert et al. observed African Americans to be more insulin resistant using HOMA-IR compared to European Americans, although both had similar insulin sensitivities as per the clamp test [174, 175]. In a study by Tripathy et al., the HOMA1 indices did not fare well in the prediction of insulin sensitivity and β-cell function in IFG and IGT [176]. Therefore, as this model was only applied to the GDS cohort of T2DM and NGT, external validation in independent cohorts and in prediabetes is required to ensure reproducibility. Moreover, the validity of this model in the state of impaired renal function also needs to be assessed. Of note, HOMA1-IR showed a strong relationship with insulin resistance derived from clamp-test in T2DM patients with kidney disease [177].

We propose this model as a practical and non-invasive alternative for the assessment of insulin resistance and β-cell function in T2DM and persons with NGT, with the potential to be utilised at home over a calculator using a fasting urine sample. If validated in independent cohorts, this could pave the way for decentralized and remote screening programs not only in diabetes but also in prediabetes and metabolic syndrome. More importantly, as the implementation of the novel diabetes subgroups is hampered by the underuse of SCP, the application of UCP-based HOMA2 indices may remove this hurdle to the execution of precision diagnostics in diabetes [6].

4.5 Cluster Analysis in Type 2 Diabetes using Urinary C-peptide

Building on the Ahlqvist classification, this study explored whether T2DM subtypes can be predicted using UCP alongside simple demographic and anthropometric variables. The multinomial logistic regression model achieved a high overall accuracy of 77.5% and showed substantial agreement with established subtype assignments (Cohen's κ = 0.62), with the highest discriminative performance being observed for the mild subtypes (MOD and MARD).

The observed overall classification accuracy and substantial agreement with established clusters should be interpreted in the context of an inherent variability in diabetes subtyping itself. The systematic review of Misra et al. showed that when model variables other than or in addition to the variable set used in the Ahlqvist classification were applied, the reproducibility of the Ahlqvist assignments across cohorts was shown to vary [141]. In this context, achieving substantial agreement using a non-invasive urinary biomarker in combination with readily available variables suggests that UCP-based models may capture key underlying metabolic features that are relevant to subtype allocation, even if some degree of misclassification is unavoidable.

An attempt to undertake cluster analysis in T2DM using UCPCR has already been made by Wang and colleagues [128]. In this study, UCPCR was used as an additional variable to the ones used in the Ahlqvist classification with the result that five clusters could be identified in T2DM. In contrast, our study adopted a supervised modelling approach aimed at predicting established subtypes rather than discovering novel clusters. This approach was chosen to prioritize comparability with existing subtypes.

The higher discriminative performance observed for the mild subtypes is plausible, as these subtypes tend to represent more metabolically homogeneous groups with relatively preserved β-cell function and lower degrees of insulin resistance [144], thereby reducing phenotypic overlap. Although the model performed well for the clusters of SIDD and SIRD, owing to the small number of test cases for the severe groups, the discriminative performance of the model for SIDD and SIRD cannot be definitively concluded. We do, however, expect the model to also perform well in the severe groups, because the UCP-based HOMA2 indices showed strong associations with SCP-based HOMA2 indices of β-cell function and insulin resistance, the disturbance in each being pathognomonic for SIDD and SIRD, respectively.

We selected these model variables owing to three factors: Firstly, the use of additional variables such as fasting blood glucose and HbA1c did not substantially improve the performance of the model. When fasting blood glucose was included additionally, the overall accuracy of the model marginally rose to 81.3% (95% CI 71.0% to 89.1%), exceeding the no-information rate of 45% ($p < 0.001$) with a Cohen's κ of 0.68 (see Supplementary Figure 4). With the inclusion of both HbA1c and fasting blood glucose, the model achieved an accuracy of 80.0% (95% CI 69.6% to 88.1%) at a no-information rate of 45% ($p < 0.001$) with a Cohen's κ of 0.67 (see Supplementary Figure 5). Therefore, no considerable benefit could be achieved with the parameters that depict hyperglycaemia in diabetes. Secondly, as UCP is the only measurand, this would minimize the dependency on a laboratory, and thirdly, all the model variables can be obtained non-invasively. While serum-based, genetic, or multi-omics approaches may provide richer information, this simple UCP-based model could substantially lower the logistical barriers to cluster allocation. Therefore, the UCP-based model could be seen as a trade-off between precision and scalability, which may be particularly relevant for future large-scale remotely conducted studies in T2DM. Moreover, repeated urine sampling may facilitate longitudinal monitoring of subtype stability over time. This could help in exploring whether individuals transition between clusters with disease progression or in response to therapeutic interventions, which was particularly noted in the study done by Zaharia et al [146].

Taken together, these findings highlight the potential of UCP-based modelling as a practical tool for subtype allocation in diabetes. While further validation in independent and ethnically diverse cohorts is required, the present results suggest that UCP-based models could help to enable a decentralized and scalable allocation of subtypes, thereby aligning with the broader goals of precision diagnostics in diabetes [6].

4.6 Limitations

In addition to the potential limitations of the GDS itself, as noted in Szendroedi et al. [148], several weaknesses of this study should be acknowledged. First, potential assay-related interferences affecting the measurement of UCP were not systematically controlled. Importantly, high-dose biotin intake is known to interfere with sandwich-immunoassays, potentially leading to falsely low results [178]. Although assay manufacturers recommend an interval of at least eight hours between biotin intake and

sample collection [100], this requirement is not explicitly mandated within the GDS protocol. Consequently, the possibility of residual assay interference cannot be fully excluded and may have influenced individual UCP measurements. Additionally, haemolysis in urine samples was not systematically assessed. However, according to the assay manufacturer, haemoglobin concentrations below a specified threshold were unlikely to lead to relevant analytical interference in UCP measurements [100].

Second, the lack of international standardization for C-peptide measurement represents an important analytical limitation [87]. Considerable inter-assay and inter-platform variability has been reported across different manufacturers, which limits direct comparability between studies [87]. As a result, the findings presented here are specific to the analytical platform used and may not be directly transferable to results obtained using other assays or laboratories.

Third, the stability of UCP and UCr at room temperature and during multiple freeze-thaw cycles was not evaluated using freshly collected samples. Instead, analyses were performed on samples that had already undergone at least two freeze-thaw cycles. As this approach does not fully reflect the pre-analytical conditions of a freshly collected urine sample, subtle biochemical degradation or concentration changes prior to the stability experiments cannot be completely ruled out. This may have introduced additional variability into the measurements. Furthermore, an alternative approach, such as pooling urine samples followed by preparation of multiple aliquots, with these aliquots being sequentially measured over time, may have been preferable for assessing the stability at room temperature, as it would have minimized repeated sample handling and potential evaporation effects during measurement.

Furthermore, the generalizability of the study findings is limited. The GDS cohort comprises participants residing exclusively in Germany, which may restrict extrapolation to populations with different ethnic backgrounds. Additionally, although participants with diabetes were recently diagnosed, most were already receiving anti-diabetic treatment at the time of sample collection. This may have influenced endogenous insulin secretion and C-peptide levels, thereby potentially attenuating associations.

Other important limitations include the retrospective nature of the analyses, which hinders causal inference, and the exclusion of individuals with impaired renal function,

limiting the applicability of the findings to patients with reduced kidney function, a group highly relevant in clinical diabetes care.

Taken together, these limitations highlight the need for cautious interpretation of the results and underscore the importance of prospective studies, standardized analytical methods, and broader population-based validation to confirm the robustness and clinical utility of UCP measurements.

5 Conclusions

This retrospective clinical study demonstrates that UCP could be a feasible, stable, and clinically meaningful non-invasive surrogate for SCP in recently diagnosed T2DM. UCP showed no significant time-dependant degradation across various storage conditions, including prolonged exposure to room temperature and long-term frozen storage. Importantly, no systematic degradation of UCP was observed at the population level, supporting its suitability for large-scale epidemiological studies and biobanking applications.

UCP correlated positively with SCP and enabled a reliable prediction of HOMA2 indices of β-cell function and insulin sensitivity when combined with basic demographic and anthropometric variables. These findings support the use of UCP as a proxy for SCP to assess endogenous insulin secretion in individuals with NGT and in those with early T2DM, provided renal function is preserved.

Moreover, UCP-based modelling was able to identify established T2DM subtypes with substantial agreement to SCP-based classifications. The supervised prediction approach achieved good overall accuracy, with particularly strong performance for the mild diabetes subtypes. The ability to allocate diabetes subtypes using a non-invasive urinary biomarker, in combination with readily available clinical variables, could address a key logistical barrier that has limited the implementation of precision diagnostics in diabetes.

Taken together, these results indicate that UCP has the capacity to offer a good balance between practical feasibility and clinical validity. By mitigating the pre-analytical challenges associated with SCP measurement, UCP has the potential to enable decentralized and scalable assessment of insulin secretion, insulin resistance, and diabetes subtypes.

6 Outlook

While the present findings provide strong proof of concept, several avenues for future research remain. First, to establish reproducibility of the model, external validation of the UCP-based prediction model is required in independent cohorts with ethnically diverse populations, in a higher number of study participants with severe subtypes, and in individuals across the full spectrum of glucose tolerance, particularly in prediabetes.

Second, the performance of UCP-based indices in individuals with impaired renal function warrants systematic investigation, given the kidney's central role in C-peptide metabolism. Defining the limits within which UCP remains interpretable in the context of chronic kidney disease will be crucial for broader clinical applicability.

Third, prospective studies comparing UCP-derived HOMA2 indices against gold-standard methods, such as clamp-based assessments of insulin sensitivity and β-cell function, are needed to clarify the degree of clinical interchangeability. In parallel, the feasibility of replacing plasma glucose with glucometer-based measurements in UCP-driven models should be explored to further enhance real-world applicability.

The non-invasive nature of UCP opens opportunities for at-home sampling, mail-based study designs, and longitudinal monitoring. Repeated urine sampling could facilitate the investigation of changes in insulin secretion, insulin resistance, and diabetes subtype stability over time, including potential transitions between clusters in response to disease progression or therapeutic interventions.

In conclusion, UCP-based assessment represents a promising step toward decentralized and scalable precision diagnostics in diabetes. If validated in broader settings, this approach could substantially lower the barriers to metabolic phenotyping and subtype classification, thereby supporting more individualized risk stratification and management strategies in T2DM and related metabolic disorders.

7 Bibliography

1. International Diabetes Federation, *IDF Diabetes Atlas, 11th edn*. Brussels, Belgium: 2025 Available at: https://diabetesatlas.org.
2. American Diabetes Association Professional Practice, C., *2. Diagnosis and Classification of Diabetes: Standards of Care in Diabetes-2025*. Diabetes Care, 2025. **48**(Supplement_1): p. S27-S49.
3. Schleicher, E., et al., *Definition, Classification and Diagnosis of Diabetes Mellitus*. Exp Clin Endocrinol Diabetes, 2022. **130**(S 01): p. S1-S8.
4. Aschner, P., *New IDF clinical practice recommendations for managing type 2 diabetes in primary care*. Diabetes Res Clin Pract, 2017. **132**: p. 169-170.
5. Deutsch, A.J., E. Ahlqvist, and M.S. Udler, *Phenotypic and genetic classification of diabetes*. Diabetologia, 2022. **65**(11): p. 1758-1769.
6. Chung, W.K., et al., *Precision Medicine in Diabetes: A Consensus Report From the American Diabetes Association (ADA) and the European Association for the Study of Diabetes (EASD)*. Diabetes Care, 2020. **43**(7): p. 1617-1635.
7. DiMeglio, L.A., C. Evans-Molina, and R.A. Oram, *Type 1 diabetes*. Lancet, 2018. **391**(10138): p. 2449-2462.
8. Deutsche Diabetes Gesellschaft (DDG) and diabetesDE - Deutsche Diabetes-Hilfe, *Deutscher Gesundheitsbericht Diabetes 2025: Die Bestandsaufnahme*. Berlin: DDG; 2024 Available at https://www.ddg.info/fileadmin/user_upload/Gesundheitsbericht_2025_final.pdf.
9. Baumert, J., et al., *Diabetes mellitus, cardiovascular and chronic respiratory diseases in Germany and Europe - results of the European Health Interview Survey (EHIS 3, 2018 - 2020)*. J Health Monit, 2024. **9**(4): p. e12920.
10. Stumvoll, M., B.J. Goldstein, and T.W. van Haeften, *Type 2 diabetes: principles of pathogenesis and therapy*. Lancet, 2005. **365**(9467): p. 1333-46.
11. Lima, J., N.C.S. Moreira, and E.T. Sakamoto-Hojo, *Mechanisms underlying the pathophysiology of type 2 diabetes: From risk factors to oxidative stress, metabolic dysfunction, and hyperglycemia*. Mutat Res Genet Toxicol Environ Mutagen, 2022. **874-875**: p. 503437.
12. Galicia-Garcia, U., et al., *Pathophysiology of Type 2 Diabetes Mellitus*. Int J Mol Sci, 2020. **21**(17).
13. Fletcher, B., M. Gulanick, and C. Lamendola, *Risk factors for type 2 diabetes mellitus*. J Cardiovasc Nurs, 2002. **16**(2): p. 17-23.
14. InterAct, C., et al., *The link between family history and risk of type 2 diabetes is not explained by anthropometric, lifestyle or genetic risk factors: the EPIC-InterAct study*. Diabetologia, 2013. **56**(1): p. 60-9.
15. Meigs, J.B., *The Genetic Epidemiology of Type 2 Diabetes: Opportunities for Health Translation*. Curr Diab Rep, 2019. **19**(8): p. 62.
16. Herder, C. and M. Roden, *A novel diabetes typology: towards precision diabetology from pathogenesis to treatment*. Diabetologia, 2022. **65**(11): p. 1770-1781.
17. Unwin, N., et al., *Impaired glucose tolerance and impaired fasting glycaemia: the current status on definition and intervention*. Diabet Med, 2002. **19**(9): p. 708-23.
18. Nathan, D.M., et al., *Impaired fasting glucose and impaired glucose tolerance: implications for care*. Diabetes Care, 2007. **30**(3): p. 753-9.
19. Tabak, A.G., et al., *Prediabetes: a high-risk state for diabetes development*. Lancet, 2012. **379**(9833): p. 2279-90.
20. Narayan, K.M., et al., *Effect of BMI on lifetime risk for diabetes in the U.S.* Diabetes Care, 2007. **30**(6): p. 1562-6.
21. Valaiyapathi, B., B. Gower, and A.P. Ashraf, *Pathophysiology of Type 2 Diabetes in Children and Adolescents*. Curr Diabetes Rev, 2020. **16**(3): p. 220-229.

22. Eckel, R.H., et al., *Obesity and type 2 diabetes: what can be unified and what needs to be individualized?* Diabetes Care, 2011. **34**(6): p. 1424-30.
23. Bournat, J.C. and C.W. Brown, *Mitochondrial dysfunction in obesity.* Curr Opin Endocrinol Diabetes Obes, 2010. **17**(5): p. 446-52.
24. Mokdad, A.H., et al., *Diabetes trends in the U.S.: 1990-1998.* Diabetes Care, 2000. **23**(9): p. 1278-83.
25. Sullivan, P.W., et al., *Obesity, inactivity, and the prevalence of diabetes and diabetes-related cardiovascular comorbidities in the U.S., 2000-2002.* Diabetes Care, 2005. **28**(7): p. 1599-603.
26. Colberg, S.R., et al., *Physical Activity/Exercise and Diabetes: A Position Statement of the American Diabetes Association.* Diabetes Care, 2016. **39**(11): p. 2065-2079.
27. Sigal, R.J., et al., *Physical activity/exercise and type 2 diabetes.* Diabetes Care, 2004. **27**(10): p. 2518-39.
28. Neuenschwander, M., et al., *Role of diet in type 2 diabetes incidence: umbrella review of meta-analyses of prospective observational studies.* BMJ, 2019. **366**: p. l2368.
29. InterAct, C., et al., *Smoking and long-term risk of type 2 diabetes: the EPIC-InterAct study in European populations.* Diabetes Care, 2014. **37**(12): p. 3164-71.
30. Chiolero, A., et al., *Consequences of smoking for body weight, body fat distribution, and insulin resistance.* Am J Clin Nutr, 2008. **87**(4): p. 801-9.
31. Singh, A., et al., *Type 2 Diabetes Mellitus: A Comprehensive Review of Pathophysiology, Comorbidities, and Emerging Therapies.* Compr Physiol, 2025. **15**(1): p. e70003.
32. Kakoly, N.S., et al., *Ethnicity, obesity and the prevalence of impaired glucose tolerance and type 2 diabetes in PCOS: a systematic review and meta-regression.* Hum Reprod Update, 2018. **24**(4): p. 455-467.
33. Ke, C., et al., *Pathophysiology, phenotypes and management of type 2 diabetes mellitus in Indian and Chinese populations.* Nat Rev Endocrinol, 2022. **18**(7): p. 413-432.
34. Wallace, T.M., J.C. Levy, and D.R. Matthews, *Use and abuse of HOMA modeling.* Diabetes Care, 2004. **27**(6): p. 1487-95.
35. Roden, M. and G.I. Shulman, *The integrative biology of type 2 diabetes.* Nature, 2019. **576**(7785): p. 51-60.
36. Khamis, A.M., *Pathophysiology, Diagnostic Criteria, and Approaches to Type 2 Diabetes Remission.* Cureus, 2023. **15**(1): p. e33908.
37. Accili, D., Z. Deng, and Q. Liu, *Insulin resistance in type 2 diabetes mellitus.* Nat Rev Endocrinol, 2025. **21**(7): p. 413-426.
38. Xie, J. and R. Weiskirchen, *What Does the "AKT" Stand for in the Name "AKT Kinase"? Some Historical Comments.* Front Oncol, 2020. **10**: p. 1329.
39. Freeman, A.M., L.A. Acevedo, and N. Pennings, *Insulin Resistance*, in *StatPearls*. 2025: Treasure Island (FL).
40. Esser, N., K.M. Utzschneider, and S.E. Kahn, *Early beta cell dysfunction vs insulin hypersecretion as the primary event in the pathogenesis of dysglycaemia.* Diabetologia, 2020. **63**(10): p. 2007-2021.
41. Staimez, L.R., et al., *Tale of two Indians: Heterogeneity in type 2 diabetes pathophysiology.* Diabetes Metab Res Rev, 2019. **35**(8): p. e3192.
42. Cerf, M.E., *Beta cell dysfunction and insulin resistance.* Front Endocrinol (Lausanne), 2013. **4**: p. 37.
43. DeFronzo, R.A., J.D. Tobin, and R. Andres, *Glucose clamp technique: a method for quantifying insulin secretion and resistance.* Am J Physiol, 1979. **237**(3): p. E214-23.
44. Bergman, R.N., D.T. Finegood, and M. Ader, *Assessment of insulin sensitivity in vivo.* Endocr Rev, 1985. **6**(1): p. 45-86.
45. Pacini, G. and A. Mari, *Methods for clinical assessment of insulin sensitivity and beta-cell function.* Best Pract Res Clin Endocrinol Metab, 2003. **17**(3): p. 305-22.

46. Cersosimo, E., et al., *Assessment of pancreatic beta-cell function: review of methods and clinical applications*. Curr Diabetes Rev, 2014. **10**(1): p. 2-42.
47. Renklint, R., et al., *Surrogate measures of first-phase insulin secretion versus reference methods intravenous glucose tolerance test and hyperglycemic clamp: a systematic review and meta-analyses*. BMJ Open Diabetes Res Care, 2024. **12**(4).
48. Otten, J., B. Ahren, and T. Olsson, *Surrogate measures of insulin sensitivity vs the hyperinsulinaemic-euglycaemic clamp: a meta-analysis*. Diabetologia, 2014. **57**(9): p. 1781-8.
49. Hudak, S., et al., *Reproducibility and discrimination of different indices of insulin sensitivity and insulin secretion*. PLoS One, 2021. **16**(10): p. e0258476.
50. Prystupa, K., et al., *Comprehensive validation of fasting-based and oral glucose tolerance test-based indices of insulin secretion against gold standard measures*. BMJ Open Diabetes Res Care, 2022. **10**(5).
51. Matthews, D.R., et al., *Homeostasis model assessment: insulin resistance and beta-cell function from fasting plasma glucose and insulin concentrations in man*. Diabetologia, 1985. **28**(7): p. 412-9.
52. Levy, J.C., D.R. Matthews, and M.P. Hermans, *Correct Homeostasis Model Assessment (HOMA) Evaluation Uses the Computer Program*. Diabetes Care, 1998. **21**(12): p. 2191-2192.
53. Wang, C., et al., *The differences in homeostasis model assessment values in type 2 diabetic patients with different lengths of history of diabetes*. Arch Endocrinol Metab, 2019. **63**(3): p. 222-227.
54. Turner, R.C., et al., *Insulin deficiency and insulin resistance interaction in diabetes: estimation of their relative contribution by feedback analysis from basal plasma insulin and glucose concentrations*. Metabolism, 1979. **28**(11): p. 1086-96.
55. McAuley, K.A., et al., *Point: HOMA--satisfactory for the time being: HOMA: the best bet for the simple determination of insulin sensitivity, until something better comes along*. Diabetes Care, 2007. **30**(9): p. 2411-3.
56. Bonora, E., et al., *Homeostasis model assessment closely mirrors the glucose clamp technique in the assessment of insulin sensitivity: studies in subjects with various degrees of glucose tolerance and insulin sensitivity*. Diabetes Care, 2000. **23**(1): p. 57-63.
57. Wallace, T.M., J.C. Levy, and D.R. Matthews, *An increase in insulin sensitivity and basal beta-cell function in diabetic subjects treated with pioglitazone in a placebo-controlled randomized study*. Diabet Med, 2004. **21**(6): p. 568-76.
58. Levy, J.C., et al., *Simple empirical assessment of beta-cell function by a constant infusion of glucose test in normal and type 2 (non-insulin-dependent) diabetic subjects*. Diabetologia, 1991. **34**(7): p. 488-99.
59. Song, Y., et al., *Insulin sensitivity and insulin secretion determined by homeostasis model assessment and risk of diabetes in a multiethnic cohort of women: the Women's Health Initiative Observational Study*. Diabetes Care, 2007. **30**(7): p. 1747-52.
60. Hanley, A.J., et al., *Homeostasis model assessment of insulin resistance in relation to the incidence of cardiovascular disease: the San Antonio Heart Study*. Diabetes Care, 2002. **25**(7): p. 1177-84.
61. Bonora, E., et al., *Insulin resistance as estimated by homeostasis model assessment predicts incident symptomatic cardiovascular disease in caucasian subjects from the general population: the Bruneck study*. Diabetes Care, 2007. **30**(2): p. 318-24.
62. *U.K. prospective diabetes study 16. Overview of 6 years' therapy of type II diabetes: a progressive disease. U.K. Prospective Diabetes Study Group*. Diabetes, 1995. **44**(11): p. 1249-58.

63. Katsuki, A., et al., *Homeostasis model assessment is a reliable indicator of insulin resistance during follow-up of patients with type 2 diabetes*. Diabetes Care, 2001. **24**(2): p. 362-5.
64. Emoto, M., et al., *Homeostasis model assessment as a clinical index of insulin resistance in type 2 diabetic patients treated with sulfonylureas*. Diabetes Care, 1999. **22**(5): p. 818-22.
65. Meyer, C., et al., *Different mechanisms for impaired fasting glucose and impaired postprandial glucose tolerance in humans*. Diabetes Care, 2006. **29**(8): p. 1909-14.
66. Festa, A., et al., *Differences in insulin resistance in nondiabetic subjects with isolated impaired glucose tolerance or isolated impaired fasting glucose*. Diabetes, 2004. **53**(6): p. 1549-55.
67. Arellano-Ruiz, P., et al., *Homeostasis Model Assessment cut-off points related to metabolic syndrome in children and adolescents: a systematic review and meta-analysis*. Eur J Pediatr, 2019. **178**(12): p. 1813-1822.
68. Lin, S.Y., et al., *Optimal Threshold of Homeostasis Model Assessment of Insulin Resistance to Identify Metabolic Syndrome in a Chinese Population Aged 45 Years or Younger*. Front Endocrinol (Lausanne), 2021. **12**: p. 746747.
69. Hockaday, D., M. Sayyad, and C. Yajnik, *Counterpoint: appreciating homeostasis model assessment: more useful earlier rather than later*. Diabetes Care, 2007. **30**(9): p. 2414-8.
70. Boyko, E.J. and C.C. Jensen, *Do we know what homeostasis model assessment measures? If not, does it matter?* Diabetes Care, 2007. **30**(10): p. 2725-8.
71. Heni, M., et al., *Insulin Action in the Hypothalamus Increases Second-Phase Insulin Secretion in Humans*. Neuroendocrinology, 2020. **110**(11-12): p. 929-937.
72. Jaspan, J. and K. Polonsky, *Glucose ingestion in dogs alters the hepatic extraction of insulin. In vivo evidence for a relationship between biologic action and extraction of insulin*. J Clin Invest, 1982. **69**(3): p. 516-25.
73. Polonsky, K.S. and A.H. Rubenstein, *C-Peptide as a Measure of the Secretion and Hepatic Extraction of Insulin: Pitfalls and Limitations*. Diabetes, 1984. **33**(5): p. 486-494.
74. Van Cauter, E., et al., *Estimation of insulin secretion rates from C-peptide levels. Comparison of individual and standard kinetic parameters for C-peptide clearance*. Diabetes, 1992. **41**(3): p. 368-77.
75. Kuzuya, H., et al., *Determination of Free and Total Insulin and C-Peptide in Insulin-treated Diabetics*. Diabetes, 1977. **26**(1): p. 22-29.
76. Jones, A.G. and A.T. Hattersley, *The clinical utility of C-peptide measurement in the care of patients with diabetes*. Diabet Med, 2013. **30**(7): p. 803-17.
77. Steiner, D.F. and P.E. Oyer, *The biosynthesis of insulin and a probable precursor of insulin by a human islet cell adenoma*. Proc Natl Acad Sci U S A, 1967. **57**(2): p. 473-80.
78. Chance, R.E., R.M. Ellis, and W.W. Bromer, *Porcine proinsulin: characterization and amino acid sequence*. Science, 1968. **161**(3837): p. 165-7.
79. Rubenstein, A.H., et al., *Secretion of Proinsulin C-Peptide by Pancreatic β Cells and its Circulation in Blood*. Nature, 1969. **224**(5220): p. 697-699.
80. Clark, J.L., et al., *Isolation of a proinsulin connecting peptide fragment (C-peptide) from bovine and human pancreas*. Biochem Biophys Res Commun, 1969. **35**(4): p. 456-61.
81. Steiner, D.F., *The proinsulin C-peptide--a multirole model*. Exp Diabesity Res, 2004. **5**(1): p. 7-14.
82. Marques, R.G., M.J. Fontaine, and J. Rogers, *C-Peptide: Much More Than a Byproduct of Insulin Biosynthesis*. Pancreas, 2004. **29**(3): p. 231-238.
83. Leighton, E., C.A. Sainsbury, and G.C. Jones, *A Practical Review of C-Peptide Testing in Diabetes*. Diabetes Ther, 2017. **8**(3): p. 475-487.
84. Horwitz, D.L., et al., *Proinsulin, insulin, and C-peptide concentrations in human portal and peripheral blood*. J Clin Invest, 1975. **55**(6): p. 1278-83.

85. Bonser, A.M. and P. Garcia-Webb, *C-peptide measurement and its clinical usefulness: a review*. Ann Clin Biochem, 1981. **18**(Pt 4): p. 200-6.
86. Maddaloni, E., et al., *C-peptide determination in the diagnosis of type of diabetes and its management: A clinical perspective*. Diabetes Obes Metab, 2022. **24**(10): p. 1912-1926.
87. Schleicher, E., et al., *Call for Standardization of C-Peptide Measurement*. J Diabetes Sci Technol, 2025: p. 19322968251362848.
88. Genuth, S.M., *Clinical utility of C-peptide measurement in diabetes mellitus*. Endocr Pract, 1996. **2**(4): p. 266-8.
89. Clark, P.M., *Assays for insulin, proinsulin(s) and C-peptide*. Ann Clin Biochem, 1999. **36 (Pt 5)**: p. 541-64.
90. Smith, S., et al., *Stability of samples for insulin, proinsulin and C-peptide*. Journal of Endocrinology, 1996. **151**: p. P20.
91. McDonald, T.J., et al., *EDTA improves stability of whole blood C-peptide and insulin to over 24 hours at room temperature*. PLoS One, 2012. **7**(7): p. e42084.
92. Nkuna, D.X., et al., *The stability of C-peptide and insulin in plasma and serum samples under different storage conditions*. Clin Chem Lab Med, 2023. **61**(12): p. 2150-2158.
93. Oddoze, C., E. Lombard, and H. Portugal, *Stability study of 81 analytes in human whole blood, in serum and in plasma*. Clin Biochem, 2012. **45**(6): p. 464-9.
94. Kaneko, T., et al., *Demonstration of C-peptide immunoreactivity in various body fluids and clinical evaluation of the determination of urinary C-peptide immunoreactivity*. Endocrinol Jpn, 1975. **22**(3): p. 207-12.
95. Bonser, A.M. and P. Garcia-Webb, *C-peptide measurement: methods and clinical utility*. Crit Rev Clin Lab Sci, 1984. **19**(4): p. 297-352.
96. ten Dam, M.A., et al., *Renal handling of insulin and C-peptide in patients with non-insulin-dependent diabetes mellitus*. Nephrol Dial Transplant, 1993. **8**(2): p. 134-9.
97. Horwitz, D.L., A.H. Rubenstein, and A.I. Katz, *Quantitation of human pancreatic beta-cell function by immunoassay of C-peptide in urine*. Diabetes, 1977. **26**(1): p. 30-5.
98. Kruszynska, Y.T., et al., *Basal and 24-h C-peptide and insulin secretion rate in normal man*. Diabetologia, 1987. **30**(1): p. 16-21.
99. Kuzuya, T., et al., *C-peptide immunoreactivity (CPR) in urine*. Diabetes, 1978. **27 Suppl 1**: p. 210-5.
100. Roche Diagnostics Deutschland GmbH, *Elecsys C-Peptide*. Infosheet C-peptide Roche Diagnostics 2022-02, V 5.0 English.
101. Rendell, M., *The expanding clinical use of C-peptide radioimmunoassay*. Acta Diabetol Lat, 1983. **20**(2): p. 105-13.
102. Rappaport, E.B., et al., *Urine C-peptide, beta-cell function, and insulin requirement*. Am J Dis Child, 1980. **134**(12): p. 1129-33.
103. Meistas, M.T., et al., *Estimation of the secretion rate of insulin from the urinary excretion rate of C-peptide. Study in obese and diabetic subjects*. Diabetes, 1982. **31**(5 Pt 1): p. 449-53.
104. Meistas, M.T., et al., *Correlation of urinary excretion of C-peptide with the integrated concentration and secretion rate of insulin*. Diabetes, 1981. **30**(8): p. 639-43.
105. Blix, P.M., et al., *Urinary C-peptide: an indicator of beta-cell secretion under different metabolic conditions*. J Clin Endocrinol Metab, 1982. **54**(3): p. 574-80.
106. Aurbach-Klipper, J., et al., *Residual B cell function in diabetic children as determined by urinary C-peptide*. Diabetologia, 1983. **24**(2): p. 88-90.
107. Katzeff, H.L., et al., *C-peptide measurement in the differentiation of type 1 (insulin-dependent) and type 2 (non-insulin-dependent) diabetes mellitus*. Diabetologia, 1985. **28**(5): p. 264-8.
108. Goto, A., et al., *Body mass index, fasting plasma glucose levels, and C-peptide levels as predictors of the future insulin use in Japanese type 2 diabetic patients*. Endocr J, 2010. **57**(3): p. 237-44.

109. Hoogwerf, B.J., et al., *Urinary C-peptide as a measure of beta-cell function after a mixed meal in healthy subjects: comparison of four-hour urine C-peptide with serum insulin and plasma C-peptide.* Diabetes Care, 1983. **6**(5): p. 488-92.
110. Tillil, H., et al., *Reevaluation of urine C-peptide as measure of insulin secretion.* Diabetes, 1988. **37**(9): p. 1195-201.
111. Jones, A.G., et al., *Urine C-peptide creatinine ratio is an alternative to stimulated serum C-peptide measurement in late-onset, insulin-treated diabetes.* Diabet Med, 2011. **28**(9): p. 1034-8.
112. Besser, R.E., et al., *Urine C-peptide creatinine ratio is a noninvasive alternative to the mixed-meal tolerance test in children and adults with type 1 diabetes.* Diabetes Care, 2011. **34**(3): p. 607-9.
113. Bowman, P., et al., *Validation of a single-sample urinary C-peptide creatinine ratio as a reproducible alternative to serum C-peptide in patients with Type 2 diabetes.* Diabet Med, 2012. **29**(1): p. 90-3.
114. Hope, S.V., et al., *Urinary C-peptide creatinine ratio detects absolute insulin deficiency in Type 2 diabetes.* Diabet Med, 2013. **30**(11): p. 1342-8.
115. Besser, R.E., et al., *Urinary C-peptide creatinine ratio is a practical outpatient tool for identifying hepatocyte nuclear factor 1-{alpha}/hepatocyte nuclear factor 4-{alpha} maturity-onset diabetes of the young from long-duration type 1 diabetes.* Diabetes Care, 2011. **34**(2): p. 286-91.
116. Besser, R.E., et al., *Home urine C-peptide creatinine ratio (UCPCR) testing can identify type 2 and MODY in pediatric diabetes.* Pediatr Diabetes, 2013. **14**(3): p. 181-8.
117. Elzahar, W., et al., *Urinary C-peptide creatinine ratio to differentiate type 2 diabetes mellitus from type 1 in pediatric patients.* Eur J Pediatr, 2020. **179**(7): p. 1115-1120.
118. Yılmaz Agladioglu, S., E. Sagsak, and Z. Aycan, *Urinary C-Peptide/Creatinine Ratio Can Distinguish Maturity-Onset Diabetes of the Young from Type 1 Diabetes in Children and Adolescents: A Single-Center Experience.* Horm Res Paediatr, 2015. **84**(1): p. 54-61.
119. Wang, Y., et al., *Clinical Implications of Urinary C-Peptide Creatinine Ratio in Patients with Different Types of Diabetes.* J Diabetes Res, 2019. **2019**: p. 1747684.
120. Pappachan, J.M., et al., *Diagnostic Test Accuracy of Urine C-peptide Creatinine Ratio for the Correct Identification of the Type of Diabetes: A Systematic Review.* touchREV Endocrinol, 2022. **18**(1): p. 2-9.
121. Hope, S.V., et al., *Random non-fasting C-peptide: bringing robust assessment of endogenous insulin secretion to the clinic.* Diabet Med, 2016. **33**(11): p. 1554-1558.
122. Oram, R.A., et al., *The majority of patients with long-duration type 1 diabetes are insulin microsecretors and have functioning beta cells.* Diabetologia, 2014. **57**(1): p. 187-91.
123. Williams, G.M., et al., *Beta cell function and ongoing autoimmunity in long-standing, childhood onset type 1 diabetes.* Diabetologia, 2016. **59**(12): p. 2722-2726.
124. Shields, B.M., et al., *C-Peptide Decline in Type 1 Diabetes Has Two Phases: An Initial Exponential Fall and a Subsequent Stable Phase.* Diabetes Care, 2018. **41**(7): p. 1486-1492.
125. Thomas, N.J., et al., *The impact of gender on urine C-peptide creatinine ratio interpretation.* Ann Clin Biochem, 2012. **49**(Pt 4): p. 363-8.
126. Reintar, S., et al., *Urinary C-Peptide to Creatinine Ratio (UCPCR) as Indicator for Metabolic Risk in Apparently Healthy Adults-A BioPersMed Cohort Study.* Nutrients, 2023. **15**(9).
127. Irilouzadian, R., et al., *Urinary c-peptide creatinine ratio (UCPCR) as a predictor of coronary artery disease in type 1 diabetes mellitus.* Endocrinol Diabetes Metab, 2023. **6**(3): p. e413.
128. Wang, Y., et al., *Urinary C-peptide/creatinine ratio: A useful biomarker of insulin resistance and refined classification of type 2 diabetes mellitus.* J Diabetes, 2021. **13**(11): p. 893-904.

129. Chung, Y.H., et al., *High 24-hour urinary C-peptide excretion in non-insulin dependent diabetes mellitus*. Korean J Intern Med, 1986. **1**(2): p. 172-7.
130. Kato, H., et al., *Urine C-peptide and atherogenic risk factors in diabetes mellitus: relevance to "syndrome X"*. Angiology, 1995. **46**(10): p. 915-21.
131. Oram, R.A., et al., *Urine C-peptide creatinine ratio can be used to assess insulin resistance and insulin production in people without diabetes: an observational study*. BMJ Open, 2013. **3**(12): p. e003193.
132. Hassan, A.A., et al., *Urinary C-peptide and urinary C-peptide creatinine ratio as markers for insulin resistance in obese children and adolescents*. Pediatr Res, 2022. **92**(3): p. 805-809.
133. Farghaly, H.S., et al., *Urinary C-peptide creatinine ratio is a significant indicator of non-alcoholic fatty liver disease in children with obesity*. Turk J Pediatr, 2022. **64**(3): p. 482-489.
134. McDonald, T.J., et al., *Stability and reproducibility of a single-sample urinary C-peptide/creatinine ratio and its correlation with 24-h urinary C-peptide*. Clin Chem, 2009. **55**(11): p. 2035-9.
135. Kuzuya, T., et al., *Human C-peptide immunoreactivity (CPR) in blood and urine - evaluation of a radioimmunoassay method and its clinical applications*. Diabetologia, 1976. **12**(5): p. 511-8.
136. Remer, T., G. Montenegro-Bethancourt, and L. Shi, *Long-term urine biobanking: storage stability of clinical chemical parameters under moderate freezing conditions without use of preservatives*. Clin Biochem, 2014. **47**(18): p. 307-11.
137. Spierto, F.W., et al., *Stability of urine creatinine*. Clin Chim Acta, 1997. **264**(2): p. 227-32.
138. Herrington, W., et al., *Effect of Processing Delay and Storage Conditions on Urine Albumin-to-Creatinine Ratio*. Clin J Am Soc Nephrol, 2016. **11**(10): p. 1794-1801.
139. Lambers Heerspink, H.J., et al., *Alkalinization of urine samples preserves albumin concentrations during prolonged frozen storage in patients with diabetes mellitus*. Diabet Med, 2009. **26**(5): p. 556-9.
140. Chapman, D.P., et al., *Stability of urinary albumin and creatinine after 12 months storage at -20 degrees C and -80 degrees C*. Pract Lab Med, 2019. **15**: p. e00120.
141. Misra, S., et al., *Precision subclassification of type 2 diabetes: a systematic review*. Commun Med (Lond), 2023. **3**(1): p. 138.
142. Kautzky-Willer, A., J. Harreiter, and G. Pacini, *Sex and Gender Differences in Risk, Pathophysiology and Complications of Type 2 Diabetes Mellitus*. Endocr Rev, 2016. **37**(3): p. 278-316.
143. Tuomi, T., et al., *The many faces of diabetes: a disease with increasing heterogeneity*. Lancet, 2014. **383**(9922): p. 1084-94.
144. Ahlqvist, E., et al., *Novel subgroups of adult-onset diabetes and their association with outcomes: a data-driven cluster analysis of six variables*. Lancet Diabetes Endocrinol, 2018. **6**(5): p. 361-369.
145. Ahlqvist, E., R.B. Prasad, and L. Groop, *Subtypes of Type 2 Diabetes Determined From Clinical Parameters*. Diabetes, 2020. **69**(10): p. 2086-2093.
146. Zaharia, O.P., et al., *Risk of diabetes-associated diseases in subgroups of patients with recent-onset diabetes: a 5-year follow-up study*. Lancet Diabetes Endocrinol, 2019. **7**(9): p. 684-694.
147. Wagner, R., et al., *Pathophysiology-based subphenotyping of individuals at elevated risk for type 2 diabetes*. Nat Med, 2021. **27**(1): p. 49-57.
148. Szendroedi, J., et al., *Cohort profile: the German Diabetes Study (GDS)*. Cardiovascular Diabetology, 2016. **15**(1): p. 59.
149. Hayrapetyan, H., et al., *Enzyme-Linked Immunosorbent Assay: Types and Applications*. Methods Mol Biol, 2023. **2612**: p. 1-17.

150. Roche Diagnostics Deutschland GmbH, *CREP2 Creatinine plus ver.2.* Infosheet Creatinine Roche Diagnostics 2024-10, V 15.0 English.
151. Ahmad-Nejad, P., et al., *Revision of the "Guideline of the German Medical Association on Quality Assurance in Medical Laboratory Examinations – Rili-BAEK".* Journal of Laboratory Medicine, 2024. **48**(6): p. 263-306.
152. Mori, T., et al., *A web-based application for diabetes subtyping: The DDZ Diabetes-Cluster-Tool.* Acta Diabetol, 2025. **62**(2): p. 281-283.
153. R Core Team (2025), *_R: A Language and Environment for Statistical Computing_*. R Foundation for Statistical Computing, Vienna, Austria. <https://www.R-project.org/>.
154. Zoppini, G., et al., *Prevalence of Cardiovascular Autonomic Neuropathy in a Cohort of Patients With Newly Diagnosed Type 2 Diabetes: The Verona Newly Diagnosed Type 2 Diabetes Study (VNDS).* Diabetes Care, 2015. **38**(8): p. 1487-93.
155. Kristensen, F.P.B., et al., *The Danish Centre for Strategic Research in Type 2 Diabetes (DD2) Project Cohort and Biobank from 2010 Through 2023-A Cohort Profile Update.* Clin Epidemiol, 2024. **16**: p. 641-656.
156. Wesolowska-Andersen, A., et al., *Four groups of type 2 diabetes contribute to the etiological and clinical heterogeneity in newly diagnosed individuals: An IMI DIRECT study.* Cell Rep Med, 2022. **3**(1): p. 100477.
157. Dennis, J.M., et al., *Disease progression and treatment response in data-driven subgroups of type 2 diabetes compared with models based on simple clinical features: an analysis using clinical trial data.* Lancet Diabetes Endocrinol, 2019. **7**(6): p. 442-451.
158. Turner, R.C., *The U.K. Prospective Diabetes Study. A review.* Diabetes Care, 1998. **21 Suppl 3**: p. C35-8.
159. Shanik, M.H., et al., *Insulin resistance and hyperinsulinemia: is hyperinsulinemia the cart or the horse?* Diabetes Care, 2008. **31 Suppl 2**: p. S262-8.
160. Johnson, J.D., *On the causal relationships between hyperinsulinaemia, insulin resistance, obesity and dysglycaemia in type 2 diabetes.* Diabetologia, 2021. **64**(10): p. 2138-2146.
161. Prasad, R.B., et al., *Subgroups of patients with young-onset type 2 diabetes in India reveal insulin deficiency as a major driver.* Diabetologia, 2022. **65**(1): p. 65-78.
162. Wasada, T., et al., *Hyperglycemia facilitates urinary excretion of C-peptide by increasing glomerular filtration rate in non-insulin-dependent diabetes mellitus.* Metabolism, 1995. **44**(9): p. 1194-8.
163. Saito, K., et al., *Usefulness of subclassification of adult diabetes mellitus among inpatients in Japan.* J Diabetes Investig, 2022. **13**(4): p. 706-713.
164. Jane Ellis, M., J.H. Livesey, and M.J. Evans, *Hormone stability in human whole blood.* Clin Biochem, 2003. **36**(2): p. 109-12.
165. World Health Organization. Diagnostic Imaging and Laboratory Technology (2002), *Use of anticoagulants in diagnostic laboratory investigations.* World Health Organization. World Health Organization. https://iris.who.int/handle/10665/65957.
166. Chakera, A.J., et al., *Current laboratory requirements for adrenocorticotropic hormone and renin/aldosterone sample handling are unnecessarily restrictive.* Clin Med (Lond), 2017. **17**(1): p. 18-21.
167. Livesey, J.H., M.J. Ellis, and M.J. Evans, *Pre-analytical requirements.* Clin Biochem Rev, 2008. **29 Suppl 1**(Suppl 1): p. S11-5.
168. Silva Junior, J.M.D., et al., *Creatinine recovery from bovine urine under the effect of different times and temperatures of storage.* PLoS One, 2023. **18**(3): p. e0282145.
169. Gonzalez-Lao, E., et al., *Systematic review of the biological variation data for diabetes related analytes.* Clin Chim Acta, 2019. **488**: p. 61-67.
170. Gjessing, H.J., et al., *Correlations between fasting plasma C-peptide, glucagon-stimulated plasma C-peptide, and urinary C-peptide in insulin-treated diabetics.* Diabetes Care, 1987. **10**(4): p. 487-90.

171. Zhou, W., et al., *Application of urine C-peptide creatinine ratio in type 2 diabetic patients with different levels of renal function.* Front Endocrinol (Lausanne), 2022. **13**: p. 1052794.
172. Fernandez-Castañer, M., et al., *Evaluation of B-cell function in diabetics by C-peptide determination in basal and postprandial urine.* Diabete Metab, 1987. **13**(5): p. 538-42.
173. Garvey, W.T., et al., *Day-long integrated serum insulin and C-peptide profiles in patients with NIDDM. Correlation with urinary C-peptide excretion.* Diabetes, 1988. **37**(5): p. 590-9.
174. Pisprasert, V., et al., *Limitations in the use of indices using glucose and insulin levels to predict insulin sensitivity: impact of race and gender and superiority of the indices derived from oral glucose tolerance test in African Americans.* Diabetes Care, 2013. **36**(4): p. 845-53.
175. Sobngwi, E., et al., *Fasting insulin sensitivity indices are not better than routine clinical variables at predicting insulin sensitivity among Black Africans: a clamp study in sub-Saharan Africans.* BMC Endocr Disord, 2014. **14**: p. 65.
176. Tripathy, D., et al., *Contribution of insulin-stimulated glucose uptake and basal hepatic insulin sensitivity to surrogate measures of insulin sensitivity.* Diabetes Care, 2004. **27**(9): p. 2204-10.
177. Shoji, T., M. Emoto, and Y. Nishizawa, *HOMA index to assess insulin resistance in renal failure patients.* Nephron, 2001. **89**(3): p. 348-9.
178. Piketty, M.L., et al., *False biochemical diagnosis of hyperthyroidism in streptavidin-biotin-based immunoassays: the problem of biotin intake and related interferences.* Clin Chem Lab Med, 2017. **55**(6): p. 780-788.

8 Appendix

8.1 Supplementary Tables

Supplementary Table 1: Intra-assay and inter-assay precision of *Elecsys C-peptide* on the e 801 module of *Cobas 8000*®.

	Sample 1	Sample 2	Sample 3	Sample 4	Sample 5
Average concentration (ng/mL)	1.07	10.1	38.5	191	391
Intra-assay CV (%)	5.5	3.8	1.8	1.4	2.0
Inter-assay CV (%)	6.2	4.8	2.2	3.9	2.4

Supplementary Table 1: Intra-assay and inter-assay precision of *Elecsys C-peptide* on the e 801 module of *Cobas 8000*®. Adapted from *Elecsys C-peptide* Infosheet (Roche Diagnostics, Mannheim, Germany) [100]. *ng/mL* nanogram per millilitre

Supplementary Table 2: Intra-assay and inter-assay precision of *CREP2* assay on the c 701 module of *Cobas 8000*®.

	Sample 1	Sample 2	Sample 3	Sample 4	Sample 5
Average concentration (mg/dL)	95.4	49.8	26.4	224	538
Intra-assay CV (%)	0.5	0.9	0.9	0.6	0.8
	Sample 1	**Sample 2**	**Sample 3**	**Sample 4**	
Average concentration (mg/dL)	81.6	158	196	79.2	
Inter-assay CV (%)	1.5	1.5	1.4	1.5	

Supplementary Table 2: Intra-assay and inter-assay precision of *CREP2* assay on the c 701 module of *Cobas 8000*®. Adapted from *CREP2 Creatinine plus ver.2* Infosheet (Roche Diagnostics, Mannheim, Germany) [150]. *mg/dL* milligram per decilitre

Supplementary Table 3: Variable-wise distribution of missing data for baseline characteristics of participants with NGT and T2DM.

Variable	**NGT (n = 192)**	**T2DM (n = 488)**
Age	0 (0%)	0 (0%)
Sex	0 (0%)	0 (0%)
BMI	0 (0%)	7 (1.4%)
Fasting SCP	6 (3.1%)	32 (6.6%)
Fasting UCP	0 (0%)	0 (0%)
Fasting UCr	0 (0%)	0 (0%)
Fasting UCP	0 (0%)	0 (0%)
Fasting UCr	0 (0%)	0 (0%)
UCPCR	0 (0%)	0 (0%)
HOMA2-S	6 (3.1%)	32 (6.6%)
HOMA2-B	6 (3.1%)	32 (6.6%)
Fasting blood glucose	6 (3.1%)	32 (6.6%)

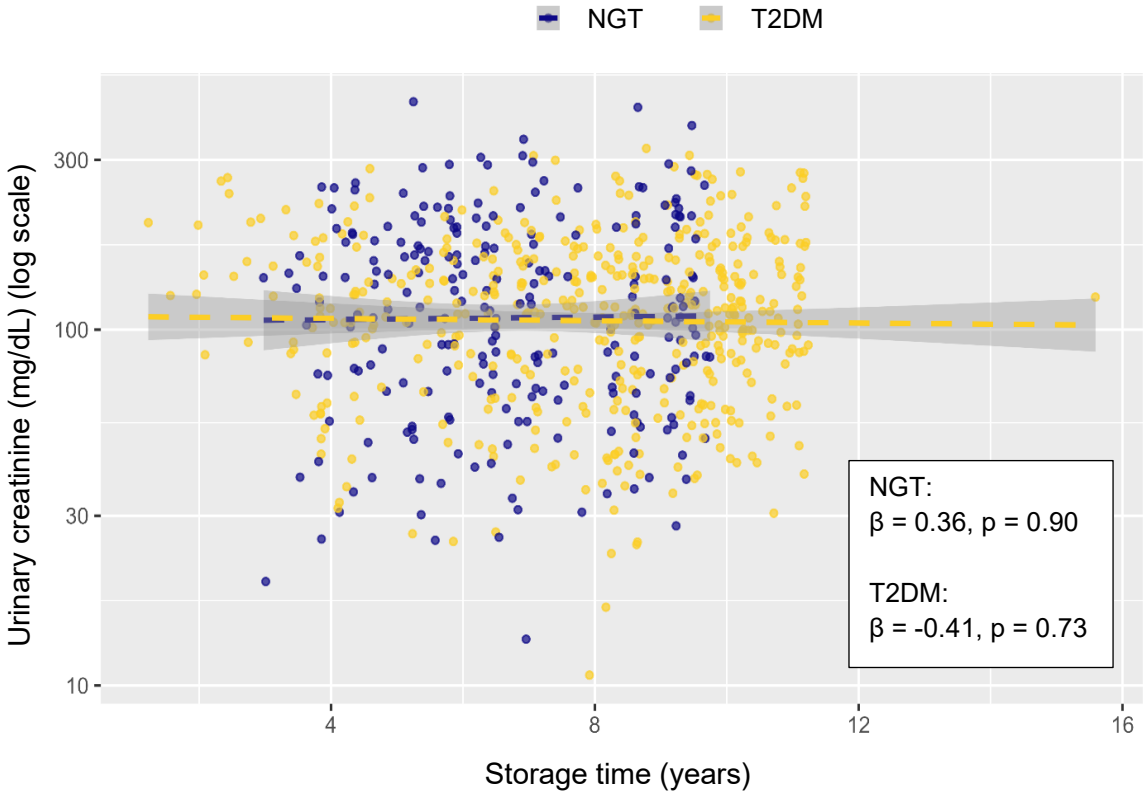
Supplementary Table 3: Variable-wise distribution of missing data for baseline characteristics of participants with NGT and T2DM. Data is presented as n (%) of total n of the respective category. *NGT* normal glucose tolerance, *T2DM* type 2 diabetes, *BMI* body mass index, *SCP* serum C-peptide, *UCP* urinary C-peptide, *UCr* urinary creatinine, *UCPCR* urinary C-peptide-to-creatinine ratio, *HOMA2-S* homeostasis model assessment 2 of insulin sensitivity, *HOMA2-B* homeostasis model assessment 2 of β-cell function, *n* number of participants

Supplementary Table 4: Variable-wise distribution of missing data for baseline characteristics of participants with T2DM subtypes and NGT.

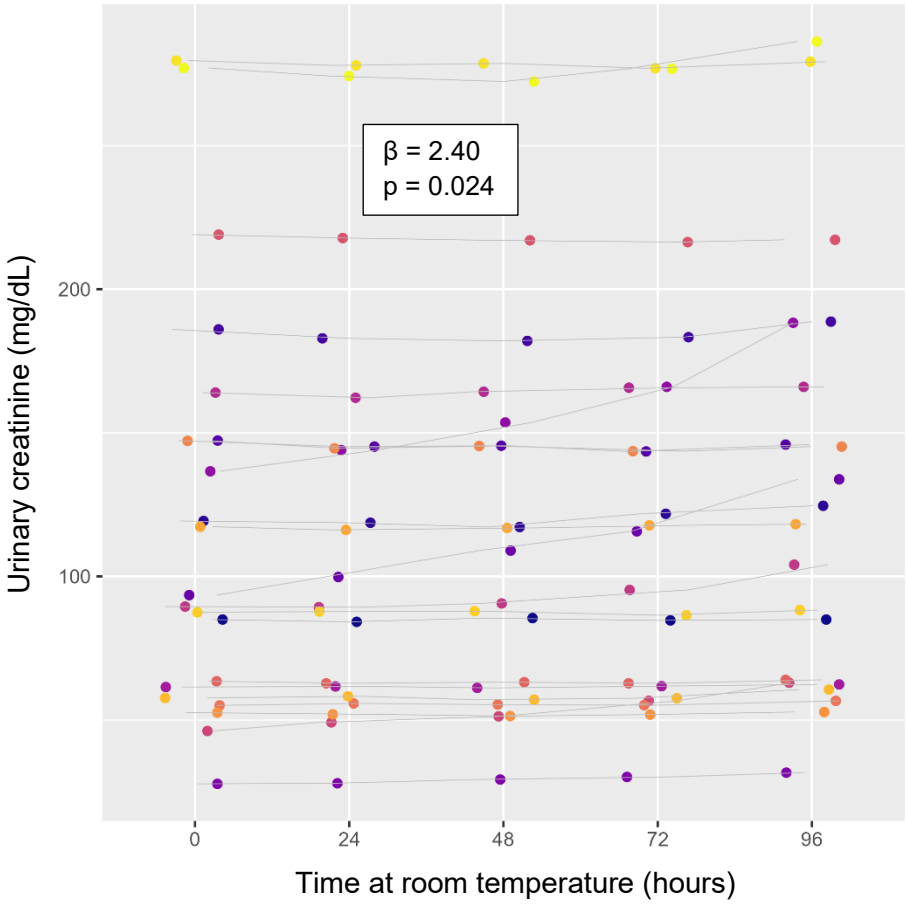
Variable	NGT (n = 192)	SIDD (n = 15)	SIRD (n = 72)	MOD (n = 190)	MARD (n = 211)
Age	0 (0%)	0 (0%)	0 (0%)	0 (0%)	0 (0%)
Sex	0 (0%)	0 (0%)	0 (0%)	0 (0%)	0 (0%)
BMI	0 (0%)	0 (0%)	1 (1.4%)	2 (1.1%)	4 (1.9%)
Fasting SCP	6 (3.1%)	1 (6.7%)	8 (11%)	11 (5.8%)	12 (5.7%)
Fasting UCP	0 (0%)	0 (0%)	0 (0%)	0 (0%)	0 (0%)
Fasting UCr	0 (0%)	0 (0%)	0 (0%)	0 (0%)	0 (0%)
Fasting UCP	0 (0%)	0 (0%)	0 (0%)	0 (0%)	0 (0%)
Fasting UCr	0 (0%)	0 (0%)	0 (0%)	0 (0%)	0 (0%)
UCPCR	0 (0%)	0 (0%)	0 (0%)	0 (0%)	0 (0%)
HOMA2-S	6 (3.1%)	1 (6.7%)	8 (11%)	11 (5.8%)	12 (5.7%)
HOMA2-B	6 (3.1%)	1 (6.7%)	8 (11%)	11 (5.8%)	12 (5.7%)
Fasting blood glucose	6 (3.1%)	1 (6.7%)	8 (11%)	11 (5.8%)	12 (5.7%)

Supplementary Table 4: Variable-wise distribution of missing data for baseline characteristics of participants with T2DM subtypes and NGT. Data is presented as n (%) of total n of the respective category. *NGT* normal glucose tolerance, *T2DM* type 2 diabetes, *SIDD* severe insulin-deficient diabetes, *SIRD* severe insulin-resistant diabetes, *MOD* mild obesity-related diabetes, *MARD* mild age-related diabetes, *BMI* body mass index, *SCP* serum C-peptide, *UCP* urinary C-peptide, *UCr* urinary creatinine, *UCPCR* urinary C-peptide-to-creatinine ratio, *HOMA2-S* homeostasis model assessment 2 of insulin sensitivity, *HOMA2-B* homeostasis model assessment 2 of β-cell function, *n* number of participants

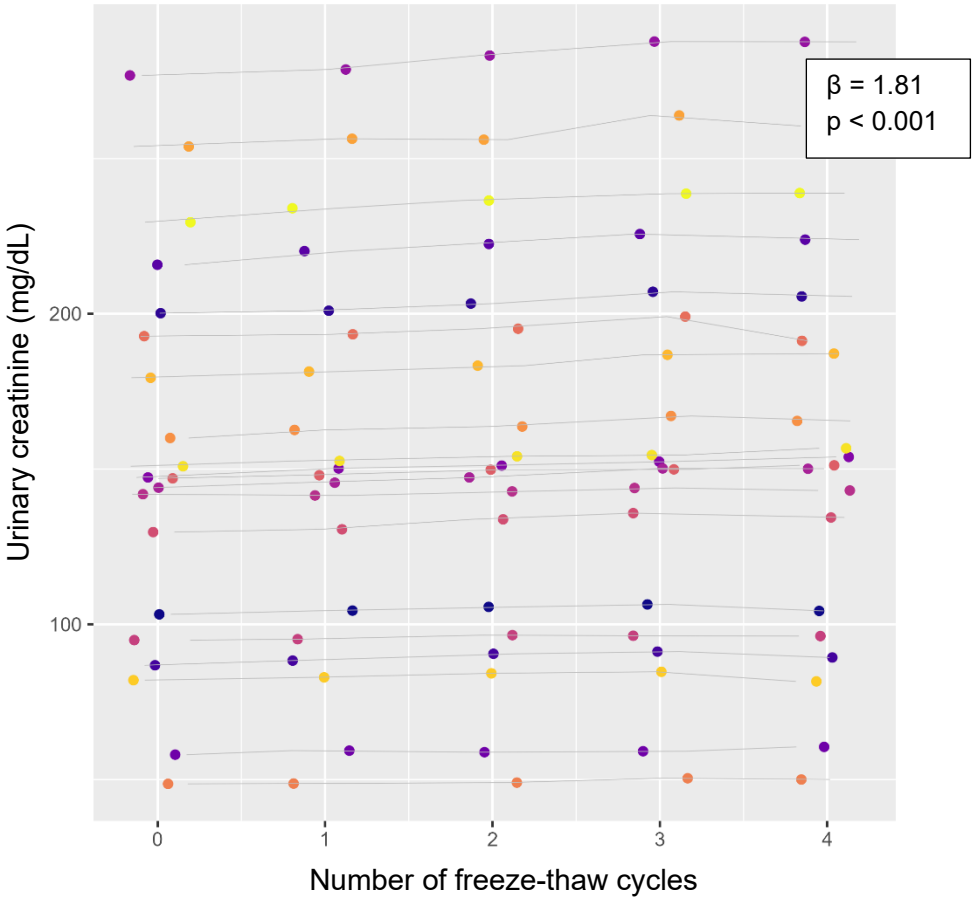
8.2 Supplementary Figures



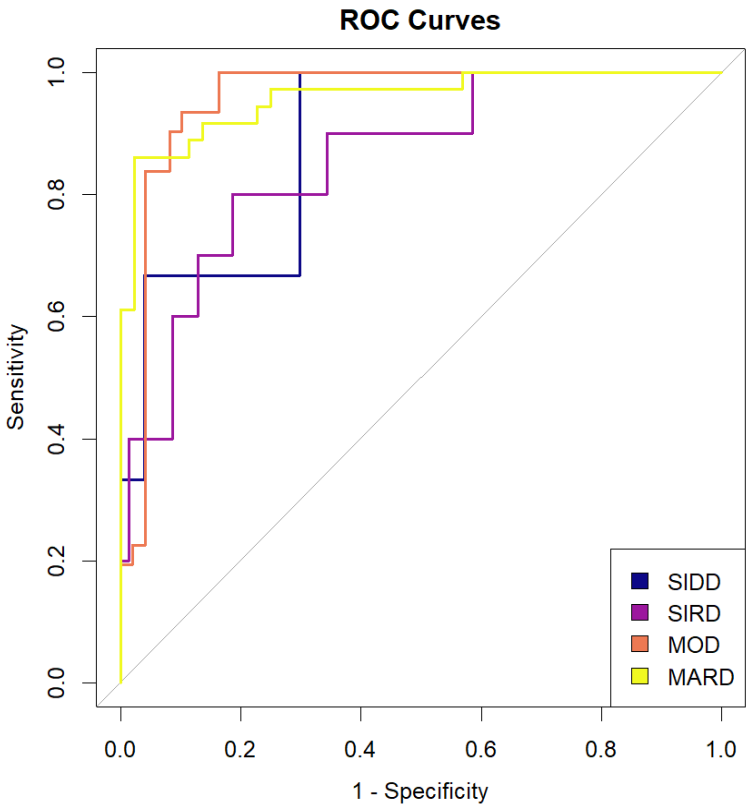
Supplementary Figure 1: Effect of time on stability of UCr at -20 °C. Scatter plot showing log-transformed UCr (mg/dL) on the Y-axis versus elapsed storage time at -20 °C on the X-axis. Group-specific regression lines (dashed) with 95% confidence intervals are shown, with the blue regression line representing participants with NGT and the yellow regression line representing participants with T2DM. Blue and yellow points correspond to individual measurements of participants with NGT and T2DM respectively. A generalized linear model was used. n (total) = 680, NGT: n = 192, β = 0.36, p = 0.90; T2DM: n = 488, β = -0.41, p = 0.73. The figure was created using the software "R". *n* number of participants, *mg/dL* milligram per decilitre



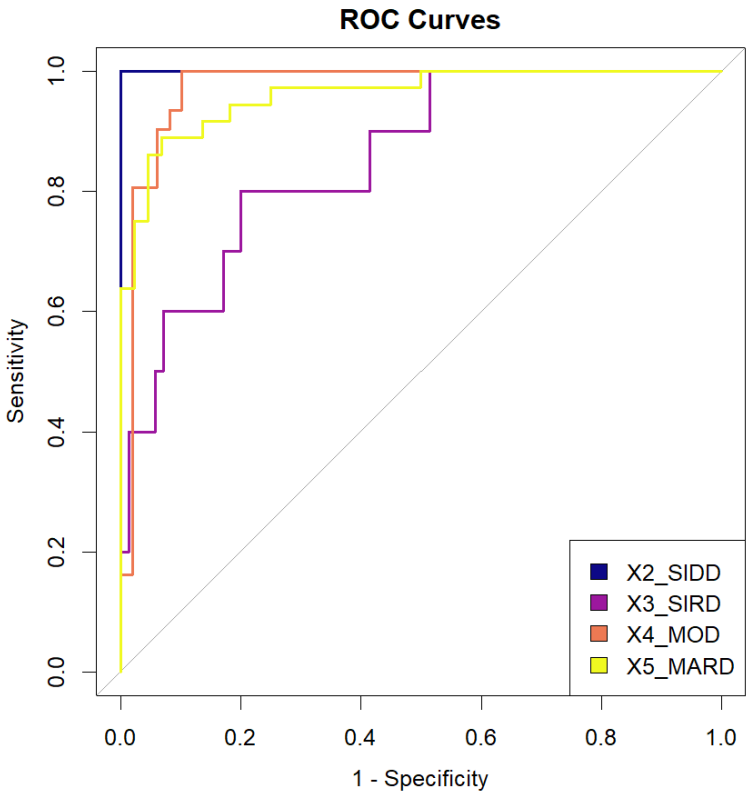
Supplementary Figure 2: Stability of UCr at room temperature over 96 hours. Spaghetti plot showing individual longitudinal trajectories of UCr concentrations (mg/dL, Y-axis) over time (hours) at room temperature (X-axis). Each point represents a single measurement, and lines connect repeated measurements from the same participant across time points. A linear mixed-effects model with random slope and intercept was used. n (participants) = 21, n (measurements = 105), β = 2.40, 95% CI 0.32 to 4.48, p = 0.024. The Figure was created using the software "R". *mg/dL* milligram per decilitre



Supplementary Figure 3: Stability of UCr across four freeze-thaw cycles. Spaghetti plot showing individual longitudinal trajectories of UCr concentrations (mg/dL, Y-axis) over time (hours) at room temperature (X-axis). Each point represents a single measurement, and lines connect repeated measurements from the same participant across time points. A linear mixed-effects model with random slope and intercept was used. n (participants) = 20, n (measurements) = 100, β = 1.81, 95% CI 1.28 to 2.33, p = < 0.001. The figure was created using the software "R". *mg/dL* milligram per decilitre



Supplementary Figure 4: ROC curves for the multinomial prediction model predicting T2DM subtypes, after inclusion of fasting blood glucose. ROC curves are shown for four predicted T2DM subtypes: SIDD (blue), SIRD (purple), MOD (orange), and MARD (yellow). Overall accuracy of the model was 81.3% (95% CI 71.0% to 89.1%), exceeding the no information rate of 45% ($p < 0.001$) with Cohen's κ being 0.68. AUC for SIDD: 0.89, for SIRD: 0.86, for MOD: 0.96, for MARD: 0.96. Variables: UCP, age at diagnosis, sex, BMI, and fasting blood glucose. The figure was created using the software "R". *ROC* receiver operating characteristic, *SIDD* severe insulin-deficient diabetes, *SIRD* severe insulin-resistant diabetes, *MOD* mild obesity-related diabetes. *MARD* mild age-related diabetes



Supplementary Figure 5: ROC curves for the multinomial prediction model predicting T2DM subtypes, after inclusion of fasting blood glucose and HbA1c. ROC curves are shown for four predicted T2DM subtypes: SIDD (blue), SIRD (purple), MOD (orange), and MARD (yellow). Overall accuracy of the model was 80.0% (95% CI 69.6% to 88.1%), exceeding the no information rate of 45% ($p < 0.001$) with Cohen's κ being 0.67. AUC for SIDD: 1.0, for SIRD: 0.85, for MOD: 0.97, for MARD: 0.96. Variables: UCP, age at diagnosis, sex, BMI, fasting blood glucose, and HbA1c. The figure was created using the software "R". *ROC* receiver operating characteristic, *SIDD* severe insulin-deficient diabetes, *SIRD* severe insulin-resistant diabetes, *MOD* mild obesity-related diabetes, *MARD* mild age-related diabetes

Acknowledgements

My first words of gratitude go towards my family, who have stood by me all along. Their continuous encouragement and motivation were essential to the completion of this work.

Secondly, I would like to thank my supervisor Prof. Dr. Robert Wagner for his unwavering support right from the beginning, guiding me throughout this journey and being approachable all the time. The comfort that I have felt to reach out to him for any matter has been unparalleled. My gratitude also goes towards my co-supervisor Prof. Dr. Friedrich Boege, who welcomed me in the world of laboratory medicine and made it possible for me take up this project. I would like to thank Dr. rer. nat. Christian Binsch not only for his help with the statistical analyses but also for his approachability, all-round expertise and patience. Apart from this, I would like to express my gratitude towards Iryna Yurchenko and Dr. med. Kálmán Bódis, whom I could go to whenever I needed help.

Thirdly, my gratitude goes towards my colleagues of the Central Laboratory, with whom I could discuss my project in detail whenever needed. I would especially like to thank Dr. med. Derik Hermsen, who kept me motivated throughout and was always there to support me and Dr. med Eva Kierysch, from whom I learned a lot. I thank the entire technical staff of the Central Laboratory, especially the team of clinical chemistry—Susanne Förster, Sabine Herrmann and Petra Meirowski for their unwavering readiness to answer my questions and help me with the measurements. Special thanks go to Thomas Lange for his support with the IT-system of the laboratory.

Apart from this, I would like to thank Dr. rer. nat. Sandra Trenkamp, Ludmila Bernowski and the entire team of the DDZ for organizing the samples needed for this study.

Last but not the least, I would like to express my gratitude towards the Medical Research School, Düsseldorf and towards all the instructors who were involved in the course-curriculum of the program.

Any number of words would not be enough to express my gratitude towards everyone mentioned above, as the magnitude of their contributions cannot be described entirely in words.